THE UNIVERSITY
of EDINBURGH

PHYTOCHROME CONTROL OF PLANT GROWTH AND METABOLISM IN *ARABIDOPSIS THALIANA*

BY **DEYUE YANG**

SUBMITTED FOR THE DEGREE OF **DOCTOR OF PHILOSOPHY**

THE INSTITUTE OF QUANTITATIVE BIOLOGY, BIOCHEMISTRY AND BIOTECHNOLOGY, SCHOOL OF BIOLOGICAL SCIENCES

UNIVERSITY OF EDINBURGH

AUGUST 2016

Abstract

Plants rely on light to supply photosynthetic energy and to provide information of the surrounding environment. Phytochromes are photoreceptors that sense external light quality and quantity, which in turn guide the strategy of plant growth. A large body of research has focused on *Arabidopsis thaliana* seedlings, where phytochrome control of responses such as hypocotyl elongation, hook opening and cotyledon greening, has been intensively explored. Mathematical models have also helped elucidate the molecular mechanism of phytochrome signalling. A smaller proportion of studies have investigated the role of phytochrome in controlling plant plasticity in adult plants. This work has shown that phytochrome depletion enhances leaf petiole elongation and slows growth, but there is a lack of information on how these marked changes alter metabolism.

In this thesis, I use phytochrome multiple mutants of to explore how phytochromes interact with metabolism to affect plant growth. My analysis revealed that phytochrome loss results in dramatically reduced biomass production, especially in high order *phyABDE* mutant that lacks four out of five phytochromes. This is caused, at least partly, by impaired photosynthesis in phytochrome mutants, including reduced chlorophyll level and less CO_2 uptake. Furthermore, cell wall synthesis and protein levels, major dry biomass constituents, are also repressed in phytochrome-depleted plants. Interestingly, these mutants accumulate more daytime sucrose and starch than wild type does, possibly due to their retarded growth in light. Further metabolic profiling reveals that these phytochrome mutants over-accumulate sugars, organic acids and amino acids. The sizable increase in raffinose and proline suggests a possible link to stress tolerance. Indeed, ABA and salt responses are significantly reduced in phytochrome mutants at both seedling and adult stages. These mutants are also more resistant to prolonged darkness, with less chlorophyll degradation in dark

and higher survival rates.

Collectively, this thesis shows that phytochromes have a novel role in plant resource management, controlling the allocation of resources for growth, switching the metabolism between growth and stress-coping states based on the availability of light from the environment. It brings new interest into phytochrome research in Arabidopsis, suggesting possible application of such knowledge to crop studies in the future.

Lay Summary

Plant life largely depends on light. Environmental light provides energy resources for photosynthesis, and notifies plants of their surroundings. Plants are able to sense changes in light quantity and quality through photoreceptors, including phytochromes. The importance of phytochromes in controlling young seedling establishment has been revealed by intensive research over the past decades. However, their role as vital regulators in adult plant development is less well understood.

This thesis presents evidence that, apart from regulating plant architecture, phytochromes are also involved in metabolism and biomass production in adult plants. Severe phytochrome mutants have compromised fresh and dry weight, less photosynthetic pigment and reduced CO_2 uptake. Plant biomass largely consists of cell wall and protein, and in line with their reduced biomass phenotype, these mutants have reduced cell wall gene expression and total protein content. Metabolic profiling results suggest that phytochrome loss leads to a general elevation of sugars, organic acids and amino acids. In phytochrome mutants, sugars over-accumulate during the day, in part because daytime growth is slow. Elevated levels of the metabolites proline and raffinose appear to render the mutant plants more tolerant to ABA, salt and dark stresses.

To summarize, this thesis presents a novel function of plant photoreceptors in regulating plant growth, metabolism and stress resilience.

Acknowledgement

First, I would like to thank my supervisor, Karen Halliday, for her insightful advice on experiments design and results interpretation, as well as her patient instructions and comments throughout my writing process. Karen is also very much appreciated for her financial support for the first two months of my final year, and a big contribution to my award application. Without her, the paper would not be published, nor would this Thesis be completed in time.

Thanks to Kelly Stewart and Gavin Steel, who kindly helped me when I first started in the lab. I thank Julia Foreman for sharing her experience of Q-PCR analysis, Gabriela Toledo Ortiz and Jayne Griffiths for their help and suggestions on metabolic assay protocols, and Keun Pyo for his help with protein quantification. Thanks to Daniel for his assistance with ANOVA analysis and contribution to the paper. I also thank John Christie's Lab and Henry Jackson at Glasgow University for their help with GC-MS experiment, and Keara Franklin (Bristol University) for providing *phyABCDE* seed stock.

I want to express my gratitude to the Darwin Trust of Edinburgh for providing scholarship to support my PhD, and the travel fund for my poster presentation at the International Conference of Arabidopsis Research in Paris. I am grateful for the British-Chinese Award for providing partial financial support for my writing up.

My greatest thank you to Yiming, who constantly supported me during all these years. Finally, a big thank you goes to Xun for her company and generous food support during my writing.

Declaration

This Thesis contains original work based on the following published paper:

Yang, D., Seaton, D. D., Krahmer, J., & Halliday, K. J. (2016). Photoreceptor effects on plant biomass, resource allocation, and metabolic state. Proceedings of the National Academy of Sciences, 113(27), 7667–7672. doi:10.1073/pnas.1601309113

I hereby declare that this Thesis is my own work except where explicitly stated.

No part of this Thesis has been previously submitted for a professional qualification or a degree at the University of Edinburgh, or any other university.

Deyue Yang

Edinburgh

August 2016

TABLE OF CONTENTS

ABSTRACT ..... **I**

LAY SUMMARY ..... **III**

ACKNOWLEDGEMENT ..... **IV**

DECLARATION ..... **V**

LIST OF FIGURES ..... **XI**

LIST OF TABLES ..... **XIII**

ABBREVIATIONS ..... **XIV**

CHAPTER 1- INTRODUCTION **1**

1.1 DUAL ROLES OF LIGHT IN PLANT LIFE 1

Light as the Ultimate Energy Source *1*

Light as the Environmental Indicator *2*

1.2 PHYTOCHROME LIGHT SIGNALLING IN ARABIDOPSIS 4

Phytochromes as 'Photoswitches' *4*

Phytochrome Signalling Networks *7*

Seedling Hypocotyl: A Model System for Phytochrome Study *10*

Shade Response Regulated by Phytochromes *11*

Arabidopsis without Phytochromes *15*

1.3 SUGAR REGULATION OF PLANT GROWTH AND INTERACTION WITH PHYTOCHROMES 17

Sugar Mediated Growth Regulation in Arabidopsis *17*

Phytochromes affect sugar metabolism partly through photosynthesis regulation *19*

Crosstalk between sucrose and phytochrome signalling *21*

1.4 PHYTOCHROME SIGNALLING IN DARK RESPONSES 23

Dark induced senescence *23*

Phytochrome Regulation of Dark Induced Senescence *25*

1.5 THESIS OVERVIEW 27

Objectives of Study *27*

Chapter Layout *28*

CHAPTER 2- EXPERIMENTAL PROCEDURES 29

2.1 PLANT MATERIAL 29

2.2 GROWTH CONDITIONS 29

2.3 FRESH AND DRY BIOMASS QUANTIFICATION 31

2.4 CHLOROPHYLL CONTENT MEASUREMENT 31

2.5 GAS EXCHANGE MEASUREMENT 32

2.6 SUGAR AND STARCH QUANTIFICATION 32

2.7 IODINE STAINING 33

2.8 TOTAL PROTEIN QUANTIFICATION 34

2.9 GROWTH MEASUREMENT 34

2.10 QUANTITATIVE REAL-TIME PCR (QRT-PCR) 35

2.11 GC-MS METABOLIC ASSAY 39

2.12 MICROARRAY ANALYSIS 42

CHAPTER 3- A NOVEL ROLE OF PHYTOCHROMES IN COUPLING CARBON RESOURCE TO GROWTH 43

3.1 INTRODUCTION 43

3.2 GROWTH CONDITION OPTIMIZATION 45

3.3 PHYTOCHROME MUTANT ADULT PLANTS POSSESS LESS CHLOROPHYLL AND FIX LESS CO_2 THAN WT 48

3.4 MORE ENDOGENOUS SUGARS AND STARCH ARE ACCUMULATED DURING DAYTIME IN PHYTOCHROME MUTANTS 50

Diurnal sucrose and starch quantification in six-week-old rosettes 50

Iodine stain result suggests different starch composition in phyABDE 53

EOD sugar quantification in shoot and root tissues 55

3.5 *PHYBD* HAS RETARDED GROWTH PARTICULARLY DURING DAYTIME 58

3.6 PHYTOCHROMES ARE MAJOR REGULATORS OF PLANT BIOMASS 61

3.7 DISCUSSION 64

CHAPTER 4- PHYTOCHROME MUTANTS HAVE REPROGRAMMED METABOLISM AND REDUCED SENSITIVITY TO ABIOTIC STRESSES. 68

4.1 INTRODUCTION 68

4.2 EXPERIMENTAL DESIGN AND GC-MS ANALYSIS PROCEDURE 70

4.3 PCA SHOWS DISTINGUISHED METABOLIC PROFILES BETWEEN WT AND PHYTOCHROME MUTANTS 73

4.4 PHYTOCHROME MUTANTS HAVE ELEVATED LEVELS OF SUGARS AND ALCOHOLS, ORGANIC ACIDS AND AMINO ACIDS COMPARED TO WT 76

4.5 Transcriptional Analysis of Enzyme Genes in Related Pathways 80

4.6 Phytochrome Mutants Have Reduced Sensitivity to Abiotic Stresses at Both Seedlings and Adult Stages 84

4.7 Stress Marker Genes are Up-regulated in Phytochrome Mutants 88

4.8 Discussion 91

CHAPTER 5- PHYTOCHROME MUTANTS HAVE ALTERED RESPONSE TO PROLONGED DARKNESS 95

5.1 Introduction 95

5.2 Phytochrome Multiple Mutants Are Less Responsive to Dark than *Ler* WT 98

Phytochrome mutants are more likely to survive through 2-week darkness 98

Phytochrome mutants have less chlorophyll loss in response to dark treatment 99

5.3 Background Effect on Phytochrome-dependent Chlorophyll Loss in Response to Darkness 102

Unlike Ler lines, 5-week phyB-9 (Col) doesn't show reduced sensitivity to dark induced chlorophyll loss and plant death 103

Similar background effect was also found in 3-week seedlings under long-day photoperiod, 23°C condition 106

5.4 Plants Grown in High-light Are More Susceptible to Dark Stress 109

5.5 Discussion 113

CHAPTER 6- DISCUSSION 116

6.1 Phytochrome Regulation of Carbon Resource 117

6.2 Phytochrome Control of Growth: Perspectives from *XTHs* Regulation 118

6.3 PHYTOCHROME AS THE METABOLIC SWITCH FOR STRESS PRIMING STATUS? . 120

6.4 POTENTIAL NATURAL VARIATION IN PHYTOCHROME CONTROL OF DARK RESPONSE 121

6.5 CONCLUDING REMARKS 123

REFERENCE 124

APPENDIX 142

List of Figures

Figure 1.1 Simplified schematic representation of light effects on plant life. 2

Figure 1.2 Plant absorption of light at certain wavelengths. 4

Figure 1.3 Phytochrome model as a 'photoswitch'. 5

Figure 1.4 PIFs act as a hub in integrating internal and external signals to regulate photomorphogenesis and stem elongation growth. 8

Figure 1.5 Plants use phytochromes to detect the neighbouring vegetation and respond in growth alteration accordingly. 13

Figure 2.1 Photo illustration of gas exchange measurement system. 32

Figure 3.1 Flowering time of *phyABDE* can be delayed by reducing growth temperature and photoperiod length. 47

Figure 3.2 Physiological study of WT and phytochrome mutant adult plants. 49

Figure 3.3 Sucrose and starch determination assay. 52

Figure 3.4 Iodine staining starch quality assay. 54

Figure 3.5 Sucrose and starch determination assay. 57

Figure 3.6 Comparing to WT, *phyBD* has retarded growth rate especially in the day. 60

Figure 3.7. Phytochrome deficiency strongly affects plant biomass. 63

Figure 4.1 GC-MS experiment procedures. 72

Figure 4.2 PCA (Principle Component Analysis) of metabolites in WT and phytochrome samples. 75

Figure 4.3 GC-MS metabolomics quantification of WT and phytochrome mutants sampled at dawn and dusk. 79

Figure 4.4 Diurnal expression profiles of metabolic enzyme genes involved in TCA and related pathways. 82

Figure 4.5 Diurnal expression profiles of metabolic enzyme genes in raffinose (A) and proline (B) metabolic pathways. 83

Figure 4.6 Salt and ABA stress response in seedlings. 86

Figure. 4.7 Salt, ABA and drought stress response in adult plants. 87

Figure 4.8. Stress marker genes and ABA pathway gene expressions are altered in *phyABDE* compared to WT plants. 90

Figure 5.1 Phytochrome mutants are more likely to survive after dark incubation than WT plants. 100

Figure 5.2 Chlorophyll quantifications in L*er* WT and phytochrome mutants at subjective dusk (D0), day 1, 7 and 10 (D1, 7, 10) of darkness. 101

Figure 5.3 Dark responses of 5-week-old plants using Ler and Col lines. 105

Figure 5.4 Dark responses of 3-week-old plants using L*er* and C*ol* lines. 108

Figure 5.5 Represent photo and fresh biomass of L*er* and *phyBD* grown in different light levels. 111

Figure 5.6 Dark test results of phytochrome mutants and WT from different light conditions. 112

List of Tables

Table 1.1 Shade avoidance syndrome. 14
Table 2.1 Sequence of primers used for qRT-PCR 36
Table 2.2 10ul reaction system for qRT-PCR 38
Table 2.3 qRT-PCR program setting 38

Abbreviations

WT	Wild Type
L*er*	Landsberg *erecta*
C*ol*	Columbia
phy	phytochrome
PIF	Phytochrome Interacting Factors
R	Red Light
FR	Far-Red light
R:FR	Red:Far-red light ratio
Pfr	Far-red light absorbing form of phytochrome (Active)
Pr	Red light absorbing form of phytochrome (Inactive)
ABA	Abscisic Acid
EOD	End of Day
EON	End of Night
wk	Week
ZT	Zeitgeber time
CO_2	Carbon Dioxide
qRT-PCR	Quantitative Real-Time PCR
GC-MS	Gas Chromatography coupled with Mass Spectrophotometry
PCA	Principle Component Analysis

Chapter 1- Introduction

1.1 Dual roles of light in plant life

Light as the Ultimate Energy Source

Light is best known to provide energy source for photosynthesis, where plants absorb light and CO_2 to synthesize carbohydrates and oxygen (Figure 1.1). Photosynthesis is rather important as its products not only directly contribute to plant growth and development, but also indirectly feed the majority of all other living organisms and provide biological fuels. However, only light between 400-700 nm wavelengths (Photosynthetically Active Radiation, PAR, see Figure 1.2), less than 50% of total solar energy can be used to drive photosynthesis. In addition, only a small fraction of light energy absorbed by plants can be converted to chemical resources, and not all the chemical energy is used to produce biomass. In other words, photosynthesis efficiency is incredibly low. Typically, only 4-6% of sunlight energy can be fixed as carbohydrates (Zhu et al., 2008). Compounding this, plant photosynthesis is also constantly challenged by environmental factors, such as changes in light quality and quantity, temperature, atmospheric CO_2 level, various stresses and pathogens (Kangasjärvi et al., 2012). As food problem becomes more urgent than ever due to the burgeoning population, reduced farmland and the challenging alterations of the

environment, researchers are making concerted efforts to promote photosynthetic efficiency, in order to improve biomass and yield production especially in crops.

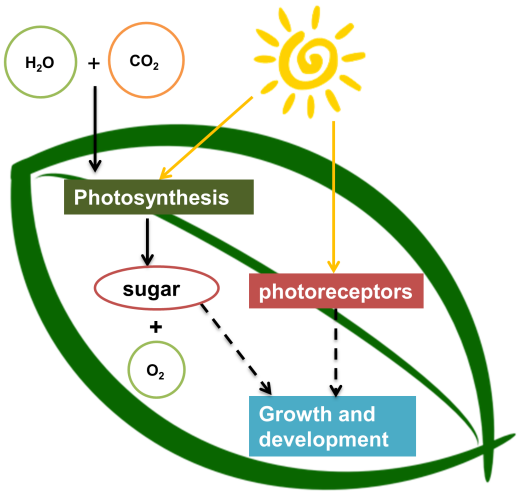

Figure 1.1 Simplified schematic representation of light effects on plant life.

Light is absorbed by plants to drive photosynthesis; it is also perceived by plant photoreceptors to provide information of the surroundings. Both processes are of vital importance in contributing to plant growth and development.

Light as the Environmental Indicator

In the plant life cycle light has an important role even before photosynthesis has been initiated. Light stimulation is required for seed germination in many species. One classical experiment (Borthwick et al., 1952) demonstrates red light exposure could increase seed germination rate from 8.5% to 98% in lettuce (*Lactuca sativa L.*). Similar results were also reported in the model plant Arabidopsis (Cho et al., 2012; Lee et al., 2012). When covered or buried in soil, seedlings undergo an etiolated growth, where the hypocotyl elongates and cotyledons fold to form a hook, enabling the seedling to emerge from soil surface to reach the sunlight. Almost immediately the rapid hypocotyl elongation stops, cotyledons open to embrace light, functional

chloroplasts are developed, leading to a photoautotrophically competent seedling (Chory et al., 1996). Afterwards, light continues to provide 'instructions' for plant growth and development, including elongating towards light when shaded by neighbouring foliage, and transiting from vegetative growth into reproductive stage at appropriate time (Franklin and Quail, 2010). Light information from the surroundings is perceived by plants throughout the entire life cycle (Neff et al., 2000). This is particularly important for sessile plants that cannot move like animals to escape from encountered enemies or stresses. Natural environmental light varies in a sophisticated way, including fluctuations of light quality, quantity, duration and direction by hours, days and seasons. During the past decades, studies on light signalling responses have discovered three types of photoreceptors in plants (Chen et al., 2004): phytochromes (PHYs) as red (600-700 nm) and far-red (700-800 nm) light receptors (Casal et al., 1998); cryptochromes (CRYs), phototropins and zeitlupe family as blue light (400-500 nm)/UV-a (315-400 nm) receptors (Fankhauser and Staiger, 2002; Galvão and Fankhauser, 2015) and the UV-B (280-315 nm) light receptor UVB-RESISTANCE 8 (UVR8) (Tilbrook et al., 2013). Briefly, photoreceptors are light sensing proteins that transduce specific wavelengths of light information (Figure 1.2) into biochemical signals, triggering a series of molecular and physiological responses to regulate plant life.

Despite that both photosynthesis and photoperception largely rely on light and greatly affect plant life, the interaction between these two processes is rarely reported (Figure 1.1). This thesis sets out to explore how photoreceptors, especially phytochromes, integrate photosynthetic carbon metabolism to regulate plant growth and biomass production in Arabidopsis.

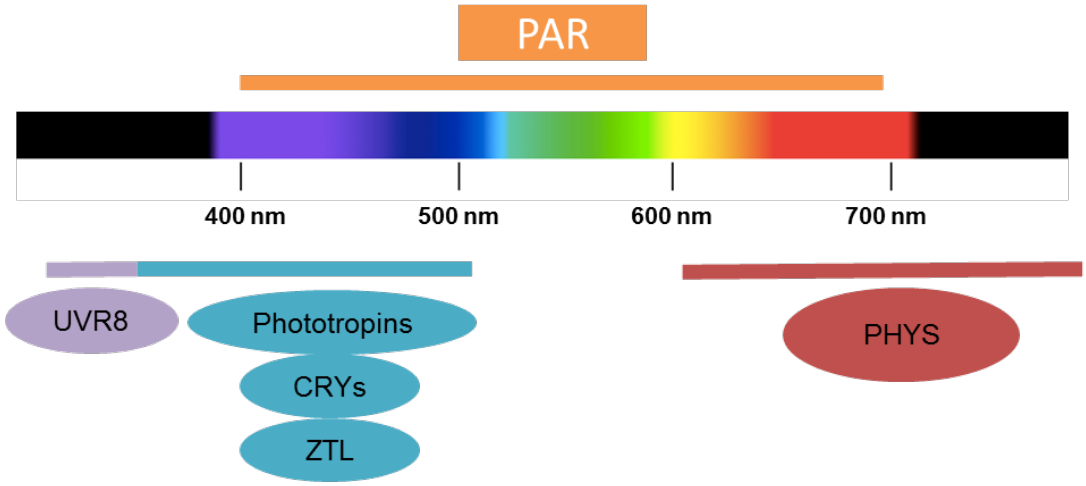

Figure 1.2 Plant absorption of light at certain wavelengths.

Plant Photosynthetically Active Radiation (PAR) ranges from 400-700 nm; UVR8 photoreceptor responds to UV-B light between 280-315 nm; Phototropins, CRYs and ZTL family respond to blue light (400-500 nm)/UV-a (315-400 nm); PHYs respond to red (600-700 nm) and far-red (700-800 nm) light.

1.2 Phytochrome light signalling in Arabidopsis

Among all photoreceptors, the red (R) and far-red (FR) light detectors, i.e. phytochromes, are probably most intensively studied. There are five members in the phytochrome family in Arabidopsis, phytochrome A (phyA) to phytochrome E (phyE) (Sharrock and Quail, 1989; Clack et al., 1994; Li et al., 2011). These phytochromes have partially redundant yet distinctive functions, working together to regulate throughout plant life, from seed dormancy and germination (Lee et al., 2012; Cho et al., 2012), seedling de-etiolation and photomorphogenesis (Chen and Chory, 2011) to reproductive transition (Chory et al., 1996).

Phytochromes as 'Photoswitches'

Phytochromes act as dimers in two forms: active (Pfr) and inactive (Pr). The attached tetrapyrrole chromophores absorb light, enabling phytochromes to undergo a

reversible conformational change between two forms upon R/FR light stimulation (Rockwell et al., 2006). In the dark, all phytochromes are in the Pr form, but can be activated by R that triggers photoconversion to the active Pfr form (Figure 1.3). Once activated, Pfrs are translocated into nucleus, where they regulate gene transcription and the downstream physiological responses through a series of transcription factors such as PIFs (Phytochrome Interacting Factors) (Leivar and Quail, 2011; Chen and Chory, 2011). The active Pfr form can be photoconverted back to the inactive Pr form by FR. In addition, the thermally unstable Pfr can be reversed back to Pr in a light-independent relaxation process called dark reversion (Rockwell et al., 2006). Due to these structure characteristics, phytochromes function as reversible photoswitches that can quickly respond to the constantly changing light conditions.

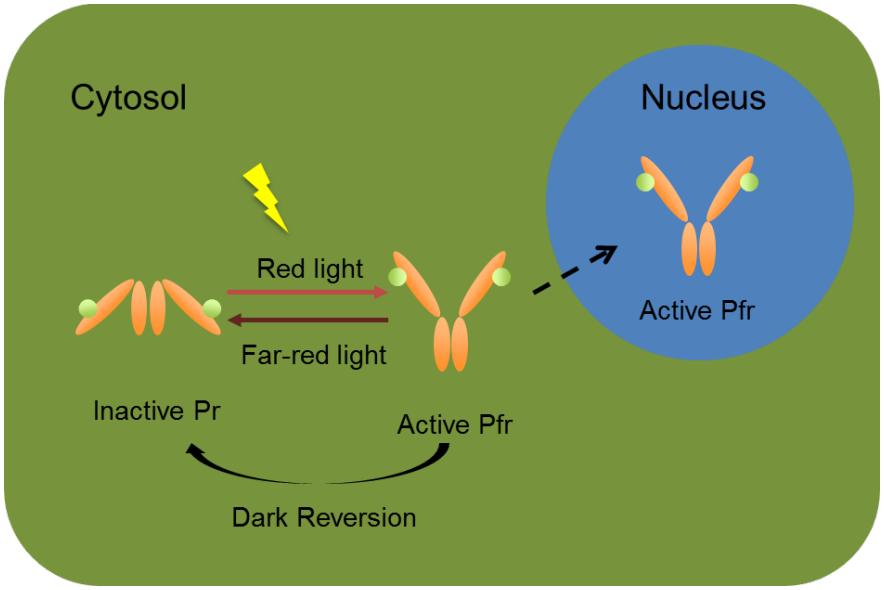

Figure 1.3 Phytochrome model as a 'photoswitch'.

Simplified illustration of activation and inactivation of phytochromes by red/far-red light induced protein conformational change.

The photoreversible switch by R and FR described above was only observed in low-fluence responses (LFR), where phyB is the dominant phytochrome (Tepperman et al., 2004; Halliday et al., 1994). As a result, a mathematical model has been proposed based on phyB protein dynamics and plant physiology (Rausenberger et al., 2010). phyD and phyE were also found to work in a similar way, sharing redundant functions with relatively minor effects (Devlin et al., 1999; Franklin, 2003). Also as a weak red light sensor, phyC was found to have a significant role in co-activating other photoreceptors (Franklin et al., 2003). While phyB and other light stable phytochromes act in LFR, phyA is light labile (Bae and Choi, 2008) and has been found to work in very-low-fluence responses (VLFR) and high-irradiance responses (HIR) (Casal et al., 1998; Rausenberger et al., 2011). PhyA is therefore responsible for a vast of growth and development processes in those conditions, including seed germination (Botto et al., 1996), seedling de-etiolation (Shinomura et al., 2000) and reproductive transition (Lin, 2000). Very recently, phyA was reported to partially work through intercellular signaling in regulating high irradiance responses to far-red light (Kirchenbauer et al., 2016).

Phytochrome Signalling Networks

Phytochrome Regulation in Nucleus

After being transported into the nucleus as active dimers, phytochromes continue to transduce environmental light signals through transcriptional regulation of hundreds of gene that are responsible for downstream physiological responses (Jiao et al., 2007). Phytochromes control light signalling transcriptional networks partly by repressing several negative regulatory proteins in the nucleus. In particular, the PIF family of phytochrome interacting transcription factors and an E3 ligase Constitutively Photomorphogenic (COP1) are the main two inhibitory regulators of light responses, such as seedling photomorphogenesis (Li et al., 2011; Xu et al., 2015).

PIFs are a small group of basic helix-loop-helix (bHLH) transcription factors that were found important for seedling etiolation (Toledo-Ortiz et al., 2003). Dark-grown Arabidopsis quadruple *pifq* mutant (*pif1 pif3 pif4 pif5*) has short hypocotyl and open cotyledons that resemble WT seedlings in light (Leivar and Quail, 2011). In addition, PIFs also work as a hub for integration of environmental (light and temperature) and internal (clock, hormone and sugars) signals to regulate various responses, including photomophogenesis and stem elongation growth (Figure 1.4 and Leivar and Monte, 2014). Phytochromes were reported to phosphorylate (Shin et al., 2016) and degrade PIFs via the 26S proteasome (Duek and Fankhauser, 2005; Leivar and Quail, 2011). Interestingly, PIFs also negatively regulate phyB abundance in the nucleus by enhancing COP1/phyB interaction to promote degradation (Figure 1.4 and Jang et al., 2010). Phytochromes also physically interact with PIFs, sequestering them from their target DNA promoters to stop gene regulation (Park et al., 2012). By repressing both

abundance and activity of PIFs, phytochromes can transduce light signal to gene transcription efficiently.

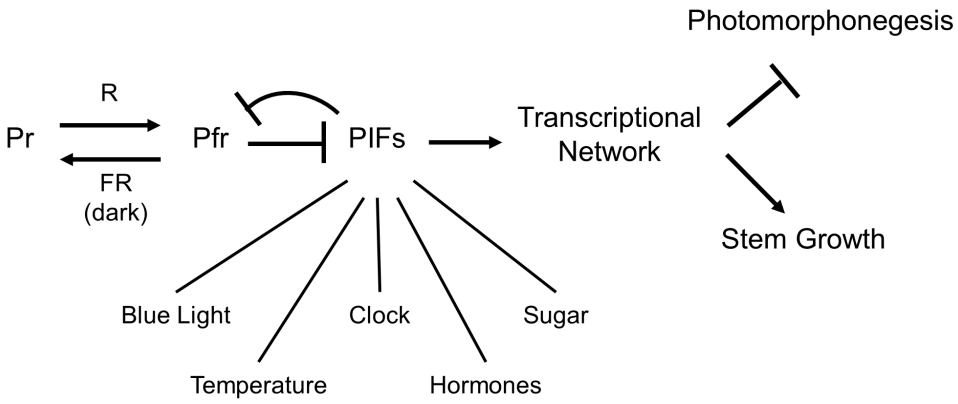

Figure 1.4 PIFs act as a hub in integrating internal and external signals to regulate photomorphogenesis and stem elongation growth.

Adapted and reproduced from (Leivar and Monte, The Plant Cell, 2014).

As an E3 ligase, COP1 represses photomophogenesis in dark by targeting several positive regulators of light responses for degradation, including ELONGATED HYPOCOTYL 5 (HY5), HY5-HOMOLOG (HYH) (Holm et al., 2002), LONG HYPOCOTYL IN FAR-RED (HFR1), LONG AFTER FAR-RED LIGHT 1 (LAF1) (Xu et al., 2015; Li et al., 2011). Arabidopsis *cop1* mutant also develops a light-grown phenotype in darkness (Deng et al., 1991). Activated phytochromes in the nucleus directly interact with SUPPRESSOR OF PHYTOCHROME A 1 (SPA1) and quickly dissociate COP1-SPA1 complex (Lu et al., 2015; Sheerin et al., 2015). In addition, COP1 was also found gradually migrating from nucleus to cytoplasm upon light stimulation (Subramanian et al., 2004; Pacin et al., 2014). Both contribute to an

inactivation of COP1 in the nucleus, stabilising the positive transcription factors for light induced photomophogenesis.

Phytochrome Regulation in Cytoplasm

Phytochromes are synthesized as inactive form in cytoplasm, only being translocated into nucleus when activated by red light. Active phytochromes regulate gene transcription in nucleus, leading to various physiological responses as described above. In contrast, role of phytochromes, especially the active Pfr form, in cytoplasm remains largely unknown. A family of cytoplasmic-specific proteins, phytochrome kinase substrate 1 (PKS1), was reported to be bound and phosphorylated by phyA and phyB (Fankhauser et al., 1999). Years later, (Paik et al., 2012) reported that besides transcriptional repression in the nucleus, Pfrs also directly inhibit the mRNA translation of protochlorophyllide reductase (PORA) in cytosol. This dual regulation enables phytochromes to respond quickly to light stimuli, helping seedlings to complete the dark to light development transition in a short time. Phytochrome cytoplasmic signaling in other plant species was also reviewed in (Hughes, 2012; Ermert et al., 2016).

Seedling Hypocotyl: A Model System for Phytochrome Study

Even though phytochromes control plant physiology through the entire life cycle, most of the signaling research has been conducted in Arabidopsis seedlings (Li et al., 2011; Chen and Chory, 2011). In particular, seedling hypocotyl response regulated by phyB through PIFs has often been used to identify potential light signaling components (Reed et al., 1998). This simple system provides a phenotype easy to measure within a short amount of time, and has contributed significantly to the current understanding of the molecular network downstream of light signaling (Leivar and Monte, 2014). Tools and softwares have been developed to monitor the hypocotyl elongation, enabling the investigation into signaling dynamics in great detail (Cole et al., 2011).

Seedling hypocotyl response also provides a biological system for mathematical modeling. These models have been developed to describe the molecular mechanism of phytochrome signaling pathway, which in turn help to promote our understanding by suggesting potential unknown candidates (Johansson et al., 2014; Rausenberger et al., 2010, 2011). A recent observation from Halliday lab reported that while the hypocotyl elongation is repressed by increasing fluence rate in cool conditions (17°C and 22°C), it is surprisingly promoted at 27°C as light increases from about 1 $\mu mol \cdot m^{-2} \cdot s^{-1}$ (Johansson et al., 2014). Modelling was used in this study as an essential tool in deciphering how a change in temperature could reverse the role of light in controlling seedling hypocotyl cell expansion. The temperature switch hypothesis was then validated with experimentation results supporting HY5 as part of the 'X' regulatory component proposed by the model.

Shade Response Regulated by Phytochromes

The proportion of active and inactive phytochromes is determined by both dark reversion rate and the R:FR ratio in the environment (Rausenberger et al., 2010). Due to this specific wavelength sensitivity, phytochromes ideally function as a detector of vegetative neighbourhoods (see Figure 1.5 A-B for comparison of the world seen by human being's eyes and that perceived by plants through phytochromes). While there is almost equal amount (1.2:1) of R and FR light in the natural sunlight, most of R light is absorbed by photosynthetic pigments, leaving a greater percentage of FR light under the vegetative canopy (Ruberti et al., 2012). This reduced R:FR light ratio (down to 0.05) leads to a promotion in phytochrome deactivation, informing plants of the neighbour density, triggering a series of shade avoidance responses (Ballaré, 1999; Smith and Whitelam, 1997). In laboratories, shade is often mimicked by reducing R: FR ratio of light in growth facilities. Also, end-of-day FR treatment can be used to quickly deactivate light stable phytochromes before night falls (Franklin and Whitelam, 2005).

Table 1.1 has listed the major shade responses in plant growth and development, from delayed seed germination (Borthwick et al., 1952), retarded leaf development to early flowering transition (Smith and Whitelam, 1997). In particular, shade induced elongation growth is probably the most dramatic phenotype (Figure 1.5 C), which appears to be a competitive strategy of plants for limited light. A set of phytochrome regulated transcription factors, PIF4 and 5, are reported to control shade induced elongation growth (Lorrain et al., 2008). While elongation is promoted in petioles by shade, leaf blade expansion is inhibited (Figure 1.5 C and Kozuka et al., 2005). In

addition, radish, as a root vegetable, produces dramatically reduced 'yield' when grown in shade (Figure 1.5 C Radish). This was supported by an earlier study that reported a shade induced reduction in dry biomass, leaf area and net assimilation rate in *Rumex obtusifolius* (Mclaren and Smith, 1978). These together indicate a possible phytochrome dependent carbon re-allocation from leaf/storage organ to petiole favouring elongation growth in shade.

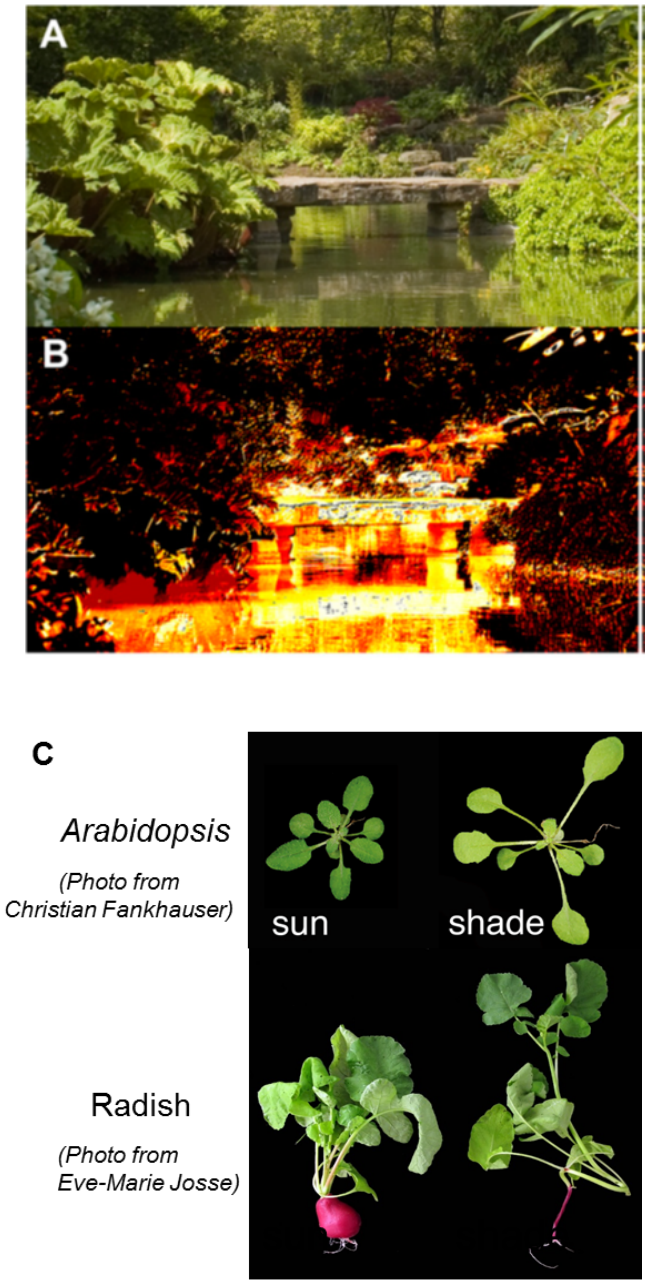

Figure 1.5 Plants use phytochromes to detect the neighbouring vegetation and respond in growth alteration accordingly.

Photo (A) shows the world perceived by humans; (B) represents the same world pictured by plant based on phytochromes. Bright colours show areas with high R:FR, typically the stone bridge and water surface where sunlight was reflected; Dark areas suggest low R:FR, indicating the density of vegetation which absorbs R and largely reflect FR. Reproduced from (Devlin, PNAS, 2016) with original photos taken by James Gillies. (C) Arabidopsis and radish grown in direct sunlight and shade conditions. Both plants show elongated stem and reduced leave size when grown in shade. Photos are reproduced as indicated.

Table 1.1 Shade avoidance syndromes.

Adapted from (Smith and Whitelam, Plant Cell and Environment, 1997).

Physiological process	Response to shade (reduced R:FR ratio)
Germination	**Retarded (delayed)**
Extension Growth	**Accelerated**
Internode extension	Rapidly increased
Petiole extension	Rapidly increased
Leaf extension	Increased in cereals
Leaf development	**Retarded**
Leaf area growth	Marginally reduced
Leaf thickness	Reduced
Chloroplast development	**Retarded**
Chlorophyll synthesis	Reduced
Chloeophyll a:b ratio	Balance changed
Apical dominance	**Strengthened**
Branching	Inhibited
Tillering (in cereals and grasses)	Inhibited
Flowering	**Accelerated**
Rate of flowering	Markedly increased
Seed set	Severe reduction
Fruit development	Truncated
Assimilation distribution	**Markedly change**
Storage organ deposition	Severe reduction

Arabidopsis without Phytochromes

Due to the function redundancy in signalling mediating responses, it was difficult to determine the individual role of each phytochrome, or to identity the overall role of phytochromes for plant life. Multiple mutants, especially those with all phytochromes deficient, were created to test the effect of severe depletion in phytochromes. Arabidopsis mutant without phytochromes was first generated in C*ol* background, where a *ft* mutation was also introduced to promote germination rate (Strasser et al., 2010). Later, another *phyABCDE* mutant in L*er* background was reported in (Hu et al., 2013), together with several other high order phytochrome mutants such as *phyABDE*. These later created alleles have *FT*, and show much earlier onset of flowering compared to WT. Both *phyABCDE* mutants are largely dependent on sufficient light illumination to survive, supporting the vital role of phytochromes in plant life cycle. In Arabidopsis, chlorophyll production is light dependent. The fact that phytochrome null mutants have much reduced but still detectable chlorophyll produced in red light suggests the existence of other red light receptors. Also, *phyABDE* and *phyABCDE* in L*er* background behave similarly in various phenotypes, suggesting that phyC could be non-functional in the absence of other phytochromes (Hu et al., 2013).

All these high order phytochrome mutants are dramatically elongated (Strasser et al., 2010; Hu et al., 2013), which is probably due to PIF mediated elongation growth without phytochrome repression. More interestingly, these mutants were also reported to have retarded grow rate. When grown in 8-h photoperiod, *phyABDE* showed delayed flowering at 16°C compared to the standard 22°C, enabling more

rosette leaves to be produced during vegetative stage. However, even in this condition, the mutant still has a significantly reduced leaf production rate compared to L*er* WT (Halliday et al., 2003), suggesting an underlying control of vegetative growth by phytochromes. In this project, I mainly use L*er* background *phyABDE* to explore the phytochrome impact on growth, biomass and metabolism. An intermediate mutant, *phyBD*, is also included in most tests for comparison.

1.3 Sugar Regulation of Plant Growth and Interaction with Phytochromes

Sugar Mediated Growth Regulation in Arabidopsis

Plant growth largely depends on the carbohydrate availability generated through photosynthesis, which is constantly challenged by various factors in the changing environment, such as light, temperature, water, nutrient and pathogens (Kangasjärvi et al., 2012). Energy stress can be induced in unfavourable conditions, leading to severe growth retardation. Luckily, plants have obtained multiple strategies through evolution to mediate growth by coordinating carbon allocation and sugar signalling.

As photosynthetic products, sugars can only be produced during the day with enough PAR, yet is still in great need at night to maintain respiration and growth. To cope with this situation, plants store part of the synthesized carbon in the form of starch during the day, and break it down into soluble sugars for nocturnal use (Stitt et al., 2010). Diurnal changes of leaf starch was found to be adjusted accordingly in different photoperiods (Lee et al., 2010), demonstrating the ability to predict the length of the coming night and calculate the proper carbon depletion rate (Smith and Stitt, 2007; Scialdone et al., 2013). Even when grown in very short day lengths, plants were still able to survive by adjusting growth, starch, protein and central metabolism (Gibon et al., 2009, 2004). More amazingly, upon an unexpected early onset of night, Arabidopsis starch degradation could be adjusted immediately to ensure depletion just before the subjective morning. However, this regulation no longer holds when plants were grown in abnormal day lengths such as 28h or 17h, indicating an internal circadian control of starch degradation (Graf et al., 2010).

Leaf starch is usually depleted at the end of night; therefore, carbon starvation can be experimentally induced by an extended night period (Lastdrager et al., 2014). Like energy stress induced in other situations, low carbon level is sensed by T6P-SnRK1 (KIN10 and KIN11) signalling, which triggers a series of transcriptional regulation to repress growth, only allowing basic life maintenance (Nunes et al., 2013; Baena-González et al., 2007). In particular, SnRK1 activates bZIP transcription factors that control a number of target genes involved in amino acid metabolism. More interestingly, resumed sucrose level not only inactivates SnRK1 and subsequent bZIPs, but also represses the translation of a subset of bZIP proteins (Rahmani et al., 2009; Hanson and Smeekens, 2009). While SnRK1 works mainly in low carbon situations, Target of Rapamycin (TOR) signalling was considered an important regulator to link high sugar availability into various growth processes (Lastdrager et al., 2014). Repression of TOR results in defects in cell expansion, seed yield, ABA regulated osmotic stress response and protein translation (Deprost et al., 2007).

Apart from energy status detection, sugars also provide signals to regulate plant growth and development. Hexokinase was identified as a sugar sensor decades ago (Jyan-Chyun et al., 1997). A hexokinase mutant, *gin2*, was first found insensitive to high glucose induced seed germination repression (Moore, 2003). Following mutant analysis demonstrated a role of HXK1 in growth regulation irrespective of its enzyme activity, supporting glucose to work as a signalling molecule (Cho et al., 2006). More recently, sucrose were reported to speed up plant life cycle, promoting early juvenile-to-adult phase transition by repressing miRNA156 expression (glucose shares this function but in a different mechanism) (Yang et al., 2013; Yu et al., 2013; PROVENIERS, 2013). T6P has been recognized as a central signalling molecule in

regulating plant growth and development (Schluepmann et al., 2011), and was also recently found to control onset of flowering (Wahl et al., 2013).

Sugar regulation of growth largely interacts with multiple phytohormones (León, 2003; Das et al., 2012) and circadian clock (Stitt and Zeeman, 2012; Moghaddam and Ende, 2013; Lastdrager et al., 2014), both of which were also reported to closely connected to light signalling (Fankhauser and Staiger, 2002; Lucas and Prat, 2014). As a result, sugars are very likely to crosstalk with light signalling in plant growth control as well.

Phytochromes affect sugar metabolism partly through photosynthesis regulation

Phytochrome mutant seedlings have been reported to have substantially reduced chlorophyll compared to WT upon red light stimulation (Strasser et al., 2010; Hu et al., 2013; Ghassemian et al., 2006). By re-analyzing the microarray data from (Hu et al., 2013), I found high percentage of light reaction genes are repressed in *phyABCDE* seedlings grown in constant red light, compared to WT (Figure 1.6). Among these genes, at least one third own G boxes in their promoter region, suggesting that they could be the target genes of light signaling components, e.g. PIFs or HY5 (Jiao et al., 2005; Hudson and Quail, 2003). Supporting these results, PIF3 has been found to repress chlorophyll biosynthetic and photosynthetic genes in etiolated seedlings associated with HDA15 (Liu et al., 2013). As a result, the reduced growth in phytochrome deficient mutants could be at least partly due to the impaired plant photosynthesis and subsequent production of carbohydrates.

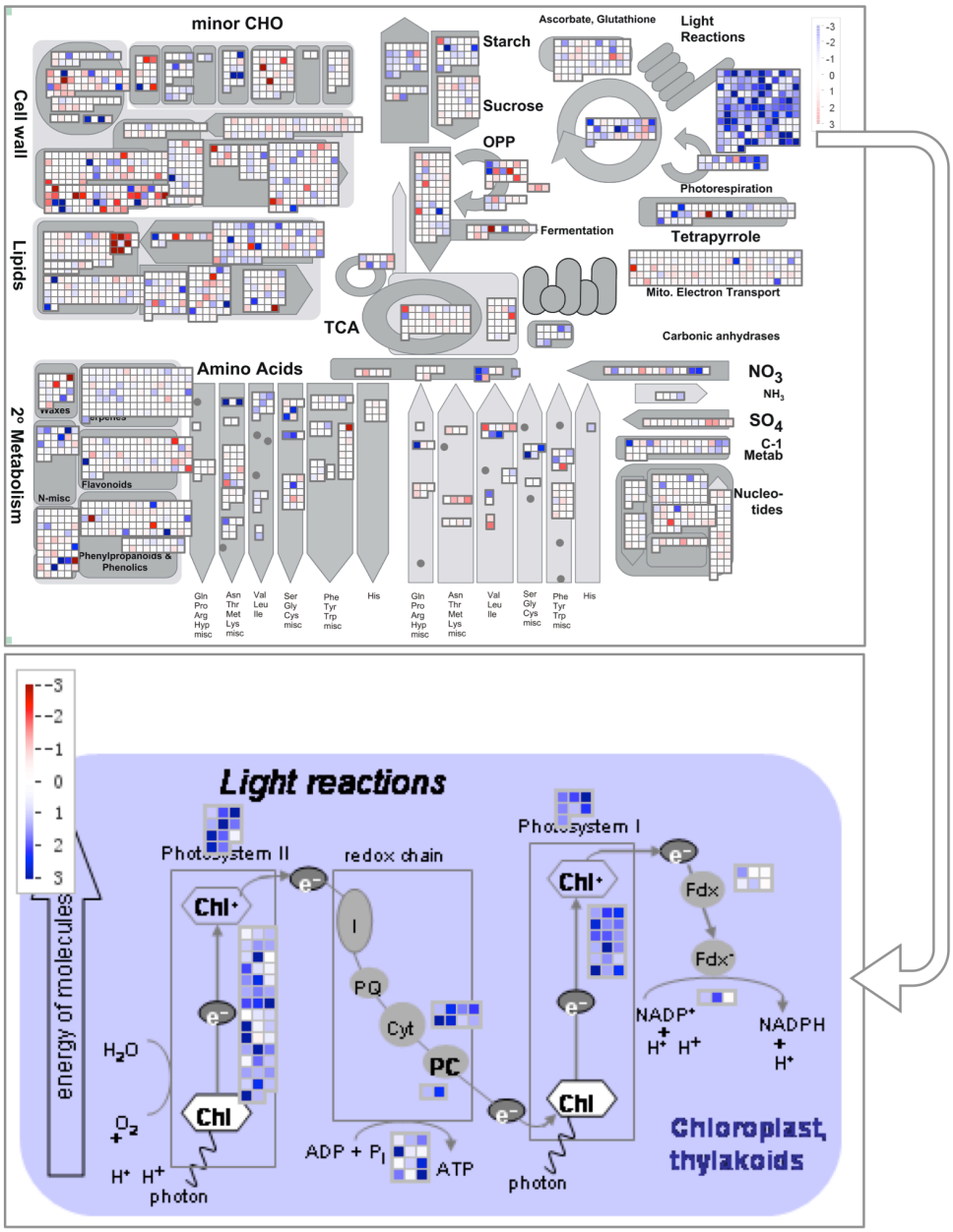

Figure 1.6 Microarray analysis shows large numbers of photosynthetic genes repressed in phytochrome null seedlings.

Samples were from 4-day-old seedlings of *phyABCDE* and L*er* grown in 50μmol·m^{-2}sec^{-1}constant red light. Microarray raw data was provided by published paper (Hu et al., PNAS, 2013). Pathway maps were generated by mapman after data analysis with GEO2R online. Log transformation was used to show the fold changes. (Blue dots in the map indicate down-regulated genes in the mutant compared to WT, red dots stand for genes promoted in the absence of all phytochromes, white or light color means this gene has similar expressions in both genotypes in this condition- difference less than two-fold change.)

Crosstalk between sucrose and phytochrome signalling

Apart from regulating chlorophyll biosynthesis and the amount of carbohydrates produced through photosynthesis, phytochromes have also been reported to interact with sucrose in controlling plant growth, especially in seedlings. An earlier study found that sucrose in the growth medium could repress the transient induction of plastocyanin gene during seedling development (Dijkwel et al., 1996). In addition, phyA mediated far-red light high-irradiance responses, including seedling cotyledon opening, inhibition of hypocotyl elongation and block of greening, were also repressed by sucrose (Dijkwel et al., 1997). Following that, (Short, 1999) reported the previously observed dominant negative phenotype in phyB overexpression seedlings grown in FR was dependent on the availability of specifically metabolizable sugars in the medium. Furthermore, sucrose was also found necessary for COP1 degradation of phyA in etiolated seedlings (Debrieux et al., 2013), adding to the evidence of sucrose crosstalk with phytochrome signaling pathways.

More recently, a series of publications reported the interaction between sucrose and PIFs in regulating seedling hypocotyl elongation (Liu et al., 2011; Stewart et al., 2011; Lilley et al., 2012; Sairanen et al., 2012). While sucrose promotes seedling hypocotyl elongation in WT, this response is eliminated in *pif* mutants (Liu et al., 2011; Stewart et al., 2011). In addition, overexpression of PIF5 results in increased hypocotyl length than WT in the absence of sucrose, and a further enhanced promotion response to exogenous sucrose application. Furthermore, sucrose was also found to increase PIF5 protein abundance (Stewart et al., 2011), supporting PIFs to be the essential regulator of sucrose promoted hypocotyl growth. Following studies

revealed the link between sugars, PIFs and auxin homeostasis, proposing an endogenous carbon-sensing pathway that promotes PIF dependent hypocotyl elongation through auxin biosynthesis and transportation (Sairanen et al., 2012; Lilley et al., 2012).

So far, the majority of phytochrome-sugar research has been conducted in seedlings, and it would be interesting to explore the crosstalk further using more developed plants, to see how light signaling and sugar interacts to regulate plant biomass.

1.4 Phytochrome Signalling in Dark Responses

Dark induced senescence

Apart from carbon starvation described above, environmental dark stress can also induce premature leaf senescence. Similar to developmental senescence, plant dark senescence also involves chlorophyll loss, protein/nucleic degradation and remobilization of nutrients (Lim et al., 2007). In particular, leaf bleaching, or the loss of greening, is the visually most dramatic phenotype in senescence response caused by chlorophyll breakdown (Hörtensteiner, 2006).

Dark induced senescence also triggers dramatic transcriptional reprogramming in plants. A large number of senescence-associated genes (SAGs), involved in processes like cellular components breakdown and hormone signalling, have been identified through microarray analysis (Buchanan-Wollaston et al., 2003; Lim et al., 2007). Due to the quick accumulation upon senescence induction, SAGs are often regarded as senescence markers. Another set of genes, which is repressed during senescence, was termed senescence down-regulated genes (SDGs), including the chlorophyll a/b binding protein (*CAB*) and the Rubisco small subunit gene (*SSU*), leading to a repression of photosynthesis (Gan and Amasino, 1997). In addition, a group of transcription factors were specifically identified in senescence regulated genes (senTFs), either promoted or repressed (Balazadeh et al., 2008; Lim et al., 2007). These senTFs controls expression of massive downstream SAGs, and are similarly regulated in developmental and stress induced senescence. For instance, *ORE1* (or *NAC2*) and *AtNAP* were found to be main senescence-promoting NAC transcription factors (Kim et al., 2009; Guo and Gan, 2006). Despite the commonly

induced genes in developmental and dark induced senescence, a transcriptome comparison assay also revealed a significant distinction in enhanced gene profiles between these two types of senescence (Buchanan-Wollaston et al., 2005), suggesting the responses are partially overlapping yet still different.

Phytohormones are extensively involved in senescence response (Lim et al., 2007). In addition to fruit ripening, ethylene has also long been known to promote leaf senescence (Grbic et al., 1995). Mutants with impaired ethylene signalling pathways, such as *ethylene-resistant1* (*etr1*), *ethylene-insensitive2* (*ein2*) and *ethylene-insensitive3* (*ein3*) *ein3-like* (*eil1*) double mutant, have significantly delayed senescence (Grbic et al., 1995; Oh et al., 1997; Li et al., 2013). In particular, EIN3 was identified as an senTF, acting downstream of another senTF EIN2, to repress expression of *microRNA164* that negatively regulates *ORE1* (Li et al., 2013; Kim et al., 2009). ABA also controls plant development especially aging and senescence. Similar to ethylene, ABA application induces senescence and SAGs (Lim et al., 2007), while ABA insensitive mutants have delayed senescence (Lee et al., 2011; Zhang et al., 2012). Very recently, Arabidopsis Late Embryogenesis Abundant (LEA) protein ABR (ABA-response protein), negatively regulated by ABI5, was found to delay dark induced leaf senescence (Su et al., 2016).

Phytochrome Regulation of Dark Induced Senescence

Phytochromes have been linked to dark induced senescence for decades. Dating back to 1971, a study on *Marchantia* reported that dark-induced chlorophyll loss could be inhibited by 5-min red light pulse per day, which can be reversed by 10-min irradiation of far-red that induces leaf bleaching (De Greef et al., 1971). Similar experiments were also reported in various other species, including barley, cucumber, tomato, mustard, etc. (Biswal and Biswal, 1984). These observations supported a role of phytochromes in regulating dark induced responses, especially chlorophyll degradation. Specifically, phytochrome activation leads to delayed leaf senescence in darkness.

Unexpectedly, however, a later study reported phytochrome mutants to be hyposensitive to dark induced chlorophyll loss. While Ws WT grown in short-day photoperiods for 6 weeks has significantly reduced chlorophyll after 6-day dark incubation, leaves of *phyB-10* and *phyA-5-phyB-10* mutants maintained similar chlorophyll level during the dark incubation (Brouwer et al., 2014). Ws WT has significantly more chlorophyll than that in both phytochrome mutants under normal growth conditions, yet after 6-day dark treatment Ws chlorophyll is reduced to the mutant level. In contrast, *phyA* mutant was shown to have increased chlorophyll reduction than WT in partial shade, but not in dark (Brouwer et al., 2012, 2014). These studies pointed out a role for phyB, but not phyA, in dark induced chlorophyll loss, and that the loss of phyB eliminates dark effect on chlorophyll level.

More recently, during the course of my thesis work, a series of studies were published, supporting the observations from original R/FR pulse experiments. Again,

phytochromes are considered as negative regulators of dark induced senescence. (Sakuraba et al., 2014) proposed an underlying molecular feed-forward loop, where PIF4 and PIF5 activate the transcription of *EIN3, ABI5* and *EEL* genes involved ethylene and abscisic acid signalling; these protein in turn, together with PIF4 and PIF5, directly activate the expression of *ORE1* to promote leaf senescence. Phytochromes, especially phyB, are considered to suppress senescence by negatively regulate PIFs. In addition, mutant analysis showed *phyB* was hypersensitive to dark stress relative to C*ol* WT, including more chlorophyll loss, ion leakage and induction of senescence marker genes (*SEN4* and *SAG12*) (Sakuraba et al., 2014). In addition, mutation or overexpression of PIF4 or 5 genes leads to delayed and accelerated dark senescence, respectively. This was observed in both physiological and molecular levels (Song et al., 2014; Zhang et al., 2015). Another study using rice phytochrome mutants confirmed the similar dark response regulated through phytochromes (Piao et al., 2015).

These recent studies have greatly improved our current understanding of the molecular mechanism underlying phytochrome regulation of dark induced senescence. Nevertheless, it is incapable of explaining the previous contradictory observation of dark induced chlorophyll loss in Ws lines as shown in (Brouwer et al., 2014). This demonstrates the complexity of dark response in plants, highlighting a possible gap in our current knowledge that remains to be understood.

1.5 Thesis Overview

Objectives of Study

Light regulation of plant growth has been established through photosynthesis and photoreceptors, yet how photoreceptors control vegetative biomass production in adult plants remains mysterious. In addition, the interaction between phytochrome signalling and metabolic sugars has been reported in seedling growth, but the underlying mechanism is unclear especially in adult plants. Finally, phytochromes were found to regulate dark induced plant growth retardation and senescence in adult plants, the mechanism of which needs further exploration. Therefore, my PhD project aimed to achieve the following objectives:

1. To explore the effect of phytochromes on plant biomass accumulation by studying phytochrome multiple mutants;

2. To reveal metabolic alteration induced by phytochrome deficiency as an indirect way to control plant biomass production;

3. To test and compare dark induced responses in both WT and phytochrome multiple mutants.

Chapter Layout

This thesis documents my PhD research work on exploring how phytochromes control growth, metabolism and stress responses in *Arabidopsis thaliana*. Chapter 1 presents a literature review on the dual roles of light in plant life focusing on phytochrome regulation of seedling hypocotyl elongation and shade response, followed by studies on phytochrome-sugar interaction. Previous observations on phytochrome involvement in dark senescence are also introduced. Chapter 2 describes all plant materials, and experimental protocols used in this project. After that, Chapter 3 focuses on how the light activated signaling pathways manipulate plant carbon resources to control biomass production. Despite of reduced biomass and repressed photosynthesis, phytochrome mutants have elevated levels of starch and sugar. This is suggested to link to the altered diurnal growth pattern, proposing a role of light activated phychromes in allocating carbohydrates into growth during daytime. The interaction between phytochrome and metabolism was further explored in Chapter 4 by assessing metabolome using GC-MS analysis. A stress like metabolic signature was identified in phytochrome mutants, which possibly underlies the reduced sensitivity to biomass repression induced by abiotic stressors like NaCl and ABA. Here phytochromes are further proposed to switch plant metabolic condition between growth-promoting and stress-priming statuses. Chapter 5 presents some preliminary tests on phytochromes mutant response to long-term darkness. The results suggest a potential re-assessment of the current knowledge by considering allele effect. Finally, general discussions were made in Chapter 6, highlighting the various questions raised from the project with perspectives of possible future work, and a brief conclusion of the findings and significance of research in this thesis.

Chapter 2- Experimental Procedures

2.1 Plant Material

Arabidopsis thaliana wild-type and mutants used in this experiment were listed as follows: Landsberg *erecta* (L*er*) and L*er* background *phyB-5* (Reed et al., 1993), *phyBD* (Devlin et al., 1999), *phyABD* (Devlin et al., 1999), *phyABDE* (Franklin, 2003) and *phyABCDE* (Hu et al., 2013); Columbia-0 (C*ol-0*) and C*ol*-0 background *phyB-9* (Reed et al., 1993), *PHYB-OX* (Kircher et al., 2002).

2.2 Growth Conditions

In all experiments, seeds were collected in a 1.5ml Eppendorf (EP) tube and sterilised by shaking in 8% commercial bleach and 1% Tween20 solution for 10 minutes. The sterilising solution was removed with a pipette and rinsed four times with distilled water. After the final wash, 0.1% autoclaved agar solution was added to suspend the seeds. The seeds were then spread on petri dishes with half strength MS-agar medium (MURASHIGE & SKOOG MEDIUM, Duchefa Biochemies; 1.2% agar; PH 5.8) and stratified at 4˚C in darkness for 3 days.

For most of adult plant studies in Chapter 3, 4 and 5, seeds on medium were moved to Binder cabinet with diurnal (8h light: 16h dark) white light (100 $\mu mol \cdot m^{-2} \cdot s^{-1}$) at

18°C to induce germination and early seedling development. Two weeks later, seedlings of the average size were transferred to soil (Levington seed and modular compost, plus sand) trays in growth room maintained at 18°C with 12h light: 12h dark photoperiods for several weeks based on experimental requirements. There light was provided by Polylux XLR 835 (GE Lighting triphosphor white fluorescent tubes) at 100 μmol $m^{-2}s^{-1}$ (except fluence rate experiments where light level is specified in the according chapter).

In Chapter 3, for shoot/root sugar quantification experiment, plants were grown in the same condition except that they were transferred to new medium plates instead of soil, for root sample collection.

For stress assays in Chapter 4, adult plants were grown in the above condition to four-week-old, watered once with ABA/NaCl solution to soil capacity followed by normal irrigation procedure every other day. Data was collected two weeks after the treatment. Alternatively, seedlings were grown in medium plates under 12h light (100 μmol $m^{-2}s^{-1}$): 12h dark photoperiod at 18°C for 11 days, then transferred to growth medium with different doses of salt (NaCl)/ABA for further 10 days.

In Chapter 5, 5-week plants were transferred to dark cabinets for about 2 weeks, then back to previous condition for observation. Alternatively, plants were grown in continuous light for a week, transferred to long day photoperiod (16h light: 8h dark) till 3-week-old, then treated with darkness for 5 days before sampling; in this case temperature was set to 23°C to match the published data.

2.3 Fresh and Dry Biomass Quantification

Whole plant rosettes (aboveground part for soil-grown plants and whole seeding for medium-grown plants except for shoot/root-specific quantification in Chapter 3) were harvested and immediately weighed using a precision balance before dehydrated. After this, plant materials were wrapped in aluminium foil, dried in an oven at 80°C for 4 days before being weighed again to obtain dry biomass data.

2.4 Chlorophyll Content Measurement

Plant rosettes were harvested in liquid nitrogen (LN) and ground into fine powder while frozen. Approximately 20mg of sample powder was weighed and mixed with 1ml of 80% acetone (cooled in ice) by shaking on the vortex. The mixture was then kept in darkness at 4°C overnight for extraction. After centrifuging (14000 rpm for 10 min) the supernatant is used to measure OD values at wavelengths of 645nm and 663nm with a spectrometer (use 80% acetone as blank). Chlorophyll content (per fresh weight of plant tissue) was calculated using the following equation (Ni et al., 2009):

Chlorophyll a (mg/g) = $(12.7*OD_{663nm}-2.69*OD_{645nm})*V/ (1000*FW)$

Chlorophyll b (mg/g) = $(22.9*OD_{645nm}-4.86*OD_{663nm})*V/ (1000*FW)$

Total Chlorophyll (mg/g) = Chlorophyll a + Chlorophyll b, where

V = volume of the extract (ml), FW = extract fresh weight of sample powder used for extraction (g). Samples were diluted if OD_{663nm} exceeds 1 and the calculation was adjusted accordingly.

2.5 Gas Exchange Measurement

For gas exchange measurement, I used a customized chamber connected to the EGM-4 (PP Systems, US) (equipment demonstration see Figure 2.1, protocol adapted from (Chew et al., 2014)). Each time a pot of plant(s) was placed inside the chamber, where the CO_2 level was recorded every 4.6 seconds for about one minute. CO_2 exchange was measured in parts per million (ppm). Flux was calculated per unit area (m^2) and results expressed relative to WT in light.

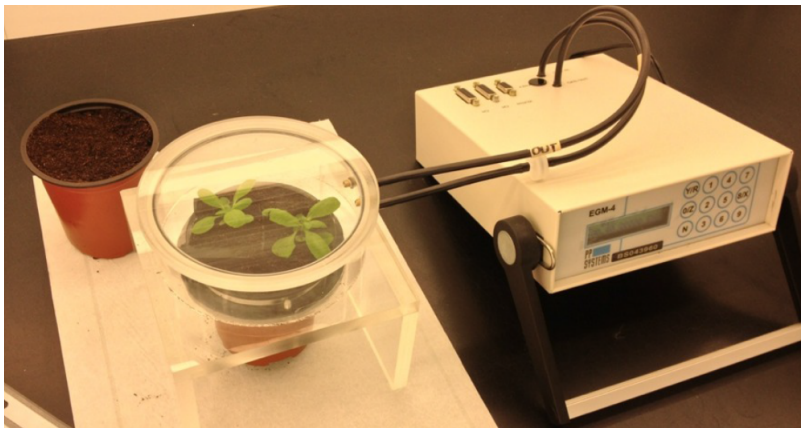

Figure 2.1 Photo illustration of gas exchange measurement system.

A customized chamber connected to a commercially purchased gas analyser used in this study.

2.6 Sugar and Starch Quantification

Plant tissue (rosettes or roots) were harvested into LN and finely ground. About 20 mg powder was weighed into a clean EP tube for extraction. Soluble sugars were extracted three times using ethanol of 80%, 80% and 50% concentration respectively. Each time sample was briefly shaken on a vortex, incubated in 80°C heating block for 20 min, spun in a centrifuge at the speed of 14000 rpm for 5 min and the

supernatant was collected into an EP tube kept on ice. All the supernatants were combined together for soluble sugar quantification.

The determination mix was prepared using 15.5 ml buffer (HEPES/KOH 0.1 M, $MgCl_2$ 3 mM, pH 7.0), 480 µl ATP (60 mg/ml), 480 µl NADP (36 mg/ml) and 80 µl G6PDH. Then 40 µl ethanoic soluble sugar extract and 160 µl mix were combined and measured using a plate reader. OD values were read at 340 nm once stabilized after adding the following enzymes in order: Hexokinase, Phosphoglucose isomerase and Invertase. Glucose, fructose and sucrose levels are then calculated from the OD change and normalized to material fresh weight.

The pellet used for starch quantification was re-suspended in 0.1 M NaOH by vigorous shake and 30 min 95°C incubation. Following PH neutralization by adding a mix of 0.5M HCl and 0.1M acetate/NaOH (PH 4.9), starch was hydrolyzed using a starch degradation mix (amyloglucosidase, amylase in acetate buffer) with overnight incubation at 37°C. Starch breakdown product, glucose, was measured the same way as soluble sugar measurement.

This protocol was adapted from Mark Stitt's lab as described in (Hendriks, 2003).

2.7 Iodine Staining

For starch qualitative assay (iodine staining), plant rosettes were harvested at the end of light period and immersed in 96% ethanol until leaves were fully de-colourized. Plant materials were then washed briefly in water before stained by Lugol's iodine solution (SIGMA) for 5 min and de-stained in water for 1-2h until colour difference

between WT and phytochrome mutants was shown. For every assay, all plants were stained and de-stained in the identical condition.

2.8 Total Protein Quantification

Plant tissue was harvested and ground into fine powder in LN and protein was extracted using homogenization buffer [recipe: 0.0625M Tris-HCl (pH 6.8), 1% (w/v) Sodium dodecyl sulphate (SDS), 10% (v/v) Glycerine (Glycerol), 0.01% (v/v) 2-Mercaptoethanol, from (Lee et al., 2012)]. Samples were incubated in heating blocks at 65°C for 10min before centrifuging at the highest speed for another 10min. Supernatant was collected into a new tube and protein was quantified using Pierce BCA kit according to manufacturer's instruction. A series dilution of 2000 µg/ml BSA protein sample was prepared to generate the standard curve used for sample calculation. Data was normalized to sample fresh weight used for each individual extraction.

2.9 Growth Measurement

For rosette expansion measurement, plants were grown in soil trays to 3-week-old and images were taken from top using a digital camera within half an hour after lights-on (i.e. 9 AM) or before lights-off (i.e. 9 PM), for a continuous week period. Photos were processed in Adobe Photoshop to achieve optimal contrast for distinguishing plant rosette from soil background. Whole rosette area of each individual plant from every time point was then measured using ImageJ software (NIHimage, http://www.rsb.info.nih.gov/nih-image/). The percentage of relative expansion rate for day and night is calculated by setting the starting area at 100 (e.g.

9 AM) and subtracting the area at the end point (e.g. at 9 PM) and expressed as a percentage of that of the starting point.

It might be worth mentioning that considering the overlap of rosette leaves, PRA will differ from the total area of dissected leaves (Vanhaeren et al., 2015). However, it is a non-invasive measurement that allows us to monitor the same plants for a period of time. Choosing to observe relatively young plants from 3-week to 4-week-old also helps to avoid too much leaf overlapping.

2.10 Quantitative Real-Time PCR (qRT-PCR)

For qRT-PCR experiments, at least 3-5 plants were pooled together as one single sample, and three sample replicates were harvested into LN. Plant tissue was ground when frozen and RNA was extracted using an RNeasy Plant Mini Kit (QIAGEN) with on-column DNase digestion. cDNA synthesis was performed using SuperScript VILO cDNA Synthesis Kit (Invitrogen) as described by the manufacturer. Primers were designed using PerlPrimer software (a list of sequence details can be found in Table 2.1). The qRT-PCR was set up as 10 µl reactions (see details in Table 2.2) using SYBR Green (Roche) in a 384-well plate, performed with the Roche Lightcycler 480 system (for program setting see Table 2.3). The results were analyzed using the LightCycler 480 Software (1.5.0) and plotted in Microsoft Excel.

Table 2.1 Sequence of primers used for qRT-PCR

Gene	Locus	Primer	Sequence (5'-3')
ACT7	AT5G09810	ACT7-F	CAGTGTCTGGATCGGAGGAT
		ACT7-R	TGAACAATCGATGGACCTGA
CSLB4	AT2G32540	CSLB4-F	ACGATTTAGGAGACGATGGA
		CSLB4-R	ACCATCTCCTTAGAATTCCCA
CSLG3	AT4G23990	CSLG3-F	TAATACCTTGCTACGAGTGTCTG
		CSLG3-R	CTGGATCGTTGGAATACATATCAC
EXP1	AT1G69530	EXP1-F	CAACGCATCGCTCAATACAG
		EXP1-R	AAACCTTATTCCTCCTCTTCTCAC
XTH7	AT4G37800	XTH7-F	GATTTCCACGAATATGCCATCTC
		XTH7-R	CCTCATTGTTCTTGTAAACCCTG
FUM1	AT2G47510	FUM1-F	GTCACTTAACACAATCGCCAC
		FUM1-R	TAGTACAAGTTCACCAAGACCAC
ATCS(CSY4)	AT2G44350	CSY4-F	TGAGTGCCAGAAAGTATTACCT
		CSY4-R	TACCTTTCCAGTTAAGAGAAGCC
FUM2	AT5G50950	FUM2-F	AGAAATGTGCTGCCAAGGT
		FUM2-R	CTTTCCTTCTGCTACTTCTTGTG
ACN1	AT3G16910	ACN1-F	GGTTGGTGTTTCCCTTGGT
		ACN1-R	GAATACACTTCCTTCGCCGT
P5CS1	AT2G39800	P5CS1-F	CTATTAGCACCCGAAGAGCC
		P5CS1-R	CAGTTCCAACGCCAGTAGAG
P5CR	AT5G14800	P5CR-F	CAATGTCTTCTCCACTAGCGA
		P5CR-R	ACAGCCTTCTTAACAACTTGAG
PRODH	AT3G30775	PRODH-F	CTGCCAAATCTTTACCAACATCTC
		PRODH-R	AGATCGCTCACTCGTTTCAG
ABI1	AT4G26080	ABI1-F	AAACTGCACTTCCATTATCCGT

		ABI1-R	ACTGAATCACTTTCCCTCCTG
ABI5	AT2G36270	ABI5-F	CAGAACAATGCTCAGAACGG
		ABI5-R	CACCAAGAAATCCTCAAGTGTC
DIN1	AT4G35770	DIN1-F	GAGGACACCAGACGAATTCAG
		DIN1-R	GTTCTTAACCATTCCTGATCCGA
DIN10	AT5G20250	DIN10-F	ATGGATCGATTCTTCGTGCTC
		DIN10-R	TATCTTTAGCAAGCTGACACCA
COR15A	AT2G42540	COR15A-F	AAAGAGGCATTAGCAGATGG
		COR15A-R	TTCTTTACCCAATGTATCTGCG
RD29A	AT5G52310	RD29A-F	ATCCCACCAAAGAAGAAACTG
		RD29A-R	TCAGGAGACTCATCAGTCAC
KIN1	AT5G15960	KIN1-F	ACCAACAAGAATGCCTTCCA
		KIN1-R	CCGCATCCGATACACTCTTT

Table 2.2 10ul reaction system for qRT-PCR

Reagents	Volume/ul
2 × Mix	5
H_2O	2
Forward primer	1
Reverse primer	1
cDNA	1
Total	10

Table 2.3 qRT-PCR program setting

Program name	Target (ºC)	Acquisition mode	Hold (hh:mm:ss)	Ramp Rate (ºC/s)	cycles	Analysis Mode
Hot start	95	none	00:05:00	4.8	1	none
Amplification	95	None	00:00:10	4.8	45	quantification
	60	None	00:00:20	2.5		
	72	single	00:00:20	4.8		
Melt curve	95	None	00:00:05	4.8	1	Melting Curves
	65	None	00:01:00	2.5		
	97	Continuous	-	0.11		
Cool down	40	None	00:00:10	2	1	None

2.11 GC-MS Metabolic Assay

During my PhD project I also put together a series of procedures to measure plant metabolites: the majority of the non-targeted GC-MS protocol, including sample extraction, metabolite derivatization and separation, was adapted from (Lisec et al., 2006); methods for data pre-processing and post-analysis were combined from various resources described below.

Plant growth and sample collection: WT and phytochrome mutants (*phyBD*, *phyABDE*, *phyABCDE*) were grown to 5-week-old in previously described condition. At each individual time point (EON and EOD), 3- 5 plants were harvested and pooled together as one individual sample; 6 samples were collected for each genotype. Samples were frozen in liquid nitrogen immediately and stored at -80ºC for later extraction.

Sample Extraction: Plant sample materials were finely homogenized in liquid nitrogen; about 100mg tissue powder was transferred into a pre-cooled EP tube. After adding pre-cooled methanol, 60 µl of ribitol (0.2mg/ml) was added to each sample, which will later be used as the internal standard for relative quantification. Following procedures shown in Figure 4.1a, sample extracts were dried in a speed vacuum concentrator and then stored in bags filled with silica gel (FISHER CHEMICAL) at -80 ºC. This is to keep samples dry and cold so that metabolites could be stable for a while before being measured.

Sample derivatization and data acquisition: For GC-MS to analyse sugars with low volatilities, plant extracts need to be derivatized before the measurement. As suggested by (Lisec et al., 2006), Methoxyamine Hydrochloride (98%, SIGMA-

ALDRICH) and N-Methyl-N-(trimethylsilyl) trifluoroacetamide (MSTFA, 98.5%, SIGMA- ALDRICH) were used for sample derivatization. In addition, a series of alkanes (C7-C30 saturated alkines, 1000 µg/ml each component in hexane, SIGMA-ALDRICH) were added into each sample before measurement as internal retention time standards to support the peak identification process. A brand new column (DB-35ms, 30m, 0.25µm, 7-inch cage by Agilent Technologies; similar to MDN35, a 35%-phenyl-65%-dimethylpolysiloxane capillary column) was installed into the GC-MS machine (Scimadzu GC-MS) with parameter settings adapted from the published protocol (Lisec et al., 2006). Samples were measured in a randomized order to exclude possible technical error through time. Blank samples were included every half-day through the measurement process to ensure that no sample residue is left in the system.

Data Processing: GC-MS data file (.cdf format) was first imported into an Automated Mass spectral Deconvolution and Identification System (AMDIS, http://chemdata.nist.gov/mass-spc/amdis/downloads/), a free tool used to analyse GC-MS data files, including chromatogram deconvolution and metabolite identification. AMDIS works with a reference library (.MSL format), which contains a list of compounds together their mass spectrums and retention time information. The GOLM metabolome database (GMD) provides reference libraries particularly for plant metabolites (http://gmd.mpimp-golm.mpg.de/download/). Considering both Column Variant (MDN35) and RI Variant (ALK, based on 9 n-alkanes C10-C36), the reference library file ‘GMD_20111121_MDN35_ALK_MSL’ was used in this case. In addition, another GC-Quadrupole-MS MSRI library, 'Q_MSRI_ID'

(http://www.csbdb.de/csbdb/gmd/msri/gmd_msri.html), was also adopted to facilitate the target matching process. The reference library files were imported into NIST (National Institute of Standards and Technology, here a free demo version was used, downloaded from http://www.sisweb.com/software/ms/nist.htm#demo), a commonly used tool that compares spectrums detected in AMDIS to those stored in the library. Since retention index could be affected by different chromatographic setup, an in-house library was generated specifically for this set of experiment by matching samples to the library and assigning actual retention time to detected components. Note that similar to the reference library, mass fragments at m/z 73, 74, 75, 147, 148 and 149 were manually excluded from the in-house library as these were generated from compounds with trimethylsilyl moiety during derivatization process. This in-house library was then used to identify each detected component based on retention time and mass spectrum. Net, i.e. the minimum match factor was set to 70 for detection. All targets with net values below 80 would be given question marks in the generated report and would be double checked manually.

Once the .MSL AMDIS library is ready, an R package "Metab" (downloaded from https://www.bioconductor.org/packages/Metab/), provided by (Aggio et al., 2011), can be used as an automated pipeline for GC-MS data analysis. As required by Metab, first the in-house library (.MSL) needs to be converted into a .CSV file, which contains the name of each metabolite, retention time and 4 ion mass fragments (including the expected relative abundance of ion 2-4 to ion 1) for metabolite identification (see the reference ion library shown in Appendix Table 2). Ion 1 was used not only for identification but also as the specific mass fragment for metabolite

quantification. Following the generation of quantification report of all experimental samples, Metab provides code instructions for further data analyses, including false positive exclusion, internal standardization (relative quantification to ribitol) and biomass normalization (final quantification results relative to EOD WT samples can be found in Appendix Table 3).

2.12 Microarray Analysis

For *phyABCDE* seedling mutant microarray analysis, raw data was downloaded from the NCBI Gene Expression Omnibus with accession no. GSE31587 according to the paper (Hu et al., 2013) and analysed with GEO2R. After that, mapman (Thimm et al., 2004) (http://mapman.gabipd.org) was used to generate diagrams of metabolic pathways based on the microarray data (Figure 1.6).

Chapter 3- A Novel Role of Phytochromes in Coupling Carbon Resource to Growth

Part of this chapter is published in (Yang et al., 2016). All the analyses conducted in this chapter were the original work of this thesis.

3.1 Introduction

During the past few decades, phytochromes have been well-studied especially in the Arabidopsis seedling system (Li et al., 2011; Chen and Chory, 2011). Researchers are now aware of the molecular pathways that regulate photomorphogenesis, especially hypocotyl elongation (Leivar and Monte, 2014). Mathematical models have been developed that describe these molecular mechanisms, which in turn helps to promote our understanding by suggesting new directions for further study (Johansson et al., 2014; Rausenberger et al., 2010, 2011). Nevertheless, it still remains unclear how these photoreceptors control plant growth after seedling stage.

Analysis of phytochrome mutants has revealed some interesting observations in post-seedling plant architecture and growth rate (Halliday et al., 2003; Strasser et al., 2010; Hu et al., 2013; Mazzella et al., 2001). For instance, Arabidopsis *phyB* mutant has longer petioles, smaller leaf blades and slower leaf production rate than L*er* wild

type (WT). Theses phenotypes become even more severe when more phytochromes are knocked out. In particular, *phyABDE* mutant grown at 16°C has a leaf production rate only about half of that in WT plants [calculated from data published in (Halliday et al., 2003)]. This indicates phytochromes are still contributing largely to plant growth regulation after the seedling stage.

Plant growth depends largely on photosynthesis to generate carbon resource. Earlier reports have demonstrated that phytochrome mutant seedlings have substantial reductions in chlorophyll levels compared to WT upon red light stimulation (Strasser et al., 2010; Hu et al., 2013; Ghassemian et al., 2006). While this has not been reported in adult plants, it is possible that phytochrome mutants have constantly reduced photosynthesis-generated carbon supply that leads to growth repression.

Apart from regulating plant growth through photosynthesis pigments and subsequent photosynthate production, phychromes could also be controlling downstream carbon metabolism. Dating back to 1990's there were studies implying sucrose involvement in phytochrome signaling (Dijkwel et al., 1997; Short, 1999), indicating a possible interaction between photosynthate and photoreceptors. More recently, (Stewart et al., 2011; Lilley et al., 2012; Sairanen et al., 2012) reported in their studies that sucrose-promoted hypocotyl elongation largely depends on PHYTOCHROME-INTERACTING-FACTORs (PIFs), especially PIF5. In addition, data from (Debrieux et al., 2013) demonstrates that sucrose is needed for CONSTITUTIVE PHOTOMORPHOGENESIS 1 (COP1) control of phyA abundance in etiolated seedlings. Like seedling chlorophyll research, these studies also focus on Arabidopsis at the very early developmental stage. Nevertheless, they do suggest a

possible interaction between photoreceptor signaling and carbon metabolism that may alter plant biomass production later on.

In this chapter, I set out to test whether phytochromes control plant growth and biomass through sugars. By quantifying chlorophyll content, CO_2 gas exchange rate I confirmed a reduction in photosynthesis in phytochrome mutants. Yet an excess of photosynthates, starch and sugars, were also found in the mutants. Potential defect in daytime sugar resource allocation were proposed to cause the alteration in diurnal growth pattern, leading to reduced biomass production in phytochrome mutants. Overall these results suggest an important role of phytochrome photoreceptors in coupling carbon metabolism to growth in Arabidopsis plants.

3.2 Growth Condition Optimization

According to earlier reports (Hu et al., 2013; Halliday et al., 2003), *phyABDE* mutant plants flower much earlier than WT in standard growth conditions. For instance, when grown at 22°C, long days (16-h L/8-h D), *phyABDE* flowers within three weeks post germination (Figure 3.1 A). This makes it difficult to get comparable vegetative materials from phytochrome mutants and WT adult plants at comparative ages. So the first task is to find the optimized growth condition to delay flowering time, allowing enough biomass accumulation in phytochrome mutants for the study.

Plant flowering transition is highly sensitive to temperature (Fitter and Fitter, 2002; Halliday et al., 2003; Kumar and Wigge, 2010). In particular, our previous work has shown that the light pathways transduce temperature signals (Fitter and Fitter, 2002; Halliday et al., 2003; Kumar and Wigge, 2010), making phytochrome mutants

increasingly sensitive to temperature. This suggests that reducing temperature can delay flowering time in severe phytochrome mutants to allow longer vegetative development. Indeed, when grown at 18°C instead of 22°C, *phyABDE* plants didn't flower until four weeks old (Figure 3.1 A-B).

Apart from temperature, photoperiod also affects flowering onset (Park, 1999; Song et al., 2012). Arabidopsis is commonly known as a long-day plant, i.e. its flowering transition is promoted under long photoperiods while delayed in short days. Although it was reported that *phyABDE* mutant flowering behavior is insensitive to photoperiod (Hu et al., 2013) in relatively warm conditions (20°C), this constitutive flowering behavior no longer exists when temperature is reduced to 16°C (Halliday et al., 2003). Indeed at 18°C, when grown in short days (SD, 8-h L/16-h D) *phyABDE* flowering transition was delayed to over seven weeks (Figure 3.1 B). Comparing to SD, 12:12 photoperiod regime is more commonly used in relevant sugar studies. In this photoperiod, *phyABDE* can grow up to six-week-old without flowering, which is more comparable to the published data.

The above evaluation of growth condition allowed me to identify an optimal regime for my experiments, as follows: short photoperiod (8-h L/16-h D) for first two weeks early seedling development, followed by 12-h L/12-h D photoperiod for further four weeks, at 18°C throughout. In this condition, I successfully harvested six-week-old *phyABDE* plant materials at their vegetative stage alongside *phyBD* and L*er* WT.

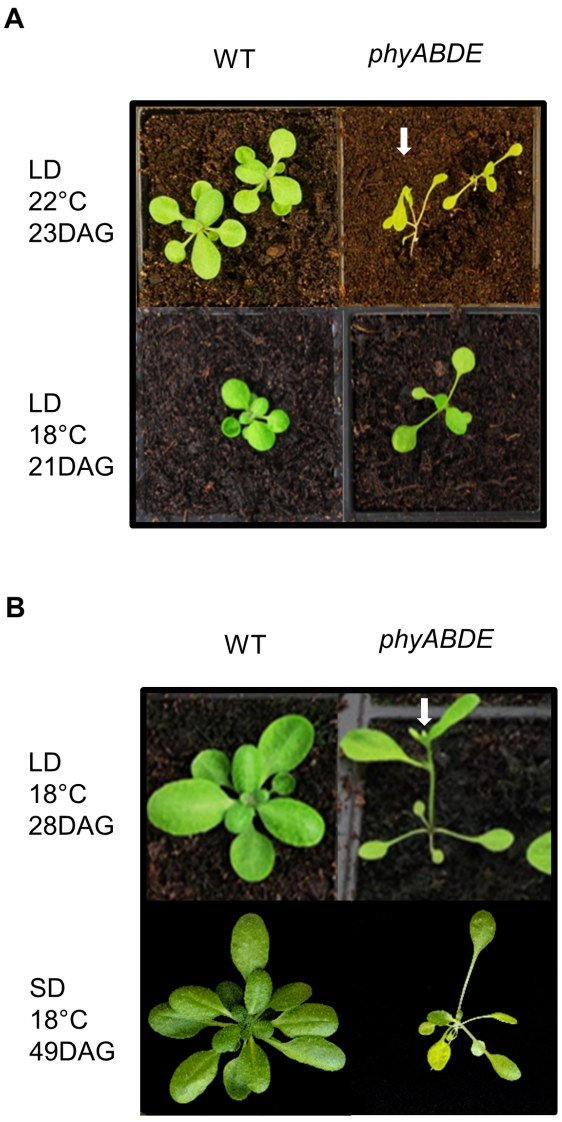

Figure 3.1 Flowering time of *phyABDE* can be delayed by reducing growth temperature and photoperiod length.

(A) Flowering time of *phyABDE* can be delayed by reducing growth temperature. When grown in 22°C, LD (long-day, 16-h L/8-h D) condition, *phyABDE* plants are flowering at 23 DAG; when grown at 18°C, *phyABDE* plants are still at vegetative stage at 21 DAG, then flower at 28 DAG. (B) At low temperature (18°C), flowering time of *phyABDE* can be further delayed by reducing photoperiod. In LD condition, *phyABDE* flowers at 4-week age; while grown in SD (short-day, 8-h L/16-h D) condition, 7-week-old *phyABDE* is still at vegetative stage. DAG: days after germination. Arrows indicate visible inflorescence buds.

3.3 Phytochrome Mutant Adult Plants Possess Less Chlorophyll and Fix Less CO_2 than WT

Whole rosettes of six-week-old L*er* WT, *phyBD* and *phyABDE* plants (growth regime described above) were harvested in light, for determination of chlorophyll level as mg per g fresh weight. A sequential chlorophyll depletion was observed in *phyBD* and the severe *phyABDE* mutants compared to WT (Figure 3.2 A), demonstrating this deficit still persists beyond the seedling stage. Nevertheless, the chlorophyll difference between phytochrome mutants and WT in our experiments is more subtle than that of red-light grown seedlings as reported in (Hu et al., 2013). This is not too surprising as chlorophyll fluorescence per 10 seedlings was presented in the publication, which could amplify the difference considering that phytochrome seedlings have much smaller cotyledons than WT (Hu et al., 2013). Also, other photoreceptors are expected to regulate this response in white light condition, which could partly compensate for the loss of phytochromes. At last, this data may reflect the comparatively reduced contribution of phytochromes to maintaining the chlorophyll pool in adult plants.

CO_2 gas exchange rate measurement is commonly used to predict photosynthetic carbon fixation efficiency. Similar to the chlorophyll data, CO_2 assimilation was also reduced in *phyBD* and *phyABDE* than WT in a mild but significant manner (Figure 3.2 B). Comparing to this, CO_2 release rate in darkness was similar in phytochrome mutants and WT plants, suggesting respiration is probably unaffected in this case (Figure 3.2 B).

Plant growth is cumulative that even small alterations in photosynthetic rate could

lead to striking changes in the final biomass (Chew et al., 2014). Therefore, the constitutive mild repression of photosynthesis in phytochrome mutants is still likely to cause vegetative growth defect in developing plants.

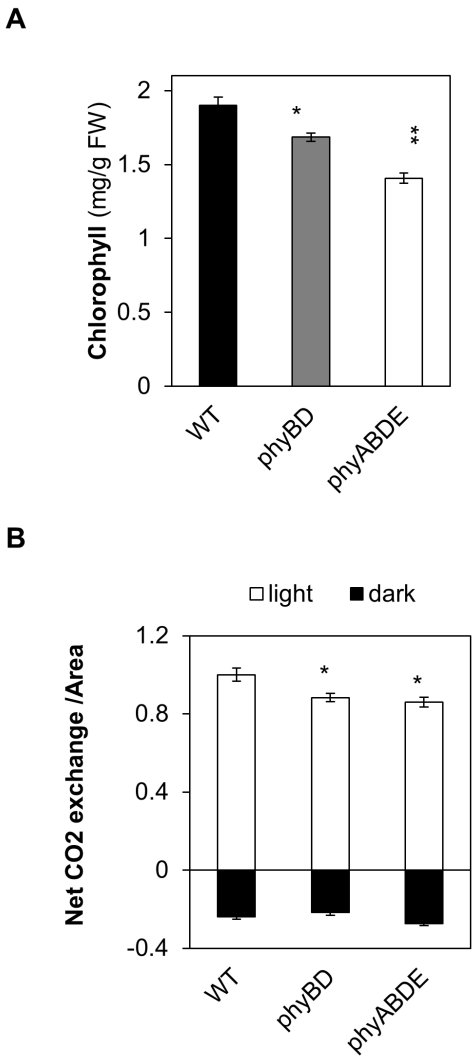

Figure 3.2 Physiological study of WT and phytochrome mutant adult plants.

(A) Total chlorophyll level quantification (mg per g fresh weight) in WT, *phyBD* and *phyABDE* whole rosette samples. (B) CO_2 gas exchange rate measurement. Flux was calculated per unit area (m²) and results expressed relative to WT in light. Values presented are mean ± SEM. Asterisks indicate a significant difference between values of the phytochrome mutants and WT by means of Student's t-test at *, $p \leq 0.05$; **, $p \leq 0.01$.

3.4 More Endogenous Sugars and Starch Are Accumulated During Daytime in Phytochrome Mutants

Plants assimilate carbon through photosynthesis to generate organic metabolites such as sugars. Sucrose is one of the most important sugars due to its high abundance, easy mobility for energy supply and special role in signaling transduction. Part of the carbohydrates fixed in light is used to synthesize starch, stored in leaves as energy reserves till night falls. Once photosynthesis ceases in dark, starch will be broken down to sucrose to sustain plant growth and metabolism (Stitt et al., 2010; Streb and Zeeman, 2012; Ruan, 2014). If impaired photosynthesis (as shown in 3.3 above) is the main cause for the repressed growth in phytochrome deficient plants, less sucrose and starch would be expected in these mutants.

Diurnal sucrose and starch quantification in six-week-old rosettes

L*er* WT and two phytochrome mutants (*phyBD* and *phyABDE*) were grown in identical conditions up to six weeks as described. Whole rosette samples were harvested from the start of the day at a six-hour interval, i.e. at ZT (Zeitgeber time) 0, 6, 12, 18 and 24 over a 24-hour period. Starch and sucrose were quantified as mg per g sample fresh weight as described in the method chapter.

Consistent with previous reports of day/night metabolite fluctuation in WT plant (Pal et al., 2013), here a similar diurnal rise and fall pattern of sucrose and starch was observed in all three genotypes. However, contrary to the expectation, more sucrose and starch are found in *phyBD* and *phyABDE* compared to WT. The difference is

particularly obvious at the end of day (EOD) when the sugar level reaches the peak (Figure 3.3 A-B). In addition, despite having more starch and sucrose at the start of dark period, phytochrome mutants deplete both carbohydrates to comparable levels relative to WT at the end of night (Figure 3.3 A-B). In brief, despite of reduced photosynthesis, phytochrome deficiency leads to elevated sucrose and starch in light and accelerated depletion in the dark, suggesting a novel role of phytochromes in carbon resource allocation.

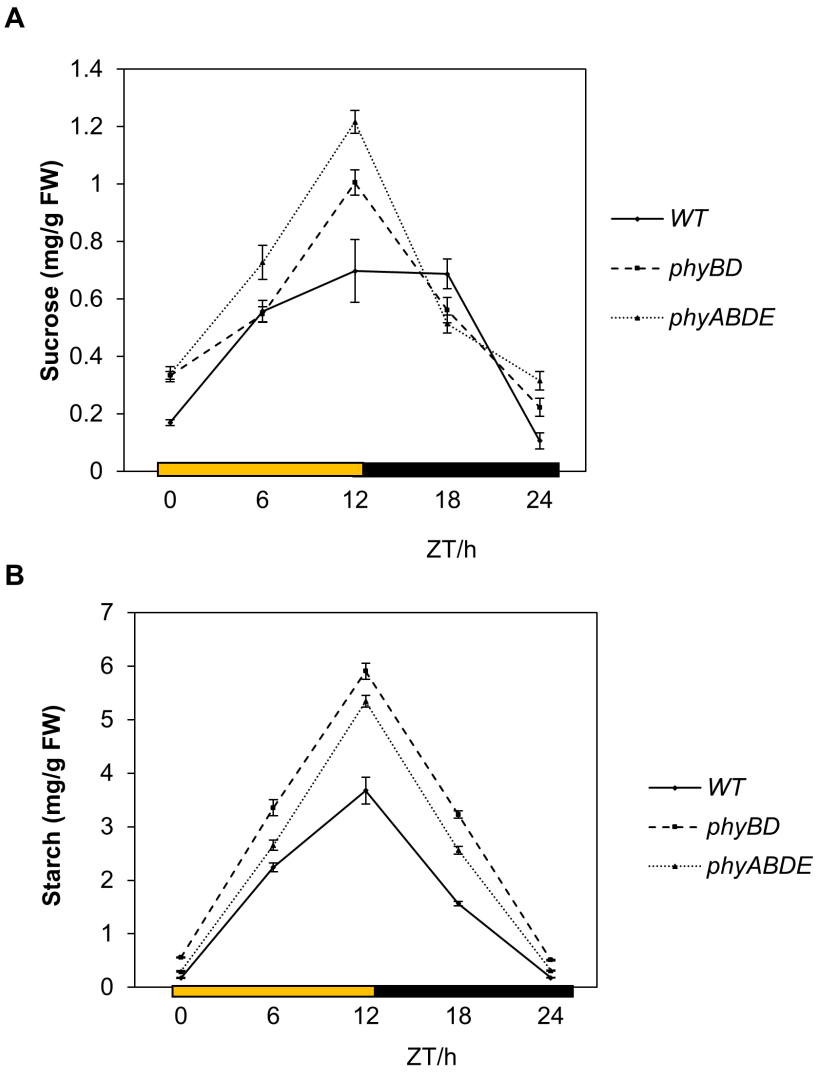

Figure 3.3 Sucrose and starch determination assay.

(A) Sucrose and (B) starch quantification in 6-week-old plant rosettes through time course. FW: fresh weight; DW: dry weight. Values presented are mean ± SEM. Statistical significance test could be found in Appendix Table1.

Iodine stain result suggests different starch composition in *phyABDE*

Lugol's iodine staining was also used to qualitatively check starch alteration in 5-week-old WT and phytochrome mutants *(phyBD, phyABD, phyABDE*). Rosettes were harvested at EOD when starch level reaches the peak. Samples were immersed in ethanol to remove chlorophyll till fully decolorized, stained in Lugol's solution for 5 min and de-stain in distilled water until difference between WT and phytochrome mutants is shown.

After being de-stained for a short while (Figure 3.4 A), L*er* started to show a lighter blue than *phyBD* and *phyABD*; this color difference became more obvious after long time de-staining (Figure 3.4 B), supporting the previous enzymatic quantification results that shows more starch in phytochrome mutants than WT (Figure 3.3 B). Interestingly, however, unlike other genotypes, *phyABDE* showed a reddish-brown staining, which was totally de-stained after long time in water (Figure 3.4 A and B). Plant starch consists of two glucose polymers, amylose and amylopectin, which behave distinctively in iodine staining due to their different structures. Amylose (linear) is stained blue, while amylopectin (branched) is stained reddish brown. Since starch level in *phyABDE* was quantified higher than L*er* at EOD (Figure 3.3 B), this result may suggest a difference in starch quality.

GBSS and PTST are two proteins directly controlling amylose synthesis without affecting amylopectin (Seung et al., 2015). Amylose-free mutants, *gbss*, *ptst-1*, and *ptst-2*, produce a brown staining that is distinct from the WT, while their total starch levels are not altered (Seung et al., 2015). Accordingly, it is possible that *phyABDE*

mutant has little amylose, but more amylopectin than total starch content of WT. In contrast, *phyBD* and *phyABD* were stained similarly to WT, implying a specific role of phyE in affecting amylose synthesis. Considering the large application of starch in various industries (Santelia and Zeeman, 2011), it would be of great interest to look into the potential regulation from phytochromes.

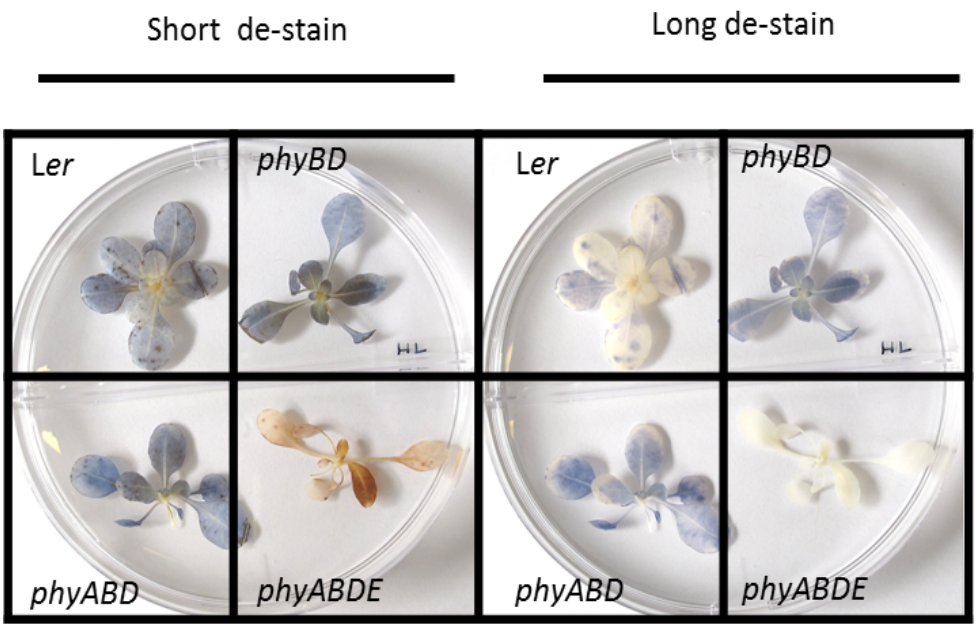

Figure 3.4 Iodine staining starch quality assay.

Representative images of 5-week-old L*er* WT, *phyBD*, *phyABD* and *phyABDE* plants after iodine staining. Rosettes were harvested at the end of the day, decolorized using ethanol, stained in Lugol's solution to visualize starch.

EOD sugar quantification in shoot and root tissues

Plants generate sugars in photosynthetic tissues and mobilize part of it to non-photosynthetic tissues mainly in the form of sucrose. Interestingly, (Kircher and Schopfer, 2012) reported possible involvement of phytochromes in this process, facilitating sucrose transport from cotyledons to roots in de-etiolated seedlings. Since my sugar quantifications were all done in aboveground rosettes, it is possible that phytochrome mutants with higher levels of sucrose in shoot actually have less in the root due to deficient sugar transportation. In this case, average sugar level across the whole plant could still be lower in phytochrome mutants than that in WT, hence consistent with the photosynthesis observation.

To test this hypothesis, I quantified fresh biomass and sugar levels (per gram fresh weight) in shoot and root of WT and phytochrome mutants (Figure 3.5). Five-week plants were grown in plates for the convenience of root sampling. In this experiment triple *phyABD* mutant was used instead of *phyABDE,* as adventitious roots emerge from the *phyABDE* hypocotyl, making it difficult to separate shoot and root.

Consistent with soil-grown plants, phytochrome mutants grown in medium also show dramatic repression of growth compared to WT. Specifically, both root and shoot fresh biomasses are similarly reduced in *phyBD* and more affected in *phyABD* (Figure 3.5 B). In agreement with the previous sucrose quantification in soil-grown plant rosettes, here *phyBD* root, *phyABD* shoot and root all show a sizable increase of sucrose relative to WT shoot and root at the end of day (Figure 3.5 C). In addition, this time glucose was also quantified in all tissues and a significantly higher accumulation was observed in phytochrome mutants, both *phyBD* and *phyABD*

(Figure 3.6 D). Note that sugar concentration (per gram tissue fresh weight) is generally higher in root than that in shoot, probably due to lower water content in root. These results disagree with the hypothesis and demonstrate that rosette accumulation of sucrose in phytochrome mutants is not caused by impairment of shoot-to-root sugar transport. Rather, the overall sugar (both sucrose and glucose) concentration is higher in phytochrome mutants than that in WT.

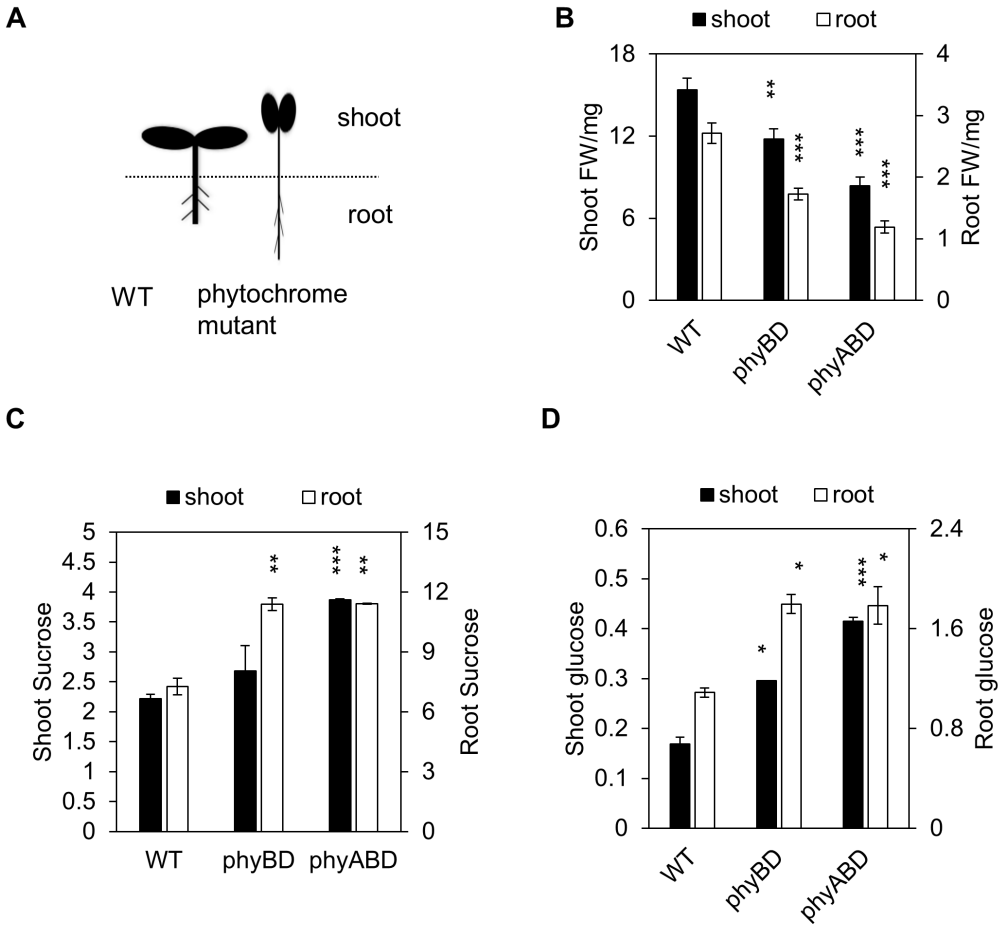

Figure 3.5 Sucrose and starch determination assay.

(A-B) Experimental design and tissue-specific fresh biomass quantification of shoot and root in WT and phytochrome mutants. (C-D) Soluble sugar (sucrose and glucose) determination (mg/g FW) in media-grown shoot and root tissues respectively. Values presented are mean ± SEM. Asterisks indicate a significant difference between values of the phytochrome mutants and WT by means of Student's t-test at *, $p \leq 0.05$; **, $p \leq 0.01$; ***, $p \leq 0.001$

3.5 *phyBD* Has Retarded Growth Particularly During Daytime

Phytochrome mutants produce less photosynthate, yet accumulate more starch and sugars during daytime (Figure 3.2 and 3.3). This suggests a possible scenario where utilization of carbon resource is impaired in these phytochrome mutants, leading to a day-specific excess of sugars. As a result, plant growth would be retarded due to the lack of resource input, particularly in light.

PRA (projected rosette area) is a plant growth measurement that represents total area occupied by the whole rosette in a top-view image. This is easily obtained by extracting information from photos without killing plants (Vanhaeren et al., 2015). To test how day/night growth is altered in phytochrome mutants compared to WT, end of light/dark period PRAs for *phyBD* and WT were obtained through a continuous week. *phyABDE* was not used in this case due to its strong hyponastic response, which skews PRA a lot from the actual rosette area.

In agreement with previously published data of leaf production rate (Halliday et al., 2003), *phyBD* rosette expansion is also generally slower than that of WT (Figure 3.6 A). More interestingly, the PRA expansion curve looks mostly smooth for WT, while that of *phyBD* has some zigzags especially between day 5 and 7 (Figure 3.6 A, enlarged section). This distinction is shown more clearly when average diurnal growth rate is quantified over the whole time period for both genotypes (Figure 3.6 B). WT has an identical relative expansion rate during day and night, implying a steady growth regardless of light availability. In comparison, *phyBD* rosette expands at a significantly lower pace during the day than that at night. While the plot seems to

suggest *phyBD* grows faster than WT at night, this difference is not significant based on student's t test ($p=0.239$). Therefore, during this period *phyBD* has a similar relative expansion rate to WT at night, while in light rosette expansion is largely retarded.

This interesting finding partially supports the hypothesis that day accumulation of sugars in phytochrome mutants is caused by less consumption for plant growth in light period. The unaffected night expansion in *phyBD* also agrees with the normal depletion of starch and sucrose in darkness. Although things might be more complicated in *phyABDE* mutant considering the dramatic repression of growth, phyB and phyD seem to be the major phytochrome regulating plant growth during daytime.

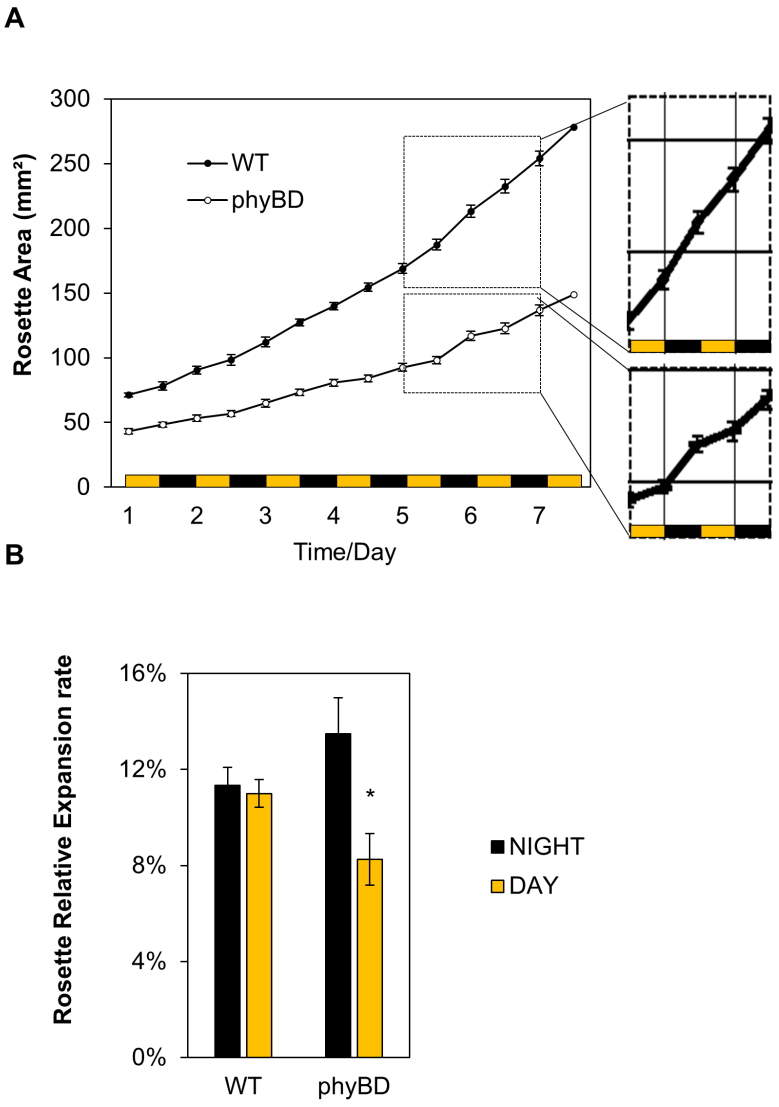

Figure 3.6 Comparing to WT, *phyBD* has retarded growth rate especially in the day.

(A) Quantification of WT and *phyBD* rosette expansion during week 3-4, post germination. The enlarged section highlights the diurnal differences in *phyBD* compared to L*er* WT. Measurements were taken at the end of each day and night. (B) Mean relative day and night expansion rates are plotted for the experimental period. Values are presented as mean ± SEM. Asterisks indicate a significant difference between values of day and night growth rate in *phyBD* by means of Student's t-test at *, $p \leq 0.05$.

3.6 Phytochromes Are Major Regulators of Plant Biomass

Previous studies have reported the growth phenotype of phytochrome mutants such as elongated petioles, reduced number of leaves and early on-set of flowering (Halliday et al., 2003; Halliday and Whitelam, 2003; Strasser et al., 2010; Hu et al., 2013). However, it might be a bit surprising that neither fresh nor dry weight per plant has ever been quantified before. Data in Figure 3.7 A-B demonstrates that two phytochrome deficient mutants have distinguished rosette appearance, revealing dramatically reduced biomass relative to WT, both fresh and dry. This reduction is particularly extreme for *phyABDE* with only one fifth of WT biomass accumulated in six weeks (Figure 3.7 B).

A large proportion of plant dry biomass comes from cell wall substance; therefore, I went on to check the expression of genes involved in cell wall synthesis and reorganization in phytochrome mutants. These gene candidates were selected based on published microarray data (Hu et al., 2013) combined with promoter search analysis. Using five-week plants (*phyABDE* and WT) grown in identical conditions described above, I harvested and extracted RNA samples every 4h through a 24h time course. The qRT-PCR results exhibit substantial transcript reduction of *CELLULOSE SYNTHASE LIKE* genes *CSLB4, CSLG3, XYLOGLUCAN ENDOTRANSGLUCOSYLASE/HYDROLASE 7 (XTH7)* and *EXPANSIN 1 (EXP1)* in *phyABDE* relative to WT (Figure 3.7 C). Specifically, all these genes show a diurnal change in expression level, largely repressed by the absence of phytochromes especially at dawn peaks.

As building blocks for most organisms, protein also contributes largely to plant dry biomass. Given that phytochrome mutants have dramatically repressed growth, their capability to synthesize major growth components could also be affected. By quantifying total protein content from five-week-old rosette samples, a mild but significant decrease was found in *phyBD* and further reduction was shown in *phyABDE,* compared to WT (Figure 3.7 D).

To summarize, the above biomass analyses show less fresh/dry weight, reduced cell wall synthesis related gene expression and reduced total protein content in phytochrome mutants. These suggest phytochromes are controlling resource allocation to biomass production through cell wall and protein synthesis**.**

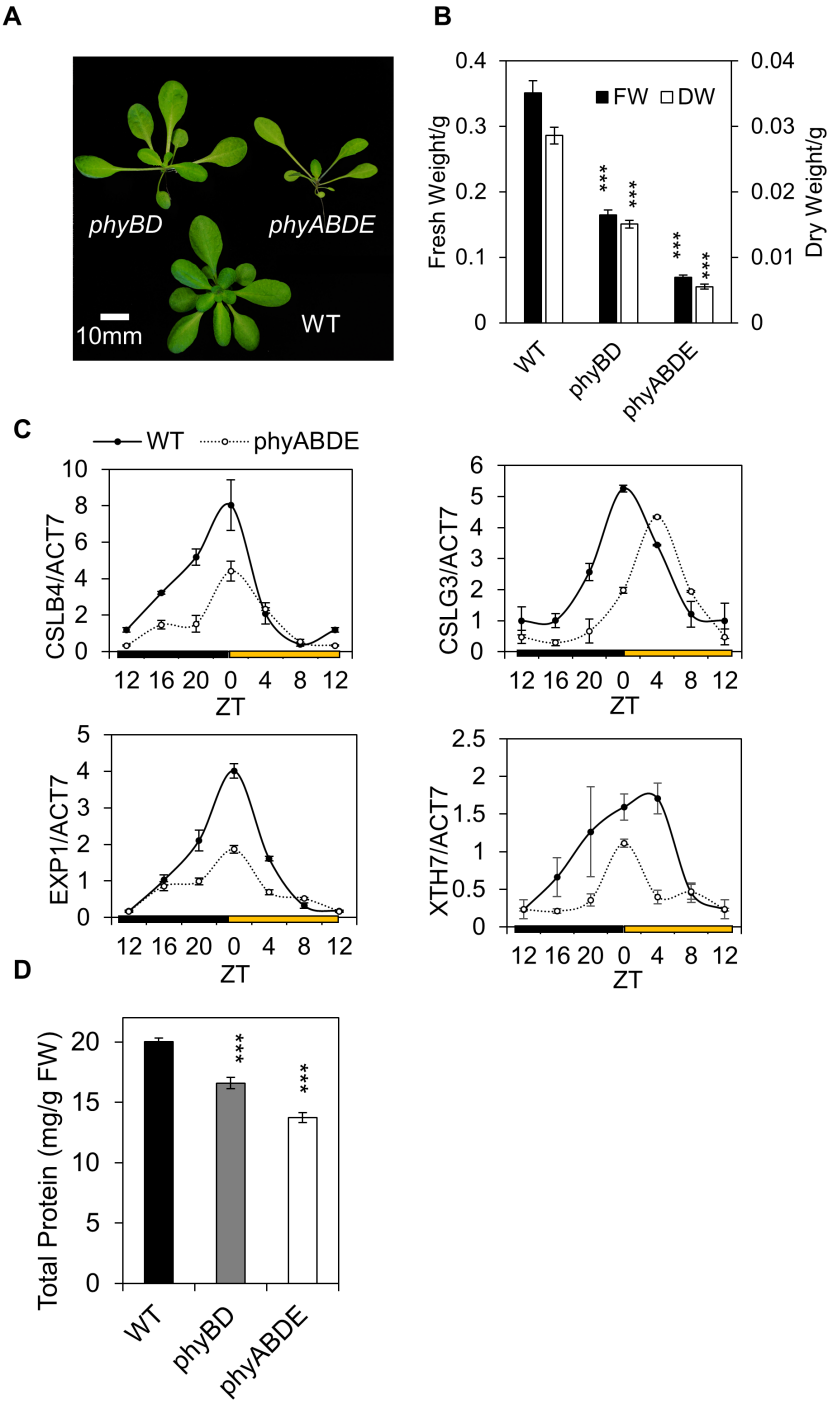

Figure 3.7. Phytochrome deficiency strongly affects plant biomass.

(A) Image depicting the severe biomass phenotypes of 6-week-old *phyBD* and *phyABDE* mutants, when compared to L*er* WT. (B) Fresh weight (FW) and dry weight (DW) of WT and phytochrome mutants. (C) Diurnal expression profiles of cell wall associated genes *CSLB4*, *CSLG3*, *EXP1* and *XTH7*, determined by qRT-PCR, in WT and *phyABDE*. (D) Total protein quantification in 5-week-old *phyBD*, *phyABDE* and WT. Values are presented as mean ± SEM. Asterisks indicate a significant difference between values of the phytochrome mutants and WT by means of Student's t-test ***, $p \leq 0.001$.

3.7 Discussion

Investigations on phytochrome control over plant growth are mostly conducted in seedlings, where hypocotyl elongation response is usually evaluated. This simple, neat system allows rapid tests of different genotypes in various conditions, largely contributing to our knowledge of how phytochromes mediate the seedling transition into photoautotrophic growth at the molecular level (Quail, 2002; Li et al., 2011). Comparing to that, much less is known about how these photoreceptors are involved in plant growth at later stages. In particular, it remains largely unknown why phytochrome deficient plants, especially the multiple mutants, have evidently reduced growth at mature stage (Hu et al., 2013; Halliday et al., 2003).

In Figure 3.7 A-B, the data demonstrates that phytochrome depletion can have a profound impact on fresh and dry weight in six-week-old plants at vegetative stage. Furthermore, cellulose, as one of the major components of plant biomass (Davison et al., 2013), might be reduced in phytochrome mutants. Although cellulose content was not directly quantified, transcript analysis results showed a clear repression of genes responsible for cellulose synthesis (*CSLB4* and *CSLG3*), cell wall expansion (*EXP1*) and reorganization (*XTH7*) over a diurnal time course especially at the peak time and rising phase in *phyABDE* relative to WT (Figure 3.7 C). Interestingly, PIF4 was found binding to the promoter of *EXP1* as shown by ChIP analysis (Bai et al., 2012), supporting a role of PHY-PIF in regulating cell wall synthesis at transcriptional level. On the other hand, (Gibon et al., 2009; HANNEMANN et al., 2009) reported that Arabidopsis (C*ol*) plants grown in 12/12 photoperiod have 15 mg protein per g FW, equivalent to 15% of dry biomass (calculated using general water

content 90%). Consistently, five-week WT (L*er*) plants have about 20 mg/g FW total protein, which was found slightly lower in *phyBD* and more reduced in *phyABDE* (Figure 3.7 D + 2-week seedling protein data in Appendix Figure 3). Together, these data indicates phytochrome photoreceptors are controlling production of major biomass components in Arabidopsis.

Phytochrome mutant seedlings are reported to have dramatically repressed chlorophyll biosynthesis compared to WT upon red light stimulation (Strasser et al., 2010; Hu et al., 2013; Ghassemian et al., 2006). This implies at the early developmental stage, phytochrome deficiency could lead to a lack of carbon resource generated from photosynthesis. Reduced availability of organic fuel can result in slower growth and less cell wall/protein production, which could possibly persist through the entire plant life. Indeed, less chlorophyll and photosynthetic CO_2 assimilation was also detected in six-week-old *phyBD* and *phyABDE* compared to WT plants (Figure 3.2 A-B). However, this photosynthesis repression does not come along with less carbon resource. Instead, these phytochrome mutants were found to possess a higher concentration of sucrose and starch in rosettes than WT (Figure 3.3). This particularly happens during daytime, while at night they mobilize these resources faster, resulting in similar sugar levels at the end of night period (Figure 3.3). To exclude the possibility that phytochrome deficiency impairs sugar translocation from aboveground to underground, sugar quantification was performed in shoot and root samples respectively. Still, five-week-old *phyABD* showed more sucrose and glucose in both tissues compared to WT, making the explanation highly unlikely (Figure 3.5).

While it is commonly accepted that plant growth depends largely on photosynthesis, this link between growth rate and carbohydrate content may need re-assessment. There have been reports of plants with reduced photosynthesis and growth yet more sugars. For instance, starch-less mutant *phosphoglucomutase (pgm)* has strongly reduced biomass than WT despite of high levels of sucrose accumulation during daytime, mostly due to the starvation stress at night given the lack of starch reserves (Caspar et al., 1985). Photosynthesis capacity is also restricted in this mutant, partly due to the feedback from high sugar substrates. In addition, other studies have revealed that in stress conditions where plant photosynthesis and growth are repressed, soluble sugars and amino acids are accumulated as part of the protection response (Arbona et al., 2013; Grant, 2012). Finally, as reported in a systematic study that tried to predict biomass from metabolic composition, no single 'magic' compound was found that could explain the biomass variance (Meyer et al., 2007). In contrast, the correlation was much higher when a combination of a large number of metabolites was considered. Interestingly, among the metabolites highly ranked in the multivariate analysis, sucrose as well as a few other sugar-derivatives and tricarboxylic acid cycle organic acids all showed weak negative correlations to biomass (Meyer et al., 2007).

So far, no satisfactory explanation has been proposed for the high level of sugars in phytochrome mutants, yet it may be linked to the altered growth behavior. By monitoring day-night rosette expansion through a continuous week, I showed that growth defect in *phyBD* is cumulative (Figure 3.6 A). More interestingly, the mutant has a tendency to grow more during night than daytime, significantly distinctive to

the WT rosettes that expand evenly in light and dark (Figure 3.6 A and B). Reduced day growth in phytochrome mutant rosettes could be possibly linked to the accumulated sugars, either the catabolism of carbohydrates to support growth is impaired in light, or that light-activated-phytochrome dependent growth is repressed therefore sugar consumption is not necessary. Either way, these results suggested a novel role for phytochromes in allocating carbon resource to day/night growth. Indeed, recent years there have been some efforts in exploring the interaction between light and sugar pathways. Researchers studying sucrose promotion of hypocotyl elongation have found this to be PIF-dependent (Stewart et al., 2011; Lilley et al., 2012; Sairanen et al., 2012). Although these experiments were done in seedlings, it does provide some insights for the possible phytochrome-sugar interplay in adult plants as well.

Phytochromes are well known to function by controlling levels and activity of key hub transcription factors such as PIFs to regulate plant growth and development, especially at the seedling stage. This chapter presents a more complete view of phytochromes, proposing their roles in carbon generation, resource allocation and biomass production in mature plants. In particular, this study provides evidence that phytochromes are involved in coordinating carbon metabolism to vegetative biomass accumulation, highlighting the significance of potential application to future crop research.

Chapter 4- Phytochrome Mutants Have Reprogrammed Metabolism and Reduced Sensitivity to Abiotic Stresses

Part of this chapter is published in (Yang et al., 2016). All the analyses conducted in this chapter were the original work of this thesis.

4.1 Introduction

It is commonly accepted that plant growth be largely driven by carbon availability, but recent studies point to a more complicated interaction. While Arabidopsis grown in low CO_2 condition unsurprisingly have reduced biomass (Li et al., 2014), increasing environmental CO_2 concentration does not necessarily lead to enhanced growth, especially when nitrogen source becomes limited (Takatani et al., 2014; Asensio et al., 2015). Similarly, feeding carbon to starved plants was proved to be effective in boosting biomass (Izumi et al., 2013); however, sugar application to non-starved plants was known to reduce photosynthetic capacity through biochemical feedback regulation (Sheen, 1990), or even to trigger severe developmental and growth stress when high doses are used (Dekkers et al., 2004 and Appendix Figure 1). In addition, analysis using Arabidopsis natural accessions revealed mild negative

correlations between starch/sucrose level and plant biomass (Meyer et al., 2007; Sulpice et al., 2009).

Plant carbon resource level is determined not only by photosynthesis rate but also how rapidly it is utilized. Since phytochrome mutants have reduced photosynthetic CO_2 assimilation (Figure 3.2), the over-accumulation of sugars (Figure 3.3) is most likely due to less carbon consumption. This leads to a potential retardation in transforming assimilated carbon into plant biomass. In addition, (Cross et al., 2006) has suggested that plant growth is not related to the absolute levels but flux of the central resources. *phyBD* mutant grows more slowly than WT (Figure 3.6), particularly during daytime when it has excess starch and sucrose (Figure 3.3). This implies that a reduced carbon flux, in addition to repressed photosynthesis, might be the major underlying cause for growth defects in phytochrome mutants. It also suggests a novel role for phytochrome photoreceptors in accommodating central resource into plant biomass production.

In this chapter, I conducted a GC-MS (Gas Chromatography coupled with Mass Spectrophotometry) analysis to gain a broader view of metabolic difference between WT and phytochrome mutants. Over 40 primary metabolites were quantified in 5-week rosettes of WT and three phytochrome mutants at EOD and EON. Using a multivariable comparison method, I was able to distinguish phytochrome mutants from WT based on the obtained metabolic profiles. Phytochrome mutants were found to have elevated levels of sugars, organic acids (mainly involved in TCA cycle) and amino acids. qRT-PCR analysis of key enzymes in these pathways suggests the metabolic alteration is not caused by transcript regulation through phytochromes.

The most dramatically accumulated metabolites in phytochrome mutants, raffinose and proline, were suggested to prime the plants more tolerant to salt/ABA stress induced growth repression/chlorophyll reduction. Some stress maker genes were also promoted in phytochrome mutants even in normal growth conditions. In summary, this chapter established a novel role of phytochromes in exerting strong effect on plant metabolic state and abiotic stress responses.

4.2 Experimental Design and GC-MS Analysis Procedure

Like many other physiological processes in living organisms, plant metabolism is also highly dynamic. Metabolite levels often vary from time to time, allowing plants to adapt to the changing environment as well as to optimize growth and development accordingly. In particular, many metabolites have rhythmic rise and fall on a daily basis. Data in Chapter 3 shows phytochrome mutants have elevated levels of sugar and starch compared to WT especially at EOD. This implies a metabolic profile at EOD would be most preferred to identify candidates affected by phytochromes. Additionally, EON time point was also included in order to capture possible diurnal changes.

I first grew WT *(Ler), phyBD, phyABDE* and the quintuple mutant *phyABCDE* (lacking all five phytochromes) in media plates under short photoperiod (8:16, 8-hr Light/16-hr Dark) condition for 2 weeks, then transferred healthy seedlings to soil with 12:12 photoperiod for further 3 weeks. Temperature was maintained at 18°C and light level was set to 100 $\mu mol \cdot m^{-2} \cdot s^{-1}$. This growth condition was designed to increase leaf number and size in phytochrome mutants, especially *phyAB(C)DE*. For

sampling, 5 rosettes were pooled together as one sample; 6 sample replicates were harvested for each genotype at each time point.

Plant tissues were frozen in liquid nitrogen, finely ground; metabolites were extracted following procedures from (Lisec et al., 2006) as shown in Figure 4.1 A. Note that in step c, same amount of Ribitol was added to each sample as internal standard for relative quantification later. MSTFA was used for sample derivatization (procedures in grey shade) so that sugars can be measured; a series of alkanes (C7-C30) were added to the sample as retention time index to help identifying metabolites in later analysis. GC-MS analysis was conducted in the University of Glasgow (Chemistry department) using Shimdazu GC-MS-QP2010 Plus with a MDN35 column. Sample orders were randomized to avoid possible technic bias through time of measurement.

For data analysis, AMDIS (Automated Mass spectral Deconvolution and Identification System) and NIST (National Institute of Standards and Technology) software together with GMD (GOLM metabolome database) mass spectrum reference libraries were used for peak detection and metabolite identification. R package 'Metab' (Aggio et al., 2011) was used for peak quantification and further normalization analysis. For a glance of the whole experiment process, see Figure 4.1 B.

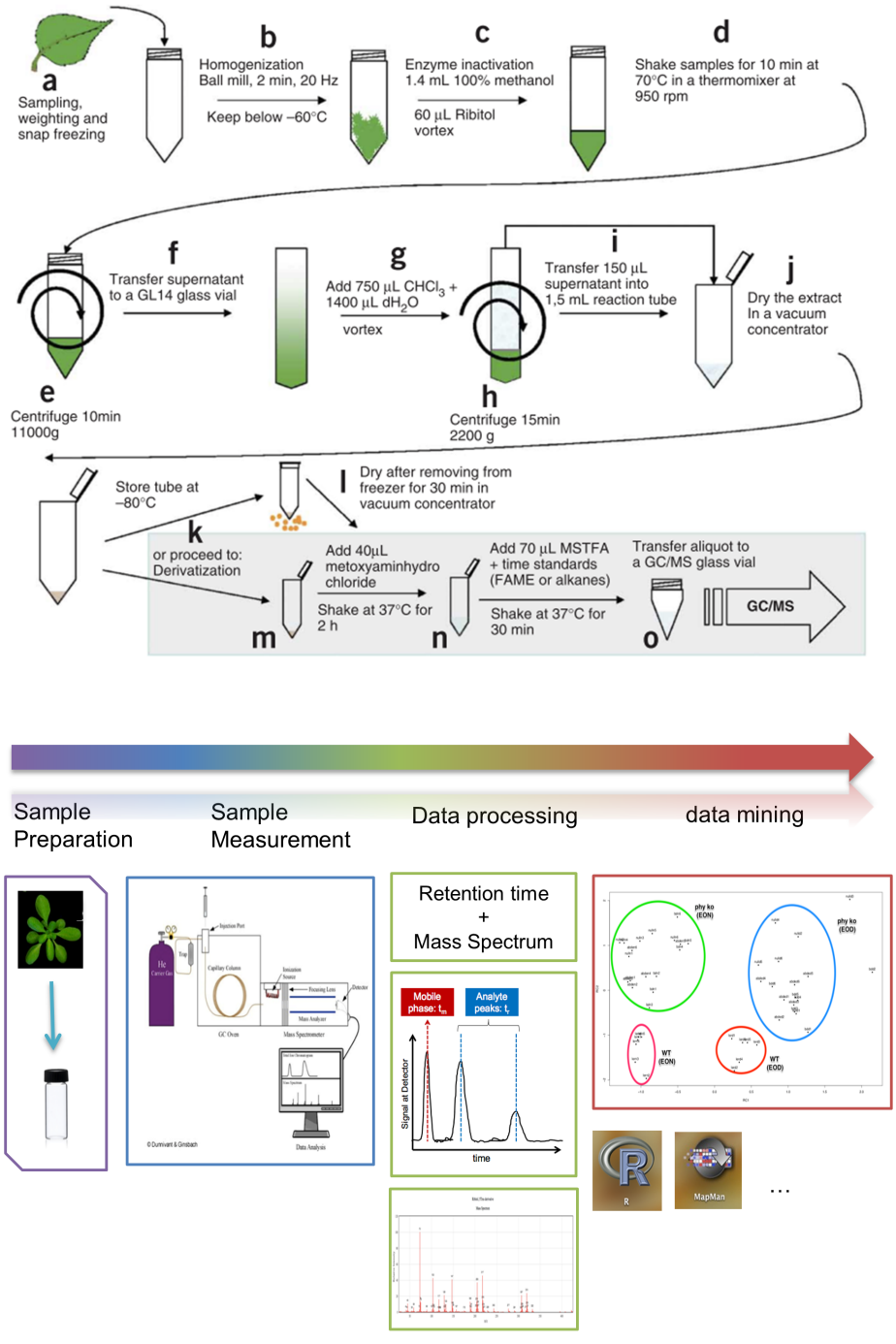

Figure 4.1 GC-MS experiment procedures.

(A) Plant sample preparation for GC-MS analysis. Reproduced from (Lisec et al., Nature protocols, 2006). (B) A brief illustration of procedures of the whole experiment conducted in this study.

4.3 PCA Shows Distinguished Metabolic Profiles between WT and Phytochrome Mutants

PCA (Principle Component Analysis) is a multivariate analytical approach commonly used in metabolomics data analysis due to its capability of reducing the dimension of variables, clustering and visualizing sample distribution (Bartel et al., 2013). It is particularly useful when samples cannot be discriminated based on the level of a single metabolite, or for exploratory experiments as a preliminary step to identify candidates of interest. Here this method is applied to check sample quality (based on the distribution of replicates), to compare metabolic profiles between samples and to find out the metabolic candidates mostly affected by the absence of phytochromes.

Figure 4.2 A shows the sample distribution of all genotypes sampled at different time points based on their PCA score results. Biological replicates were grouped in ellipses of different colours, demonstrating the metabolic variance of each type of sample. This plot also reveals four distinct groups of all samples, i.e. EON phytochrome mutants, EON WT, EOD phytochtome mutants and EOD WT, which indicates the biological meaning of PC1 to be sampling time and PC2 as genotype. Not surprisingly, the clear separation on the axis of PC1 suggests that metabolic profiles differ between EOD and EON samples. At the same time, distinctions between phytochrome mutant and WT samples at both EOD and EON on the PC2 axis confirmed the effect of phytochrome photoreceptors on plant metabolism.

At the first glance, *phyABDE* and *phyABCDE* samples are almost indistinguishable, or even largely overlapped at EOD, suggesting a comparable metabolic status shared by the two severely deficient phytochrome mutants. Meanwhile, *phyBD* samples are

located between WT and *phyAB(C)DE* at both time points. This is perhaps not surprising as phytochromes are reported to have redundant functions in many physiological responses through transcript regulation (Franklin, 2003; Hu et al., 2013); here this data also imply that they have overlapping roles in controlling metabolism.

Figure 4.2 B plots all variables (metabolites being quantified in this study) according to their transformation weights used to score distribution of samples as shown in Figure 4.2 A on the same coordinate system. Top ten significant variables are marked with individual names, among which succinic acid, citric acid, aspartic acid, proline, malic acid, fumaric acid and glutamic acid are the main contributors of PC2, which differentiates phytochrome mutants from WT.

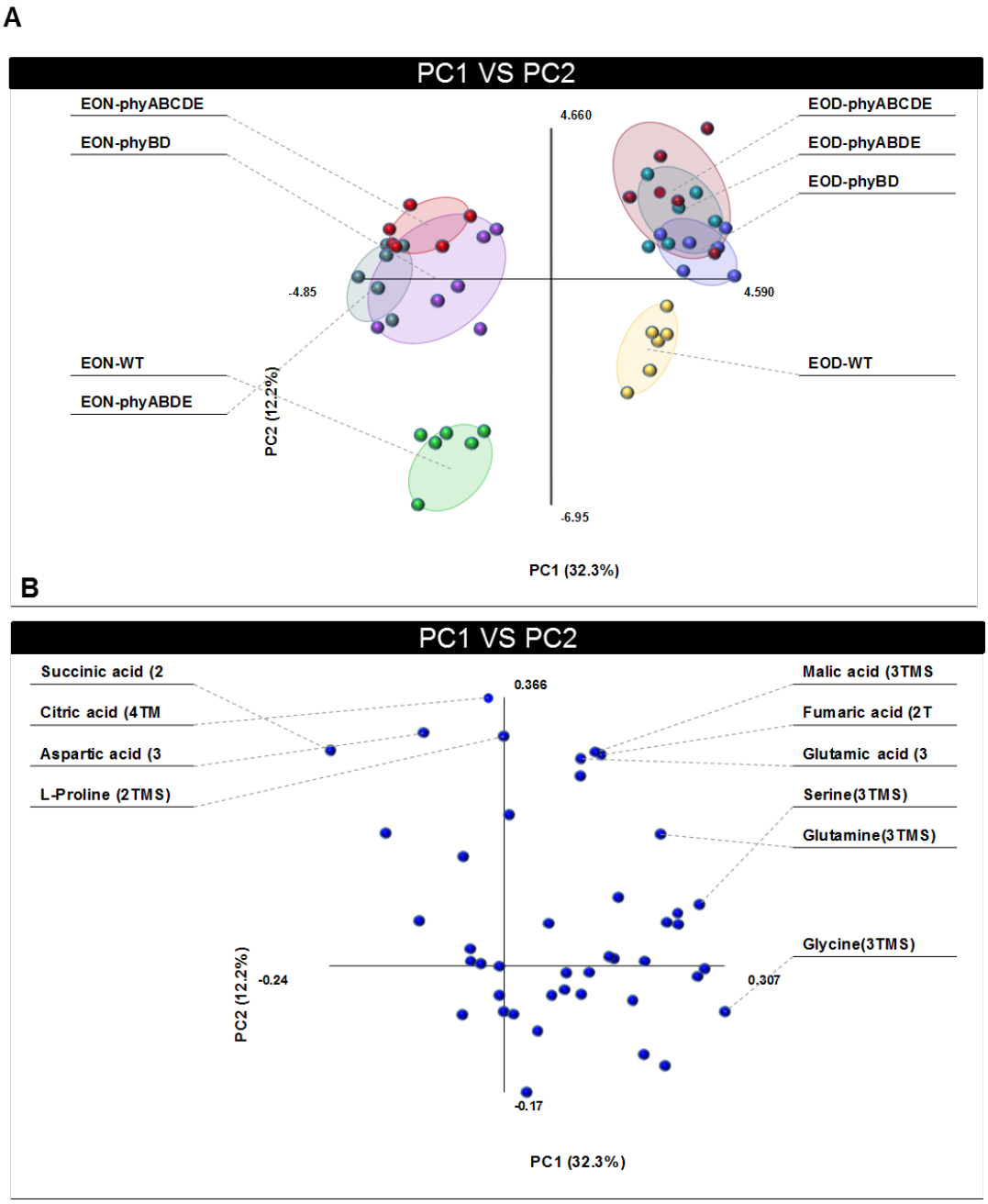

Figure 4.2 PCA (Principle Component Analysis) of metabolites in WT and phytochrome samples.

(A) Distribution of samples clustered using PCA score results. Sample replicates from the same genotype at certain time point were grouped in ellipses of different colours. Here PC1: time differentiation, PC2: mutant differentiation. (B) Loading variables (metabolites, represented as blue dots here) that contributes to the scoring process. Dots with marked names are the top ten significant variables contributing to sample distribution as shown in A. Data was log-transformed before applying PCA analysis. PCA was performed using the Multibase Excel add-in provided by Numberical dynamics, Japan.

4.4 Phytochrome Mutants Have Elevated Levels of Sugars and Alcohols, Organic Acids and Amino Acids Compared to WT

PCA results show that overall metabolic profiles of phytochrome mutants are different to that of WT at both EON and EOD (Figure 4.2). To take a closer look at each metabolite altered in these mutants, we classified the metabolites into three major classes (sugars, organic acids and amino acids) and plotted the data in bar charts with classical univariate statistical approach (Appendix Table 2).

Consistent with our sugar quantification (Figure 3.3), when compared to WT, *phyBD*, *phyABDE* and *phyABCDE* all have significantly elevated levels of metabolizable sugars including glucose, sucrose, especially at EOD (Figure 4.3 A). In particular, raffinose, often indicative of stress (Krasensky and Jonak, 2012), is much higher in mutants than in WT (Figure 4.3 A).

In the case of organic acids, three phytochrome mutants all show significantly elevated levels than WT at both EOD and EON. This includes succinic acid, malic acid, fumaric acid, citrate acid, glutamic acid and aspartic acid (Figure 4.3 B). All of these are also in the top ten list of significant variables contributing to the sample scoring analysis (Figure 4.2 B), supporting the consistency between two different analytical approaches.

Similarly, phytochrome-deficiency also leads to an over-accumulation of specific amino acids at EOD and EON, e.g. proline, 4-hydroxy-proline, glutamine, leucine, valine, phenylalanine, serine and glycine (Figure 4.3 C). Of note, proline levels are markedly elevated, a phenomenon that also has been linked with stress responses

(Hare et al., 1999; Bhaskara et al., 2015). Again, proline was among the top ten variables list (Figure 4.2B).

Collectively, phytochrome mutants have over accumulation of sugars, tricarboxylic acid (TCA) cycle intermediates (most of the organic acids) and amino acids compared to WT. This type of metabolic profile may be an inevitable consequence of the retarded growth phenotype. As phytochrome loss does not give rise to obvious differences in cellular respiration rate (Figure 3.2 B), a reduced in demand for protein synthesis and cellulose production (Figure. 3.7 C-D) could lead to an accrual of intermediates and products of the metabolic supply pathways. It might also be worth pointing out that for most of these metabolites, loss of phyB and phyD appears to have the greatest impact. This is possible as that the cell wall genes shown in Chapter 3 also have a similar reduction in *phyBD* as to that in *phyABDE* (Appendix Figure 2).

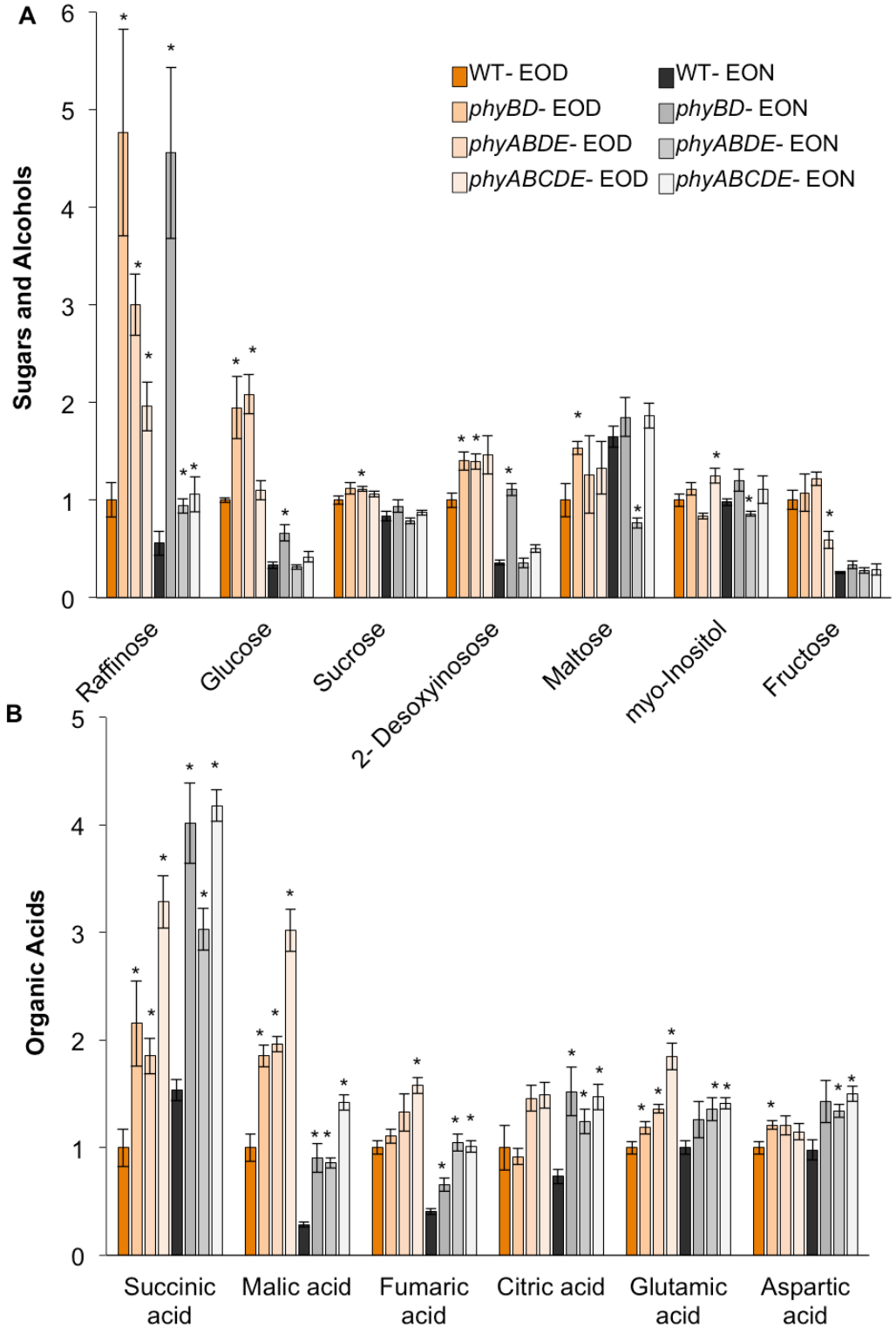
A
Sugars and Alcohols
WT- EOD
WT- EON
phyBD- EOD
phyBD- EON
phyABDE- EOD
phyABDE- EON
phyABCDE- EOD
phyABCDE- EON
Raffinose
Glucose
Sucrose
2- Desoxyinosose
Maltose
myo-Inositol
Fructose
B
Organic Acids
Succinic acid
Malic acid
Fumaric acid
Citric acid
Glutamic acid
Aspartic acid

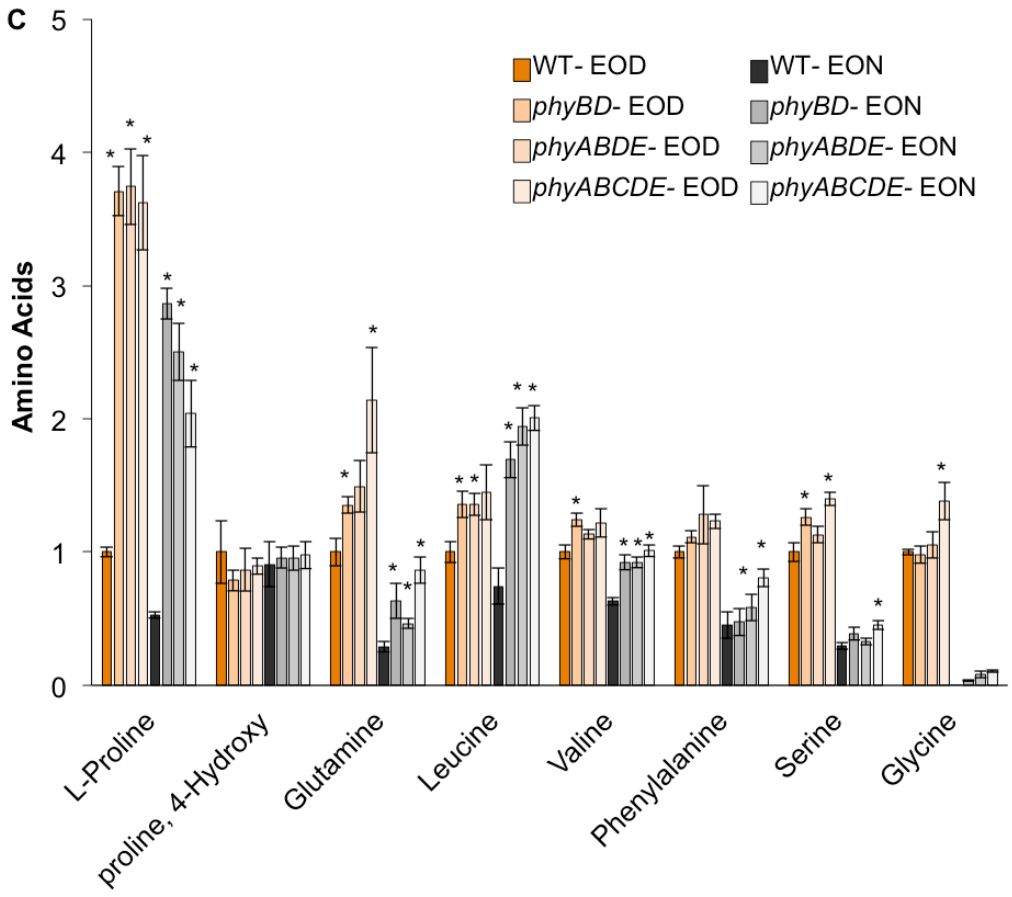

Figure 4.3 GC-MS metabolomics quantification of WT and phytochrome mutants sampled at dawn and dusk.

(A) Relative quantification of sugars and alcohols in WT and phytochrome mutants at EON and EOD respectively. (B) Relative quantification of organic acids. (C) Relative quantification of amino acids. Values presented are mean ± SEM. Asterisks indicate a significant difference between values of the phytochrome mutants and WT at EOD and EON respectively, by means of Student's t-test at *, $p \leq 0.05$.

4.5 Transcriptional Analysis of Enzyme Genes in Related Pathways

Phytochromes are reported to control plant growth and development mostly through transcriptional network regulation (Jiao et al., 2007). Therefore, I conducted a series of time course qRT-PCR experiments to explore whether gene expression of the key enzymes responsible for the elevated metabolites are also up-regulated in phytochrome mutants.

I first checked the group of organic acids, as they are constitutively elevated in phytochrome mutants at both EON and EOD (Figure 4.3 B). Also these metabolites are nicely clustered in the TCA cycle and related pathways. I picked candidate genes of two mitochondria localized TCA cycle enzymes, *FUMARASE* 1 (*FUM*1) and *CITRATE SYNTHASE* 4 (*ATCS* or *CSY4*), a cytosolic fumarase *FUM2* and a glyoxylate enzyme *ACETATE NON-UTILIZING* 1 (*ACN1*) that generates a potential second source of organic acid metabolites. Surprisingly, despite that fact that all the organic acids quantified in this study are elevated, these genes are generally repressed in *phyABDE* (Figure 4.4), especially for the two fumarases at their peak times. This implies that the increased abundance of organic acids in phytochrome mutants is not caused by upregulated enzyme transcription. Instead, the excess metabolites could possibly repress relevant enzyme gene expression through negative feedback.

I went on the check two other elevated metabolites, raffinose and proline (Figure 4.3 A, C), which were reported to have special roles in abiotic stress responses (Hare et al., 1999; Bhaskara et al., 2015; Krasensky and Jonak, 2012). Similar to the TCA enzymes, gene expressions of biosynthetic enzymes for raffinose (*RAFFINOSE*

SYNTHASE 1/2, *SIP1* and *SIP2*) and proline (*DELTA1-PYRROLINE-5-CARBOXYLATE SYNTHASE 1* or *P5CS1*, and *PYRROLINE-5- CARBOXYLATE REDUCTASE* or *P5CR*) are also repressed in a relatively milder manner (Figure 4.5 A and B). In contrast, one synthetic pathway enzyme gene was indeed found to be induced in *phyABDE* compared to WT, i.e. *RAFFINOSE SYNTHASE 6 / DARK INDUCED 10 (DIN10)* (Figure 4.5 A). At the same time, the main catabolic enzyme of proline pathway, *PROLINE DEHYDROGENASE* (*PRODH*), is also suppressed (Figure 4.5 B). This might be due to a negative feedback from the product Pyrrolin-5-Carboxylate, though its level was not revealed in our metabolome study. The up-regulation of *DIN10*, together with the repression of *PRODH*, may partly contribute to the elevation of raffinose and proline content.

The above results demonstrate that the increased abundance of certain metabolites in phytochrome mutants is not due to elevated enzyme gene expression in the synthesis pathways. Instead, the generally repressed enzyme transcription indicates a retarded flux of the metabolites, highlighting the novel role of phytochromes in directing carbon and nitrogen resource to growth.

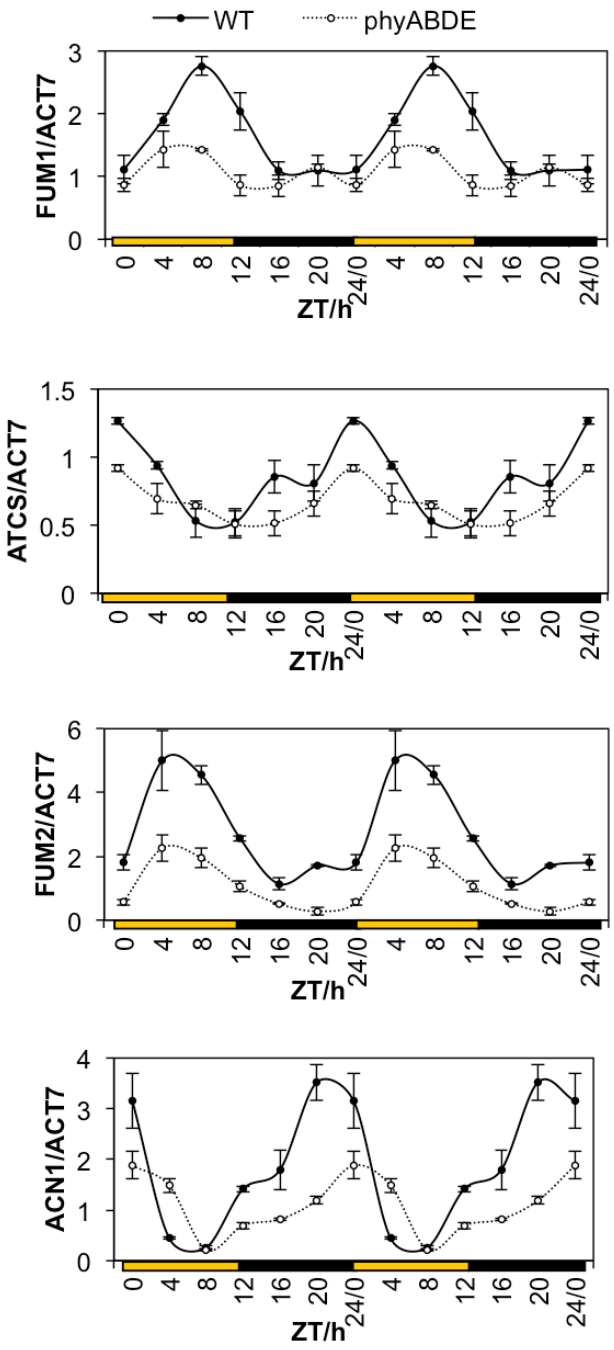

Figure 4.4 Diurnal expression profiles of metabolic enzyme genes involved in TCA and related pathways.

qRT-PCR results of metabolic enzyme genes *(FUM1, FUM2, ATCS* and *ACN1*) in 5-week WT and *phyABDE* samples through a 24-hour time course. Data was double plotted for visualization purposes. ZT: Zeitgeber time. Values are presented as mean ± SEM.

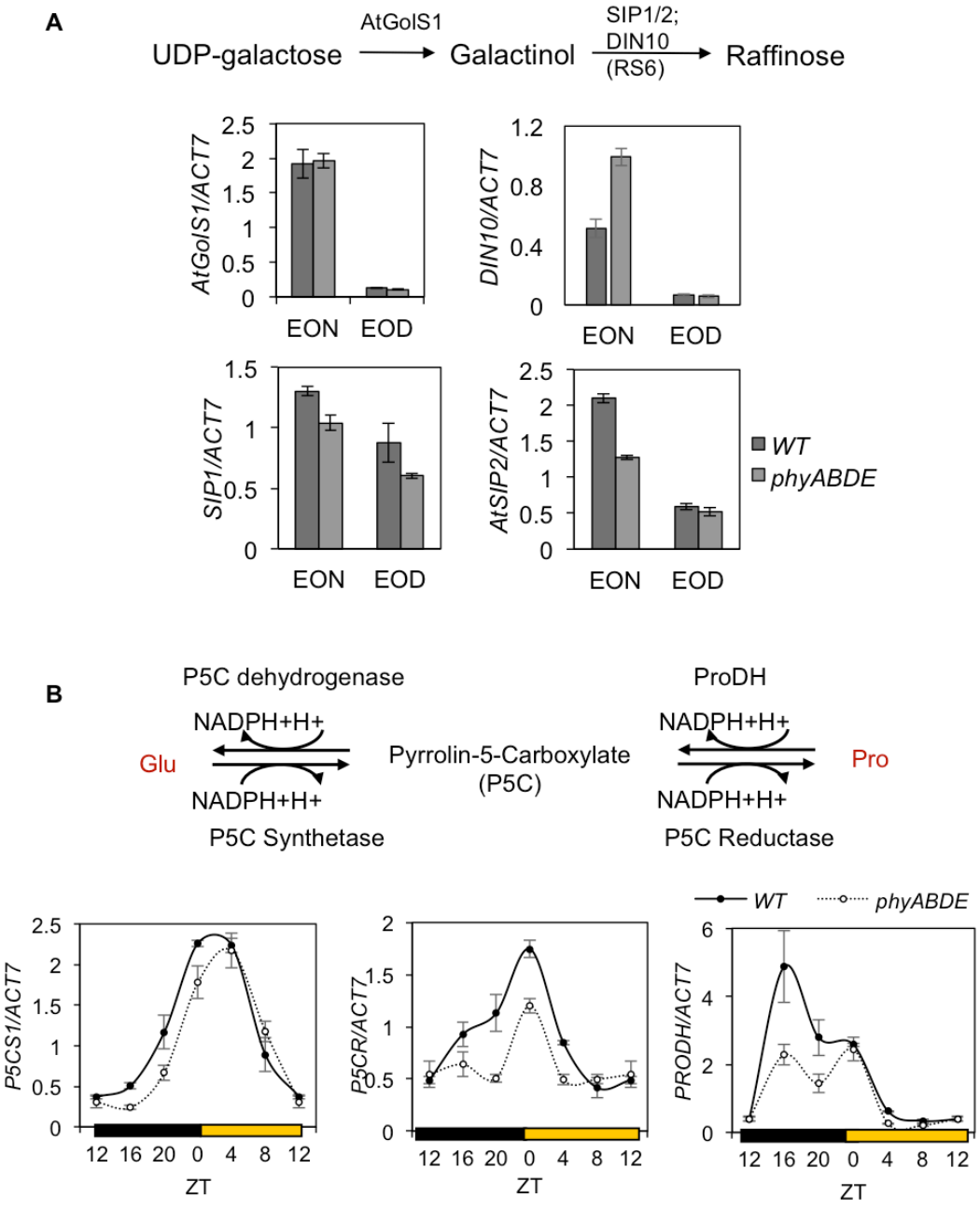

Figure 4.5 Diurnal expression profiles of metabolic enzyme genes in raffinose (A) and proline (B) metabolic pathways.

qRT-PCR results in 5-week WT and *phyABDE* samples at EON and EOD, or over 24-hour time course. ZT: Zeitgeber time. Values are presented as mean ± SEM.

4.6 Phytochrome Mutants Have Reduced Sensitivity to Abiotic Stresses at Both Seedlings and Adult Stages

It has been widely reported some metabolites, such as proline and raffinose, will be elevated in plants upon abiotic stress, including ABA, salt and drought (Hare et al., 1999; Bhaskara et al., 2015; Krasensky and Jonak, 2012; Urano et al., 2009; Kempa et al., 2008). This is commonly regarded as a protection response, not only to enhance plant tolerance through osmotic adjustment but also to supply energy resource for resumed growth once the stress is removed. The GC-MS analysis revealed that phytochrome mutants have significantly more proline and raffinose than WT when grown in non-stress conditions, which may prime the mutants to be more prepared for the up-coming stresses.

Plant growth is commonly repressed when resources are deployed to cope with stressors such as salt or ABA (Colebrook et al., 2014; Skirycz and Inzé, 2010). The retarded growth of phytochtome mutants was previously proposed to be the result of improper resource allocation, which, in this case, could be a prior stress preparation. Therefore, I speculated the metabolites might provide some stress protection in phytochrome mutants, making them less affected by stress induced growth repression.

I first tested this hypothesis in young seedlings. 11-day old seedlings of WT, *phyBD*, *phyABDE* and *phyABCDE* were transferred to growth media with different doses of salt (NaCl) or ABA for 10 days. Photos were taken before biomass data was collected (Figure 4.6 A), which shows salt-induced bleaching response in WT was very much reduced in all three phytochrome mutants. The biomass data also concurs with the prediction. Indeed, while a dose-dependent inhibition of growth by ABA or

NaCl is shown in WT plants, the effect is sequentially less marked in *phyBD*, *phyABDE* and *phyABCDE* (Figure 4.6 B).

In adult plants, similar results were obtained when treated with ABA or NaCl. In Figure 4.7, four-week-old soil-grown plants were watered once with ABA/NaCl solution to soil capacity followed by normal irrigation procedure every other day till data was collected two weeks later. Again, biomass reduction response was alleviated in *phyABDE* compared to WT with either ABA or NaCl treatment (Figure 4.7 A). NaCl application has also been shown to reduce chloroplast levels (Jiang et al., 2013), which was observed in WT plants upon salt treatment from our results. In contrast, the *phyBD* and *phyABDE* plants once again showed less sensitivity in this response (Figure 4.7 B-C). In comparison, both phytochrome mutants in this case have similar biomass response to drought stress as compared to WT (figure 4.7 A).

Overall, the data demonstrates that phytochrome mutants have increased levels of stress indicative metabolites and reduced abiotic stress response to ABA and salt. This suggests an interesting role of phytochromes in switching metabolic states between growth-promoting and stress-priming statuses.

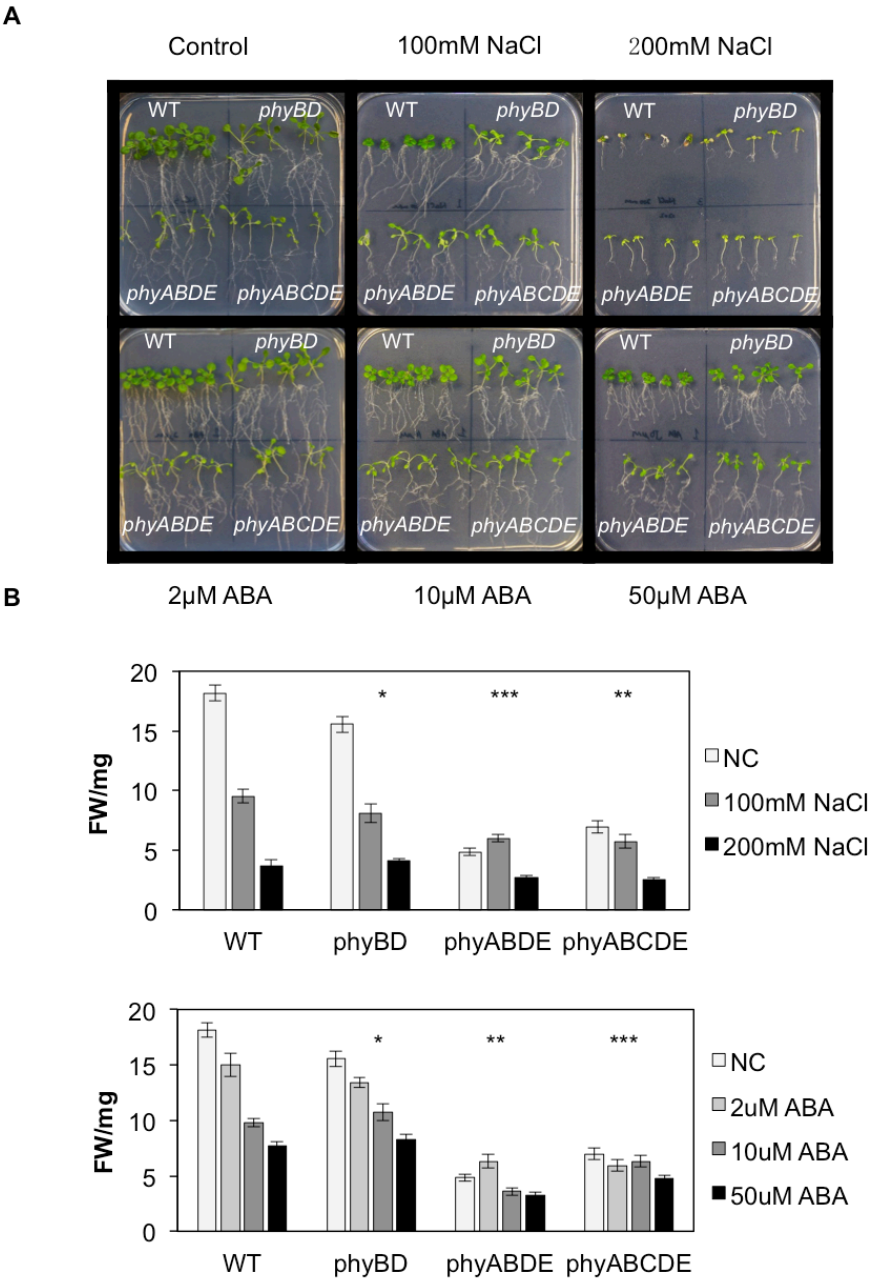

Figure 4.6 Salt and ABA stress response in seedlings.

(A) Representative photo of seedlings after stress treatment. Genotypes tested are L*er* (WT), *phyBD*, *phyABDE* and *phyABCDE*. (B) Fresh weight quantification of seedling after stress test. Values presented are mean ± SEM. Asterisks indicate significant differences in biomass response to the maximum dose treatment for each phytochrome mutant vs WT, as assessed by two-way ANOVA (data log-transformed for analysis) (* $p \leqslant 0.05$, ** $p \leqslant 0.01$, *** $p \leqslant 0.001$). ANOVA analysis was generated using the Real Statistics Resource Pack software (Release 4.11 Excel 2010/2013/2016) by Charles Zaiontz.

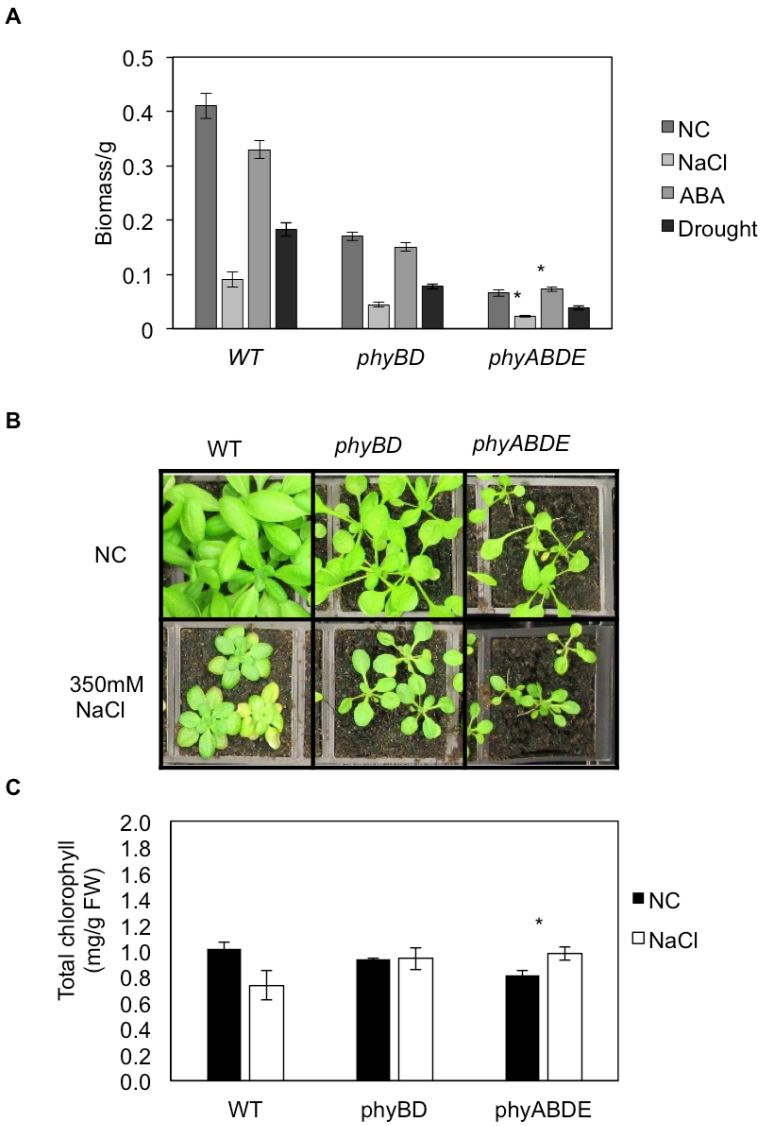

Figure. 4.7 Salt, ABA and drought stress response in adult plants.

(A) Quantification of salt (NaCl) and ABA stress repression of biomass (fresh weight) in adult plants. (B) Appearance of WT and phytochrome plants 14 days after watering same amount of 350mM NaCl solution once. (C) Chlorophyll determination in each genotype from salt stress test as shown in (B). Values are presented as mean ± SEM. Asterisks indicate significant differences in the response to ABA/salt treatment for each mutant compared to WT, as assessed by two-way ANOVA (fresh weight data log-transformed for analysis)(* $p \leqslant 0.05$). ANOVA analysis was generated using the Real Statistics Resource Pack software (Release 4.11 Excel 2010/2013/2016) by Charles Zaiontz.

4.7 Stress Marker Genes are Up-regulated in Phytochrome Mutants

Phytochrome deficiency leads to elevated stress indicating metabolites and reduced sensitivity to salt/ABA stress, raising the question whether stress response genes are induced in these mutants in normal growth conditions.

Candidate genes were picked from published reports, all shown to be induced in plants upon abiotic stress treatments such as salt, ABA, cold, etc (Pandey et al., 2005). Among these, morning genes *DARK INDUCIBLE 1 (DIN1), DIN10* and *RESPONSIVE TO DESICCATION 20 (RD20)* were the most induced at their individual peak time in *phyABDE* (Figure 4.8 A). Comparing to this, stress genes that peak at dusk, such as *COLD-REGULATED 15A (COR15A), RD29A and KIN1* (*At5g15960*), showed milder up-regulation in *phyABDE* (Figure 4.8 B). Nevertheless, this induction remains sustained through the entire rising phase of diurnal expression profile. In addition, some ABA specific signalling components, *ABA INSENSITIVE 1* (*ABI1*) and *ABI5*, showed a diurnal waveform alteration in *phyABDE* adult plants comparing to WT, indicating an increased transcript level during the daytime as well (Figure 4.8 C).

Similar observation in stress gene regulation was also found in seedlings. By analyzing published array data (Michael et al., 2008), Daniel Seaton from the Halliday lab found that *phyB-9* young seedlings have mild yet globally up-regulated stress gene expressions relative to C*ol-0* WT (Yang et al., 2016). Considering the function redundancy of phytochromes, this remains consistent with our results from *phyABDE* adult plants.

Overall, a general up regulation of stress genes was shown in phytochrome mutants, indicating a transcriptional preparation for unknown stresses. This, together with previous metabolic data, suggest an interesting scenario where plants in shade with phytochromes switched off might be more primed for upcoming environmental stress conditions at both metabolic and transcript levels.

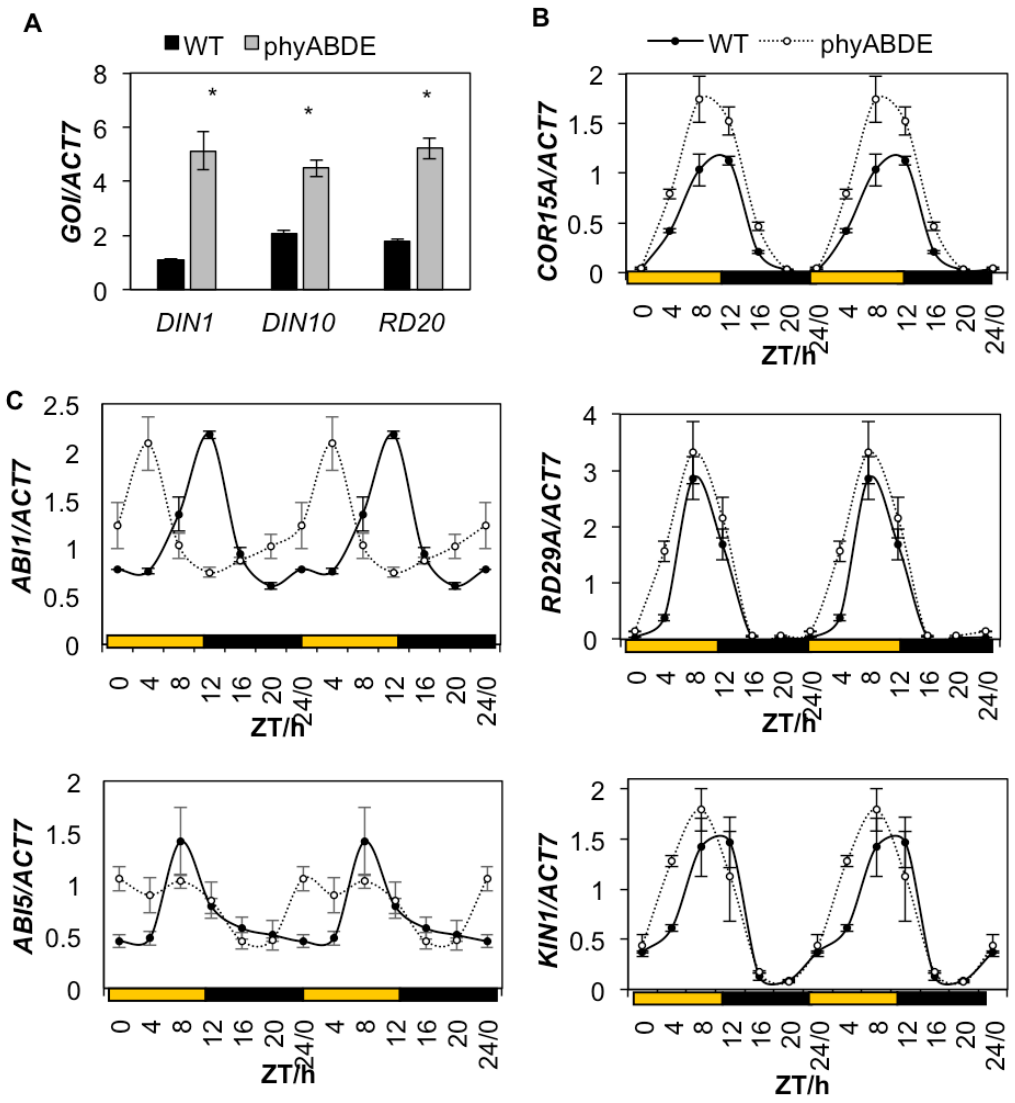

Figure 4.8. Stress marker genes and ABA pathway gene expressions are altered in *phyABDE* compared to WT plants.

(A) qRT-PCR analysis of stress genes induced in in 5-week-old *phyABDE* compared to WT (Ler) at peak time (ZT0 for *DIN1* and *DIN10*; ZT4 for *RD20*). GOI: gene of interest. (B) Diurnal gene expression of stress marker genes peaking later in the day (*COR15A, KIN1, RD29A*) in WT and *phyABDE*. (C) qRT-PCR analysis of ABA signalling pathway genes (*ABI1, ABI5*) through a diurnal time course. Time course data is double plotted for visualization purpose. Values presented are mean ± SEM. Asterisks indicate a significant difference between values of the *phyABDE* and WT, by means of Student's t-test at *, $p \leq 0.05$.

4.8 Discussion

Phytochrome photoreceptors are well known to regulate elongation growth and development in plants, yet their effect on metabolism has not been extensively explored. Following the interesting observation of elevated sugar levels in *phyBD* and *phyABDE*, this chapter shows 5-week-old phytochrome mutants have distinguished metabolic profiles compared to WT by probing the metabolome using non-targeted GC-MS approach (Figure 4.2). In particular, the data indicates phytochrome loss disrupts core metabolism, including a higher accumulation of sugar and sugar derivatives at EOD as well as constitutively elevated levels of TCA organic acids and several amino acids (Figure 4.3).

The result has confirmed our time-course quantification of sugars in Chapter 3 (Figure 3.3), and is broadly consistent with a rice study where phytochrome null mutant *phyABC* was reported to have a comparable metabolic profile (Jumtee et al., 2009). Young leaf blades of rice *phyABC* also has excessive amino acids, organic acids, sugars, though relative to our results it over-accumulates monosaccharides to a remarkable degree with glucose level promoted more than 50 folds compared to WT rice. This suggests a cross-species role for phytochromes in regulating plant metabolism.

A similar observation in metabolism alteration was also found in a clock mutant *prr975* (*PSEUDO- RESPONSE REGULATORs 9, 7, 5*), which has a higher accumulation of raffinose and proline together with defect in TCA cycle at both metabolic and transcriptional level (Fukushima et al., 2009; Nakamichi et al., 2009). More recently, another clock mutant *tic-2* (*TIME FOR COFFEE*) was reported to

have starch-excess phenotype with alteration in soluble carbohydrates including sucrose and fructose (Sanchez-Villarreal et al., 2013). Considering the close relationship between light and circadian signaling pathways, it may be unsurprising to propose a common role for both phytochromes and clock oscillators in regulating metabolic homeostasis.

Phytochromes are well known to control plant physiology through transcriptional regulation; hence the metabolite accumulation in phytochrome mutants might be caused by an activation of relevant enzyme genes. However, this hypothesis is denied by the result that shows several metabolic genes are repressed in *phyABDE*, demonstrating the metabolite excess phenotype is not due to enhancement of enzyme gene expression (Figure 4.4- 4.5). Instead, the general repression of enzymes might be the result of negative feedback from excess metabolites. Over accumulated products may inhibit synthetic enzyme genes, leading to a slowed down metabolic process. These results partly agree the idea that growth is not related to the absolute levels but the flux of the central resources (Cross et al., 2006).

Interestingly, the metabolic phenotype of phytochrome mutants partly resembles that of plants under ABA/NaCl treatment [Figure 4.3 and (Urano et al., 2009; Kempa et al., 2008)]. In particular, the remarkably elevated levels of raffinose and proline are commonly regarded as key indicators of abiotic stress (Krasensky and Jonak, 2012). The *prr975* clock mutant with elevated raffinose and proline also has an accumulation of ABA content and is reported to be more resistant to abiotic stress such as drought and freezing (Fukushima et al., 2009; Nakamichi et al., 2009). Furthermore, a recent study shows maize PIF3 transgenic rice has increased

tolerance to salt and drought abiotic stress (Gao et al., 2015). All these suggest phytochrome mutants might also have enhanced resistance to stress compared to WT.

Plants under salt or ABA conditions would re-allocate resource to cope with the stress, leading to a temporal alleviation of growth. This was confirmed in our stress tests of WT plants, where fresh biomass was largely reduced when treated with NaCl or ABA at both seedling (Figure 4.6) and more developmental adult (Figure 4.7 A) stages. In contrast, phytochrome mutants (both young and mature) with compromised growth are less responsive to the stress induced biomass repression (Figure 4.6, 4.7 A). Similarly, leaf bleaching, or chlorophyll reduction, as another stress phenotype is also very much alleviated in phytochrome mutants (Figure 4.6 A, 4.7 B-C). In addition, stress marker genes are elevated in phytochrome deficient plants grown in non-stress conditions (Figure 4.8), suggesting a possible scenario where phytochrome absence primes plants at both metabolic and transcriptional level to better cope with future stresses.

It is worth noting that, the above stress observation in phytochrome mutants probably depends on ambient temperature. A previous study on freezing tolerance revealed a similar induction of cold responsive genes like COR15A in Arabidopsis seedlings under low R: FR light at 16°C but not 22°C (Franklin and Whitelam, 2007). Similarly, (Patel et al., 2013) reported low R: FR grown Arabidopsis has elevated levels of soluble sugars, glycine and proline, again at 16°C but not 22°C. In this chapter, all plants were grown at 18°C, closer to the cool temperature used in previous research. A different metabolic profile and stress response in phytochrome mutants might be shown at warm temperatures. This adds to the scenario where

phytochromes are coordinating plant growth and stress physiology in a temperature-dependent manner.

In summary, following results from Chapter 3, this chapter further uncovered a broader metabolic change in phytochrome mutants, including a general induction of sugars, organic acids and amino acids. In particular, the elevated levels of raffinose and proline are likely to contribute to the reduced sensitivity of growth inhibition by abiotic stresses such as ABA and NaCl. An extensive up regulation of stress genes in non-stress conditions may also prime phytochrome mutants to better cope with the upcoming stresses. Taken together, this chapter provides evidence that phytochromes have a great impact on plant metabolism, and may control the switch between growth and stress physiology at both metabolic and transcriptional level. This knowledge could be helpful in estimating the effect of natural shade on plant biomass and stress resilience.

Chapter 5- Phytochrome Mutants Have Altered Response to Prolonged Darkness

5.1 Introduction

Plants have evolved to adapt to the ever-changing light in natural environment, especially the diurnal light alternate. Starch mobilisation in plants is finely optimized to maintain respiration and continuous growth at night when sunlight is unavailable (Stitt and Zeeman, 2012). More amazingly, plants can predict the length of the coming night and adjust starch degradation rate right from the beginning of dusk to ensure carbon depletion just before dawn (Smith and Stitt, 2007; Graf et al., 2010; Scialdone et al., 2013). Even in very short photoperiods, where carbon resource is limited, plants can still survive by precisely coordinating growth, starch, protein and central metabolism (Gibon et al., 2009, 2004).

When plants are left in darkness longer than expected night, starch supply will run out, inducing a carbon starvation response. Low carbon level is detected by T6P-SnRK1 signalling components that trigger a series of transcriptional regulation to repress growth, only allowing minimum life maintenance (Nunes et al., 2013; Baena-González et al., 2007). Following responses include remobilization of chlorophyll, proteins and lipids, accompanied by changes in chloroplast size and number, a process known as autophagy (Izumi et al., 2013; Wang et al., 2013; Rose et al., 2006;

Wada et al., 2008). At this point, leaf colour is changed to yellow visibly; plant senescence is triggered.

Dark induced plant senescence seems similar to age induced senescence in many ways, including chlorophyll loss and induction of several senescence associated genes (Woo et al., 2001; Guo and Gan, 2006; Kim et al., 2009). As a result, dark treatment has long been used as a rapid approach to study developmental senescence (Weaver and Amasino, 2001). Despite of the known shared mechanism, however, a transcriptome assay reveals a significant distinction between dark and age induced senescence (Buchanan-Wollaston et al., 2005). In addition, unlike age senescence that usually develops from leaf tip to base, dark induces leaf senescence without directional preference (Song et al., 2014).

It might not be too surprising that phytochromes have been linked to dark induced senescence for decades. Early work reported that 5-min red light pulse per day inhibits dark-induced chlorophyll loss in *Marchantia*, while a following 10-min far-red light can reverse this effect and induce bleaching (De Greef et al., 1971). This was also observed in Arabidopsis in a recent study, where a detailed molecular mechanism has been proposed (Sakuraba et al., 2014): PIF4 and PIF5 promote leaf senescence through ethylene and abscisic acid signalling, as well as direct activation of *ORE1* (a main NAC transcription factor that promotes senescence). Phytochromes, especially phyB, are considered to suppress senescence by negatively regulating PIFs. This was also supported by the observation that *phyB* mutant has more chlorophyll loss, ion leakage and senescence marker genes expression (*SEN4* and *SAG12*) in response to darkness than C*ol* WT (Sakuraba et al., 2014). This is further supported

by following studies using *phytochrome*/*pif* mutants or transgenic lines in Arabidopsis (Song et al., 2014; Zhang et al., 2015) and rice (Piao et al., 2015). PIF3, 4 and 5 are also reported to regulate developmental senescence in Arabidopsis (Song et al., 2014), indicating the PHY-PIF might control the shared pathway of both dark and age induced senescence in plants.

Surprisingly, however, phytochrome mutants are also reported to be hyposensitive to dark induced chlorophyll degradation (Brouwer et al., 2014): 6-week W*s* WT had significantly reduced chlorophyll after 6-day dark treatment, while *phyB-10* and *phyA-5-phyB-10* mutants maintained their chlorophyll levels throughout the dark period. *phyA* mutant, however, was shown to have increased chlorophyll reduction than WT in partial shade but not in dark (Brouwer et al., 2012, 2014). These indicate a more complicated relationship between phytochromes and dark induced response that cannot be fully explained by current knowledge.

So far, it remains unclear how high order phytochrome mutants react to prolonged darkness. Data from Chapter 4 suggests altered metabolic profiles may prime phytochrome mutants more tolerant to external salt and ABA (Figure 4.3, 4.6, 4.7). Dark induced stress shares some common responses to other stressors; likewise, phytochrome mutants could also be protected from darkness through the accumulation of metabolites like proline and pre-induced stress genes like *DINs* (Figure 4.8). In this chapter, I performed some dark experiments to find that L*er* phytochrome mutants, including *phyBD* and the more severe *phyABD*, *phyABDE*, have reduced sensitivity to darkness in terms of survival rate and chlorophyll loss. The results agree with a published study in Wassilewskija (W*s*) phytochrome

mutants, yet go against other reports using C*ol* lines. A preliminary test of background effect on dark induced chlorophyll loss in phytochrome mutants is then carried out.

5.2 Phytochrome Multiple Mutants Are Less Responsive to Dark than L*er* WT

For consistency, L*er* (WT), *phyBD*, *phyABD* and *phyABDE* plants were grown in previous condition: 100 $\mu mol \cdot m^{-2} \cdot s^{-1}$ white light, 8L: 16D short photoperiod for the first two weeks, followed by 12L: 12D photoperiod for three weeks; Temperature was maintained at 18°C throughout the whole experiment. Five-week plants were transferred to dark cabinets for two weeks, then back to 12L: 12D photoperiods to score survival rate.

Phytochrome mutants are more likely to survive through 2-week darkness

After dark treatment, a large proportion of WT plants turned yellow, particularly the older leaves. In contrast, *phyBD*, *phyABD* and *phyABDE* showed less leaf yellowing (Figure 5.1, 5wks+D14). The difference was even more striking after plants were transferred back to diurnal conditions for a week. Re-introduction to light/dark cycles caused widespread bleaching and death of WT plants, while a high percentage of phytochrome mutants recovered and resumed growth (Figure 5.1, 5wks+D14+L7). This implies that dark treatment caused more damage in WT than in phytochrome mutant plants.

Phytochrome mutants have less chlorophyll loss in response to dark treatment

In line with the survival test, I quantified chlorophyll level in these plants before and after 1, 7 and 10 days' dark incubation. Consistent with published results (Sakuraba et al., 2014; Song et al., 2014; Brouwer et al., 2012), WT plants have reduced chlorophyll content during prolonged darkness. In particular, after 7-day dark treatment, L*er* chlorophyll level dropped to half of that in normal growth conditions (Figure 5.2, L*er* D10 vs D0). In contrast, phytochrome mutants have significantly less chlorophyll than L*er* before the treatment (Figure 5.2, D0; consistent with Figure 3.1 A); their chlorophyll content also fell after 7 days in darkness, but at a significantly reduced rate compared to the WT (*phyBD* 0.28, *phyABD* 0.34, *phyABDE* 0.27 vs L*er* 0.46, Figure 5.2).

Observations above suggest that phytochrome mutants withstand prolonged darkness better than WT, and are more likely to survive afterwards. Similar to other stress tests described in Chapter 4, the absence of phytochromes, mainly *phyB* and *phyD*, reduced plant sensitivity to dark stress, highlighting a potential advantage of these plants in certain environmental conditions where light is blocked unexpectedly.

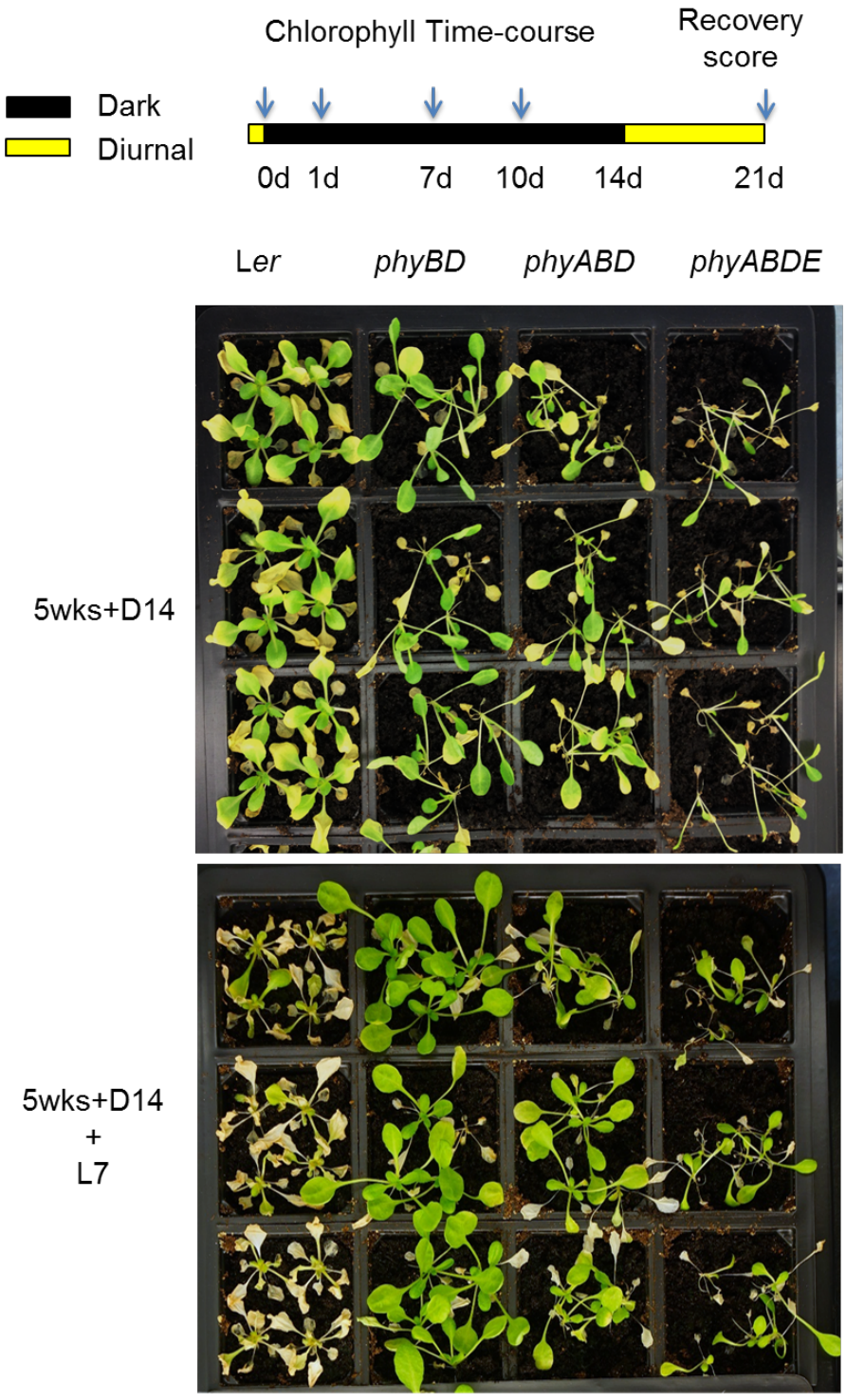

Figure 5.1 Phytochrome mutants are more likely to survive after dark incubation than WT plants.

Five-week-old plants (Ler, phyBD, phyABD, phyABDE) were moved to dark cabinets for 2 weeks (5wks+D14) and returned to 12: 12 light/dark cycle for another week (5wks+D14+L7).

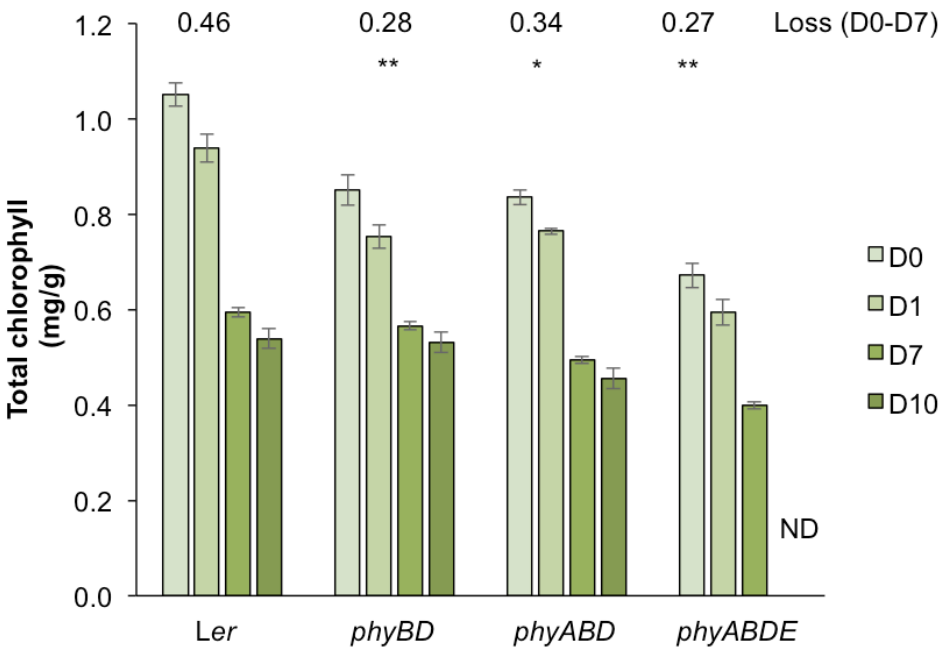

Figure 5.2 Chlorophyll quantifications in L*er* WT and phytochrome mutants at subjective dusk (D0), day 1, 7 and 10 (D1, 7, 10) of darkness.

ND: D10 data for *phyABDE* is missing due to sample availability. Values are presented as mean ± SEM. Numbers above the bars indicate the difference of chlorophyll levels between D7 and D0 for each genotype. Asterisks indicate significant differences in chlorophyll loss for each phytochrome mutant vs WT, assessed by two-way ANOVA (* $p \leq 0.05$, ** $p \leq 0.01$). ANOVA analysis was generated using the Real Statistics Resource Pack software (Release 4.11 Excel 2010/2013/2016) by Charles Zaiontz.

5.3 Background Effect on Phytochrome-dependent Chlorophyll Loss in Response to Darkness

The finding that phytochrome mutants are hyposensitive to dark induced chlorophyll loss is consistent with a published study using *phyB-10* and *phyA-5-phyB-10* in W*s* background (Brouwer et al., 2014). However, an opposite result has been reported that *phyB* is hypersensitive to dark induced leaf yellowing- *PHYB-OX* and *pif* mutants are the opposite- compared to C*ol* WT (Sakuraba et al., 2014; Song et al., 2014; Zhang et al., 2015). This inconsistency raises an interesting question whether dark induced chlorophyll loss response in phytochrome mutants is accession-dependent.

To test this, I grew C*ol* and L*er* lines in identical growth conditions to same age. Chlorophyll content was quantified using whole rosette samples both before and after dark incubation.

Unlike L*er* lines, 5-week *phyB-9* (C*ol*) doesn't show reduced sensitivity to dark induced chlorophyll loss and plant death

Plants were first grown in previous condition described in 5.2. This is a cool condition with short photoperiods that allows all genotypes to grow up to 5-week-old before initiation of flowering. It is noteworthy that this condition is similar to that of W*s* study in (Brouwer et al., 2014), where *phyB-10* and *phyA-5-phyB-10* were grown in short-day condition for 6 weeks.

Again, all genotypes (L*er* and *phyBD*, *phyABDE*; C*ol* and *phyB-9*) showed more or less leaf bleaching (Figure 5.3 A) and chlorophyll reduction (Figure 5.3 B) after dark incubation. Consistent with data from Figure 5.2, a significantly reduced chlorophyll loss was shown in *phyBD* relative to L*er* WT after 2-week dark treatment (0.25 vs 0.63, Figure 5.3 B). Particularly, at the end of dark incubation, *phyBD* had more chlorophyll than L*er* WT (Figure 5.3 B). In contrast, 5-week *phyB-9* had less chlorophyll than C*ol* WT after darkness, agreeing with published data in (Sakuraba et al., 2014). Meanwhile, unlike the L*er* lines, C*ol* and *phyB-9* had similar amount of chlorophyll loss during the dark period (0.59 vs 0.54, Figure 5.3 B).

When plants were returned to previous diurnal condition for 4, 7 and 14 days, most L*er* rosettes gradually bleached and died, while a high percentage of *phyBD* and *phyABDE* resumed growth (Figure 5.3 C; consistent with data in Figure 5.1). In comparison, both C*ol* and *phyB-9* plants survived at a similar rate, in agreement with their indistinctive chlorophyll loss in dark treatment (Figure 5.3 B-C).

Briefly, these observations support the hypothesis that phytochrome control of chlorophyll loss (and post-dark survival rate) in response to dark incubation is background-dependent.

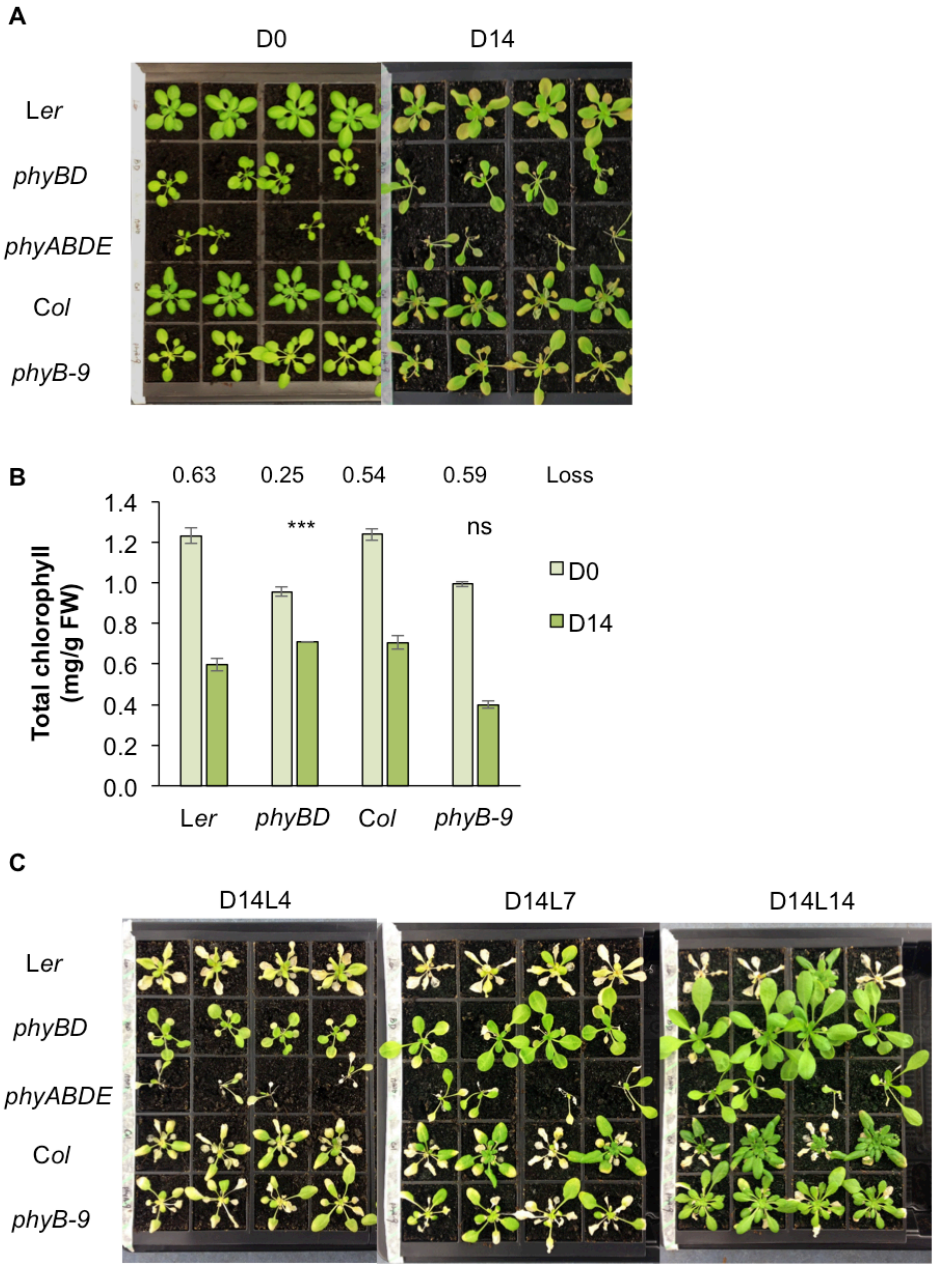

Figure 5.3 Dark responses of 5-week-old plants using Ler and Col lines.

(A) Photo of plants before and after dark treatment. (B) Total chlorophyll quantification of plants shown in (A). Data for *phyABDE* is missing due to sample availability. Numbers above the bars indicate the difference of chlorophyll between D14 and D0 for each genotype. Values are presented as mean ± SEM. Asterisks indicate significant differences in the response to 14-day dark treatment compared to the D0 between phytochrome mutants and respective WTs, as assessed by two-way ANOVA (ns: $p>0.05$; *** $p \leq 0.001$). ANOVA analysis was generated using the Real Statistics Resource Pack software (Release 4.11 Excel 2010/2013/2016) by Charles Zaiontz. (C) Photos of plants after being returned to light/ dark diurnal cycle for 4, 7 and 14 days respectively.

Similar background effect was also found in 3-week seedlings under long-day photoperiod, 23°C condition

In the second test, a completely different growth condition was used to test the robustness of the background-dependent dark response. Specifically, plants were grown in continuous light for one week before transferred to long day (16L: 8D), 23°C condition for further two weeks. This condition, comparing to the previous one, is longer in photoperiod and warmer in temperature, both accelerating flowering transition in WT and even more rapidly in phytochrome mutants (Figure 5.4 A). In addition to genotypes used in the first test, L*er phyB* and C*ol PHYB-OX* were also included to facilitate data comparison.

First of all, plants in this test also showed leaf bleaching and chlorophyll reduction after 5-day darkness (Figure 5.4 A-B), implying a similar dark response in this condition. Again, each L*er* phytochrome mutant has significantly less chlorophyll loss than WT (*phyB* 0.31, *phyBD* 0.32 vs L*er* 0.55, Figure 5.4 B), demonstrating a robust dark hyposensitivity in L*er* phytochrome mutants. In particular, *phyB* and *phyBD* had similar chlorophyll level both before and after darkness, suggesting phyB to be the main phytochrome in controlling chlorophyll response to darkness.

In this very condition, Col *phyB-9* has been reported to be more sensitive to dark induced response, while PHYB-OX transgenic line does the opposite (Sakuraba et al., 2014). Consistently, *phyB-9* had significantly less, while *PHYB-OX* had more, chlorophyll than C*ol* WT after dark treatment (Figure 5.4 B). Unlike that in L*er* lines, dark induced chlorophyll losses in *phyB-9* and C*ol* are indistinctive (0.37 vs 0.41, $p>0.05$). Meanwhile, *PHYB-OX* has significantly reduced chlorophyll loss than C*ol* (0.3 vs 0.41), supporting the published observation.

To summarize, similar results were obtained from a dramatically different growth condition, despite the distinction in developmental stages, implying that the accession effect on dark response in phytochrome mutants is fairly robust.

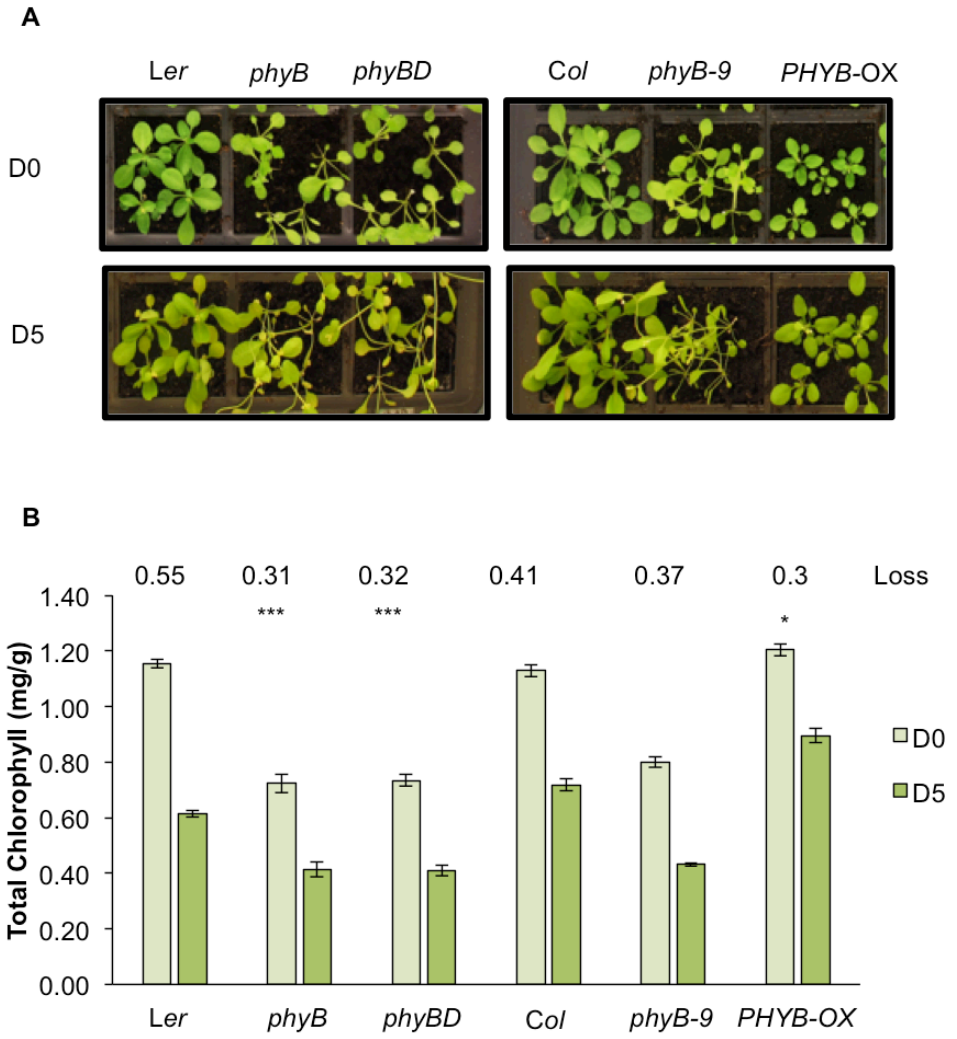

Figure 5.4 Dark responses of 3-week-old plants using L*er* and C*ol* lines.

Photos of plants (A) and total chlorophyll quantification (B) before and after 5-day dark treatment. Numbers above the bars indicate the difference of chlorophyll between D5 and D0 for each genotype. Values are presented as mean ± SEM. Asterisks indicate significant differences in chlorophyll loss between phytochrome mutants and respective WTs, as assessed by two-way ANOVA (* $p \leqslant 0.05$, *** $p \leqslant 0.001$). ANOVA analysis was generated using the Real Statistics Resource Pack software (Release 4.11 Excel 2010/2013/2016) by Charles Zaiontz.

5.4 Plants Grown in High-light Are More Susceptible to Dark Stress

While testing the accession effect, I also postulated that the dark hyposensitivity observed in L*er* phytochrome mutants might be related to retarded growth rate. This hypothesis came from the idea that plants with slower growth (Figure 3.6) and higher accumulation of sugar (Figure 3.3, 3.5) may require less fuel to sustain life maintenance, therefore survive longer in darkness.

Plant growth rate is easily manipulated by altering light intensity. Plants grown in high light conditions, with increased photosynthesis rate, are expected to grow faster and accumulate biomass more quickly than in low light. Indeed, as suggested by a previous growth test, both L*er* WT and *phyBD* accumulate more biomass under high light (Figure 5.5). Interestingly, the data also illustrates that *phyBD* is more responsive that L*er* WT to high light, suggested by a greater fold-change of fresh biomass between two light levels.

To test whether prior exposure to different light levels could alter the severity of the dark-induced response, I grew L*er* WT, *phyBD* and *phyABD* under 50, 100 or 170 $\mu mol \cdot m^{-2} \cdot s^{-1}$ for 5 weeks. Again, faster growth, indicated by larger rosettes, was observed for both WT and phytochrome mutants as fluence rate increases (Figure 5.6, Dark 0). Plants were then transferred to a dark cabinet for 13-day incubation.

Interestingly, after dark treatment, L*er* WT from three light levels show a gradient yellowing of leaves, implying that high light grown plants are more susceptible to dark induced bleaching (Figure 5.6, L*er*, Dark 13). This fluence rate-dependent dark response is even more obvious after plants were returned to previous growth

condition for 4 days (Figure 5.6, L*er*, Dark 13 + Light 4). In contrast, however, despite that phytochome mutant growth was also promoted by increased light (Figure 5.5 and 5.6 Dark 0), this gradient response was mostly missing in *phyBD* or *phyABD* (Figure 5.6, *phyBD* and *phyABD*, Dark 13). In addition, after re-introduction of light for 4 days, *phyBD* and *phyABD* under all three light conditions had similar yet significantly higher survival rates than L*er* WT (Figure 5.6, Dark 13 + Light 4).

This result implies that growth rate *per se* may not underlie the enhanced susceptibility to dark treatment, while at the same time, the level of irradiance to which the plants are exposed to before dark treatment may have a strong impact on the severity of dark senescence. Furthermore, phytochromes, especially phyB and phyD, are playing important roles in mediating this fluence rate-dependent response, suggesting the activation of phytochromes under high (red) light condition might cause plants to be more susceptible to unexpected darkness.

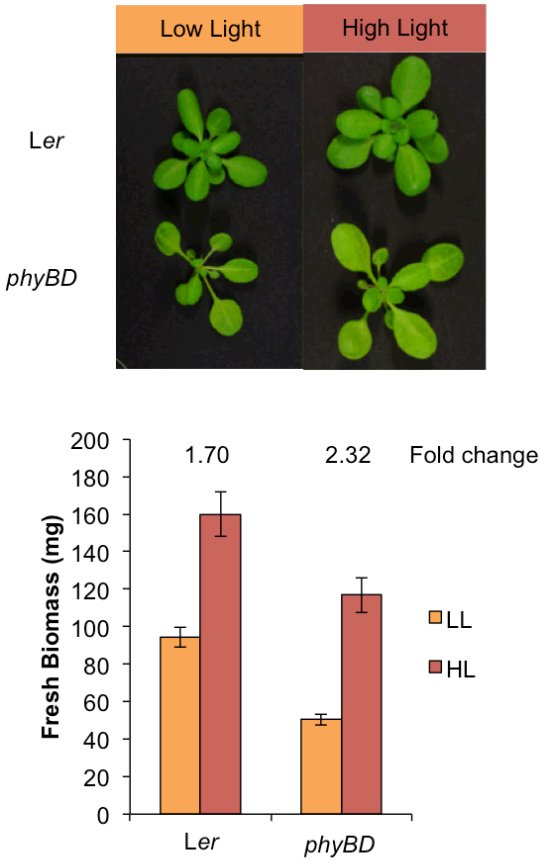

Figure 5.5 Represent photo and fresh biomass of L*er* and *phyBD* grown in different light levels.

LL: low light (90 μmol·m^{-2}·s^{-1}); HL: high light (175 μmol·m^{-2}·s^{-1}). Plants were harvested at 5-week-old. Numbers above the bars indicate the fold change of fresh biomass of plants grown in HL relative to LL. Values are presented as mean ± SEM.

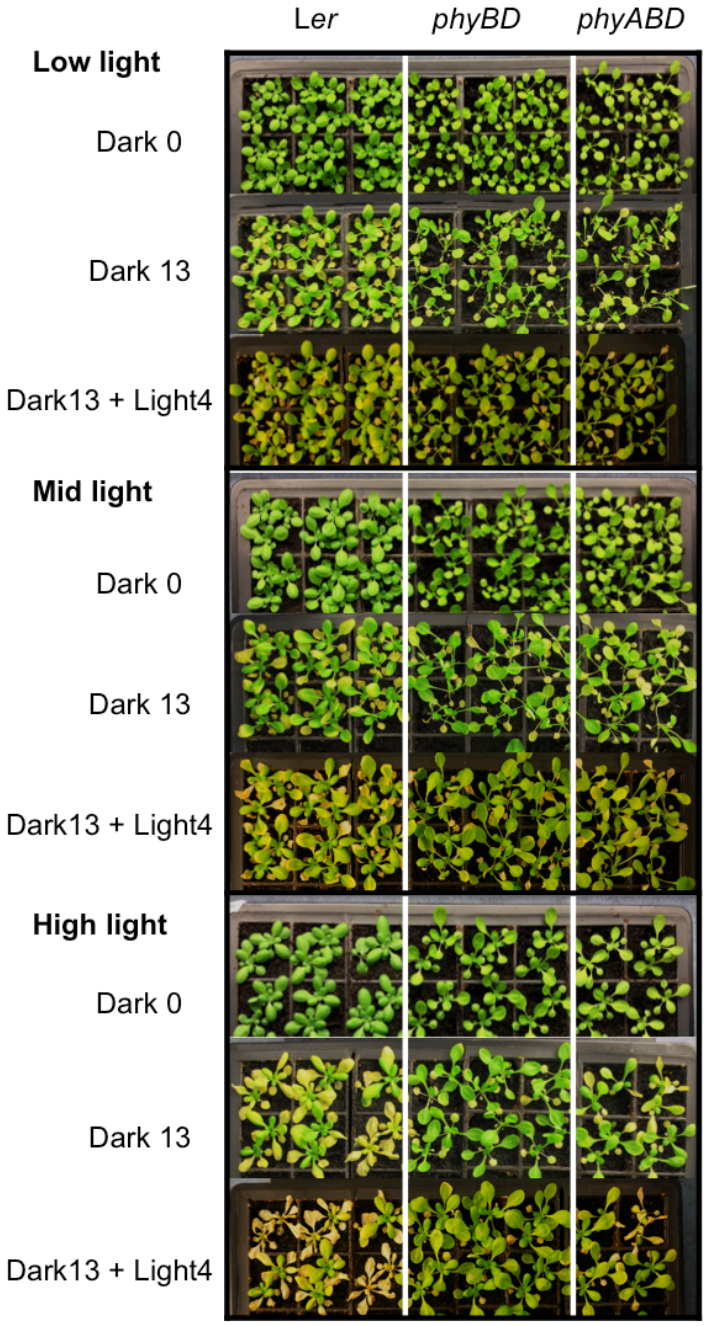

Figure 5.6 Dark test results of phytochrome mutants and WT from different light conditions.

Low light: 50 μmol·m^{-2}·s^{-1}; Middle (Mid) light: 100 μmol·m^{-2}·s^{-1}; High light: 170 μmol·m^{-2}·s^{-1}. 5-week plants were transferred to dark cabinets for 13 days, and then transferred back to original light conditions respectively for 4 days.

5.5 Discussion

In this chapter, I set out to test dark response in L*er* and high order phytochrome mutants by assessing chlorophyll loss and survival rate after dark incubation. The results demonstrated a hyposensitive response in *phyBD*, *phyABD* and *phyABDE* compared to L*er* (Figure 5.1 and 5.2), indicating the loss of phytochromes could protect plants from dark induced stress. This may not be too surprising, as phytochrome mutants were found less sensitive to ABA/salt stresses Figure 4.6 and 4.7). These mutants were believed to benefit from their altered metabolism, particularly the accumulation of stress indicators like proline and raffinose (Figure 4.3), and pre-induced stress genes (see Figure 4.8). Likewise, phytochrome mutants could also be protected from dark stress through the same mechanism as plants in dark exhibit similar phenotypic responses like growth retardation, leaf bleaching and transcript alterations (e.g. induction of *DIN* genes).

An alternative hypothesis was that growing slowly might enable plants to withstand darkness for a longer period. In this scenario, *phyBD* grows at a much slower rate than L*er* WT (Figure 3.6), implying a reduced necessity for energy resource to sustain growth; therefore, less chlorophyll is degraded in the dark (Figure 5.2). However, this growth rate hypothesis is unlikely to be true when two sets of data were cross-compared: *phyBD* under around 170 $\mu mol \cdot m^{-2} \cdot s^{-1}$ light grows faster (Figure 5.5) and survived (Figure 5.6); L*er* at about 100 $\mu mol \cdot m^{-2} \cdot s^{-1}$ grows more slowly (Figure 5.5) but died after dark treatment (Figure 5.6).

Interestingly, data in Figure 5.6 also demonstrated that increasing light level could enhance plant susceptibility to darkness in a phytochrome-dependent manner. While

L*er* WT plants showed a fluence rate response in leaf bleaching and survival chance after darkness, this response was mostly diminished in *phyBD* and *phyABD* (Figure 5.6). The idea that phytochromes are important in mediating light intensity-dependent dark response is rather novel. Not only prior light level effect on dark response has never been reported before, but also a red light pulse was known to inhibit dark induced bleaching in various species (De Greef et al., 1971; Sakuraba et al., 2014). It seems phytochrome activation before darkness enhances plant dark sensitivity, while phytochrome activation during darkness inhibits dark response. In natural conditions, plants in shade, such as high densities, perceive a decrease in red to far-red light ratio and receive less photosynthetic light. These plants, as suggested by my results, might be more tolerant to sudden darkness than those in direct sunlight.

By the time my results were obtained, there had already been a published study showing Ws background *phyB-10* is hyposensitive to dark induced chlorophyll loss (Brouwer et al., 2014). Because Ws wt contains a naturally occurring *phyD* mutation (Aukerman et al., 1997), a PHYD-expressing line (PHYD+) was also introduced and no distinction was found in chlorophyll level between Ws and PHYD+ either before or after darkness (Brouwer et al., 2014). These suggest a specific function of PHYB in promoting dark induced bleaching. In contrast, however, the majority of studies point to an opposite role for PHYB, which inhibits dark induced senescence by negatively regulating PIFs and various downstream pathways (Sakuraba et al., 2014; Song et al., 2014). Since almost all these experiments were conducted using C*ol* background accessions, I speculated there might be variations between the backgrounds. Phytochrome effect on dark induced chlorophyll loss response was then compared between L*er* and C*ol* accessions, including wt and phytochrome

mutants. Results from two different conditions both showed a reduced chlorophyll loss in L*er* background phytochrome mutants, which was missing in C*ol* lines (Figure 5.3 and 5.4). This preliminarily supports the background effect on phytochrome involvement in dark response, necessitating potential re-evaluation of the general conclusions drawn from C*ol*.

It might be worth pointing out that the absolute chlorophyll level after darkness *per se* does not seem to correlate with plant survival rate. *phyB-9* with the least chlorophyll at the end of dark incubation survived, while L*er* are all bleached, after 14 days back to light (Figure 5.3). Rather, the amount of chlorophyll loss during darkness is more likely to implicate the severity of tissue damage caused by dark. Also, whether age or developmental stage affect the results of dark test still remains mysterious. Plants grown under long photoperiod, 23°C condition for 3 weeks have already entered reproductive phase, particularly for phytochrome mutants (Figure 5.4 A).

Collectively, this chapter explored the role of phytochromes in dark induced stress response, particularly chlorophyll loss and the post-dark survival rate. A reduced dark sensitivity was shown in phytochrome mutants from L*er* but not C*ol* background, suggesting potential underlying variations between natural accessions. Further, increasing light intensity was found to promote plant susceptibility to dark induced bleaching in a phytochrome-dependent manner.

Chapter 6- Discussion

Previous phytochrome studies have mainly focused on elucidating the early molecular signaling events that follow photoreceptor activation in seedling developmental stage. More recently, new interests have been raised to explore phytochrome-signaling interaction with sugars, from chlorophyll synthesis regulation to hypocotyl elongation promoted by exogenous sucrose application. Phytochrome effects on adult plant growth and biomass has also been reported; yet relevant knowledge is rather fragmented. This thesis sets out to study how phytochromes control biomass production through carbon metabolism, especially in adult plants. I have shown that phytochrome mutants have reduced photosynthesis, growth and biomass, yet excess sugars and proline together with enhanced stress tolerance. A hypothesis was then proposed that phytochromes are playing important roles in regulating plant metabolic switch between growth-promoting and stress-coping statuses. Following observations presented in Chapter 3-5, here I want to discuss some intriguing questions raised by my data, and propose some perspectives for potential future work that would help uncover the molecular mechanism underlying phytochrome control over growth and stress.

6.1 Phytochrome Regulation of Carbon Resource

Chapter 3 shows phytochrome mutants accumulate more starch and sugars (Figure 3.3). This is rather surprising considering photosynthesis is partly repressed in these mutants (Figure 3.2). The observation of altered diurnal growth pattern in *phyBD* implies less carbon being invested into growth especially during daytime (Figure 3.6). In other words, phytochromes were suggested to regulate carbon allocation into growth particularly in light. However, how this regulation works remains mysterious. Below are some potentially interesting ideas I have come up to pursue this question.

First, it is still unclear how sucrose consumption is regulated by phytochromes. One possible way could be through manipulating sucrose allocation and partitioning between the sink and source leaves. This is partly supported by a metabolic study in rice that shows the *phyABC* null mutant differs greatly from WT in young leaves but not so much in mature leaves (Jumtee et al., 2009). This hypothesis could presumably be tested by tracking sucrose directly using CO_2 isotopes labeling analysis as described in (Kölling et al., 2013). It would be even more helpful if attached young single leaf expansion can be monitored to see how it is affected by both sucrose import and CO_2 assimilation. By comparing these parameters between WT and mutants, we will be able to establish which of these processes is phytochrome dependent.

Second, phytochrome mutants may not always have more starch and sucrose than WT. Certainly, at the 2-week-old both WT and phytochrome mutant seedlings have little starch, and there is no obvious difference at this stage (Appendix Figure 3). In addition, these young seedlings without phytochromes were found to have more

glucose, instead of sucrose, than WT (Appendix Figure 3). This involves the transition of dominant sugars used by plants at different developmental stages, also the change in their photosynthesis and carbon consumption rate. As a result, a time course quantification of sugars from seedling to mature plant would be helpful in elucidating phytochrome effect on carbon content.

Third, apart from regulating starch quantity, phytochromes might also affect starch quality. Chapter 3 presents an interesting preliminary finding that *phyABDE* has much less amylose than WT (iodine staining results, Figure. 3.4), which is probably caused by the absence of phytochrome E. The idea that light signaling could affect starch composition through plant photoreceptor is rather interesting and could be of great value to biotechnology research in starch industries.

6.2 Phytochrome Control of Growth: Perspectives from *XTHs* Regulation

A large body of photoreceptor research has established the role of phytochromes in inhibiting elongation growth. For plants in dark, shade (e.g. low R: FR light experimental conditions where phytochromes are inactivated), or plants without phytochromes, seedling hypocotyl length, or leaf petiole elongation, is promoted partly through auxin pathways by PIFs (Lorrain et al., 2008). More recently, brassinosteroid, gibberellin signaling and temperature are also found to work closely with PIFs in regulating elongation (Bai et al., 2012; Sun et al., 2012). However, these plants have reduced biomass as longer petioles are often accompanied by reduced leaf blade area.

CHAPTER 6 DISCUSSION

This thesis aimed to explore the biomass regulation through phytochromes; therefore, focus has been leaf blade expansion rather than petiole elongation. In Chapter 3 phytochrome mutants are shown to have retarded growth based on lower biomass, less rosette expansion (Figure 3.5) and reduced expression of a few cell wall synthesis/reorganization genes including *XTH7* (Figure 3.7 C). Down-regulation of *XTH7* was also found in a *phyABDE* seedling microarray analysis, together with *XTH6, 12, 13, 14, 24, 26* (Hu et al., 2013). Interestingly, however, other *XTH* genes such as *XTH5, 8, 11, 15, 17, 19, 25, 30, 31, 33* were promoted in *phyABDE* seedlings (Appendix Table 4). This is also supported by earlier studies where *XTH 9, 15, 16, 17, 19* were found induced in low R: FR light conditions (Sasidharan and Pierik, 2010; Sasidharan et al., 2010).

The differently regulated *XTHs* by phytochromes suggest distinctive functions of these genes in the respective locations. Following a study that shows both photoreceptors and sugars are responsible for the different growth response to shade in leaf blade and petiole (Kozuka et al., 2005), the same lab reported that several *XTH* genes express differently in these two locations (Kozuka et al., 2010). *XTH19* and *XTH22*, together with auxin pathway genes such as *IAA6* and *19*, are induced by far-red light treatment at the end of day in petioles but much less in blades. Likewise, it would be interesting to test weather genes like *XTH7* and *CSLB4, CSLG3, EXP1* (Figure 3.7 C) are repressed in leaf blades rather than petioles in phytochrome mutants.

33 *XTH* genes in Arabidopsis are classified into three groups based on their gene structures (Rose et al., 2002). Interestingly, the most repressed *XTH6* and *7* in

phyABDE seedlings are from group 1, while *XTH15* and *19* that are promoted by phytochrome inactivation both belong to group 2. This implies that *XTHs* might be regulated differently based on their gene structures. Actually, even *XTHs* induced by shade were reported to be regulated differently: *XTH15* is regulated by PIFs in leaf blade/lamina and does not respond to auxin, while *XTH19* responds to auxin and is not a PIF target based on ChIP data (de Wit et al., 2015). So far, how XTH6 and 7 genes are regulated by phytochromes has not been studied yet, and it would be interesting to see how phytochrome and related transcription factors manipulate these *XTH* genes to control expansion growth.

6.3 Phytochrome as the Metabolic Switch for Stress Priming Status?

Chapter 4 shows Arabidopsis phytochrome mutants have altered metabolic profile compared to L*er* WT (Figure 4.3) and suggests this could help prime plants more tolerant to unexpected stressors, such as exogenous salt and ABA application (Figure 4.6-4.7). Indeed, we have detected accumulation of metabolites like proline and raffinose that have long been reported to accumulate upon stresses (Kempa et al., 2008). However, the idea to connect phytochrome and stress pathway through metabolism is still quite novel and awaits further inspections.

Just like sugars, it is unclear how other metabolites accumulate in phytochrome mutants, especially proline. Apart from being induced by stress, proline has also been found to accumulate in reproductive organs upon developmental transition to flowering (Mattioli et al., 2009). In particular, proline catabolic genes, including *PRODH*, were found to be promoted in developmental but repressed in stress-

induced proline accumulation (Nakashima et al., 1998). The catabolism of proline in flowers, siliques and seeds were suggested to provide energy during reproductive phase (Mattioli et al., 2009). In Figure 4.5, *PRODH* was shown upregulated in *phyABDE* mutant, suggesting at least part of the excess proline might be due to earlier on-set of flowering. This hypothesis could be tested by quantifying proline content locally, such as in apical meristem where flowers would emerge.

It would also be interesting to explore how light and other factors interplay in this metabolic switching process. As similar metabolic profiles were found in several clock mutants, including *prr975* (Fukushima et al., 2009; Nakamichi et al., 2009) and *tic-2* (Sanchez-Villarreal et al., 2013), it is very possible that light and clock share this metabolic control. In addition, temperature is also likely to be involved in this regulation, not only because it has long been reported to interact with light signalling components, but also that Arabidopsis metabolism responds to shade at 16°C but not at 22°C (Patel et al., 2013). This provides potential research directions to common downstream regulators of these pathways in regulating metabolites associated with stress response.

6.4 Potential Natural Variation in Phytochrome Control of Dark Response

Chapter 5 presents some preliminary dark tests that show C*ol* and L*er* background phytochtome mutants respond to dark induced chlorophyll loss in distinctive ways. Similar results from L*er* and Ws alleles (Brouwer et al., 2014) suggested C*ol* might be the outlier in this case. Considering most of our knowledge on phytochrome control over dark induced senescence came from studies using C*ol* lines, it is

necessary to find out the potential allelic variation and perhaps re-evaluate the current conclusions.

Studies on Arabidopsis natural variation have revealed unique knowledge in biology from plant development, physiology to ecology and evolution (see thorough reviews in Alonso-Blanco and Koornneef, 2000; Koornneef et al., 2004; Weigel, 2012). Typical case examples include the onset of flowering, pathogen resistance and various aspects of plant growth (Koornneef et al., 2004). In particular, L*er* has natural disruption in a receptor-like kinase ERECTA (Torii et al., 1996), which was found to regulate plant shade response at 16°C through natural genetic variation analysis (Patel et al., 2013). Interestingly, *erecta* mutant was reported to have enhanced susceptibility to Verticillium longisporum disease (Häffner et al., 2014), suggesting potential difference in stress resistance response between L*er* and C*ol* alleles. As another example, the key repressor of gibberellin (GA) responses, DELLA, previously largely studied in L*er* background, was reported essential for fertility in C*ol* but not in L*er* allele (Plackett et al., 2014). Since DELLA has been found to coordinate light and GA signalling by sequestering and degrading PIFs (Li et al., 2016; Lucas et al., 2008; Feng et al., 2008), it further adds to the possibility that light signaling related responses could differ between L*er* and C*ol* alleles.

Still, it is worth noting that in chapter 5 only chlorophyll phenotype (and post-dark-survival rate of 5-week plant) was inspected between L*er* and C*ol* lines. Dark response also includes many other aspects, such as ion leakage and induction of senescence-associated genes. Whether these phenotypes differ in L*er*/Ws phytochrome mutants and C*ol* lines remains to be tested.

6.5 Concluding Remarks

This thesis presents a novel role of photoreceptors in regulating plant growth, metabolism and stress resilience, making a conceptual advance in the way we view light signaling. By studying phytochrome multiple mutants, I have shown that changes in light signaling are accompanied by important adjustments in carbon metabolism and biomass production. Furthermore, phytochromes might switch plant metabolism between growth-promoting and stress-coping states. Finally, my data proposes that the current knowledge about phytochome regulation of dark induced senescence might need re-evaluation of background allele effect. Taken together, these new findings have brought new interest into the field, highlighting the role of phytochromes in coordinating growth and stress physiology, suggesting potential application of such knowledge to crop biomass studies.

Reference

Aggio, R., Villas-Bôas, S.G., and Ruggiero, K. (2011). Metab: An R package for high-throughput analysis of metabolomics data generated by GC-MS. Bioinformatics **27**: 2316–2318.

Alonso-Blanco, C. and Koornneef, M. (2000). Naturally occurring variation in Arabidopsis: An underexploited resource for plant genetics. Trends Plant Sci. **5**: 22–29.

Arbona, V., Manzi, M., Ollas, C., and Gómez-Cadenas, A. (2013). Metabolomics as a Tool to Investigate Abiotic Stress Tolerance in Plants. Int. J. Mol. Sci. **14**: 4885–4911.

Asensio, J.S.R., Rachmilevitch, S., and Bloom, A.J. (2015). Responses of Arabidopsis and wheat to rising CO2 depend on nitrogen source and nighttime CO2 levels. Plant Physiol. **168**: 156–63.

Aukerman, M.J., Hirschfeld, M., Wester, L., Weaver, M., Clack, T., Amasino, R.M., and Sharrock, R.A. (1997). A deletion in the PHYD gene of the Arabidopsis Wassilewskija ecotype defines a role for phytochrome D in red/far-red light sensing. Plant Cell **9**: 1317–26.

Bae, G. and Choi, G. (2008). Decoding of Light Signals by Plant Phytochromes and Their Interacting Proteins. Annu. Rev. Plant Biol. **59**: 281–311.

Baena-González, E., Rolland, F., Thevelein, J.M., and Sheen, J. (2007). A central integrator of transcription networks in plant stress and energy signalling. Nature **448**: 938–42.

Bai, M.-Y., Shang, J.-X., Oh, E., Fan, M., Bai, Y., Zentella, R., Sun, T., and Wang, Z.-Y. (2012). Brassinosteroid, gibberellin and phytochrome impinge on a common transcription module in Arabidopsis. Nat. Cell Biol. **14**: 810–817.

Balazadeh, S., Riaño-Pachón, D.M., and Mueller-Roeber, B. (2008). Transcription factors regulating leaf senescence in Arabidopsis thaliana. Plant Biol. **10**: 63–75.

Ballaré, C.L. (1999). Keeping up with the neighbours: Phytochrome sensing and other signalling mechanisms. Trends Plant Sci. **4**: 97–102.

Bartel, J., Krumsiek, J., and Theis, F.J. (2013). Statistical methods for the analysis of high-throughput metabolomics data. Comput. Struct. Biotechnol. J. **4**: e201301009.

Bhaskara, G.B., Yang, T.-H., and Verslues, P.E. (2015). Dynamic proline metabolism: importance and regulation in water limited environments. Front. Plant Sci. **6**: 1–7.

Biswal, U. and Biswal, B. (1984). Photocontrol of Leaf Senescence. Photochem. Photobiol. **39**: 875–879.

Borthwick, H., Hendricks, S., and Parker, M. (1952). A reversible photoreaction controlling seed germination. Proc. Natl. Acad. Sci. **38**: 662–666.

Botto, J.F., Sanchez, R.A., Whitelam, G.C., and Casal, J.J. (1996). Phytochrome A Mediates the Promotion of Seed Germination by Very Low Fluences of Light and Canopy Shade Light in Arabidopsis. Plant Physiol. **110**: 439–444.

Brouwer, B., Gardeström, P., and Keech, O. (2014). In response to partial plant shading, the lack of phytochrome A does not directly induce leaf senescence but alters the fine-tuning of chlorophyll biosynthesis. J. Exp. Bot. **65**: 4037–4049.

Brouwer, B., Ziolkowska, A., Bagard, M., Keech, O., and Gardeström, P. (2012). The impact of light intensity on shade-induced leaf senescence. Plant, Cell Environ. **35**: 1084–1098.

Buchanan-Wollaston, V., Earl, S., Harrison, E., Mathas, E., Navabpour, S., Page, T., and Pink, D. (2003). The molecular analysis of leaf senescence--a genomics approach. Plant Biotechnol J **1**: 3–22.

Buchanan-Wollaston, V., Page, T., Harrison, E., Breeze, E., Pyung, O.L., Hong, G.N., Lin, J.F., Wu, S.H., Swidzinski, J., Ishizaki, K., and Leaver, C.J. (2005). Comparative transcriptome analysis reveals significant differences in gene expression and signalling pathways between developmental and dark/starvation-induced senescence in Arabidopsis. Plant J. **42**: 567–585.

Casal, J.J., Sánchez, R. a., and Botto, J.F. (1998). Modes of action of phytochromes. J. Exp. Bot. **49**: 127–138.

Caspar, T., Huber, S.C., and Somerville, C. (1985). Alterations in Growth, Photosynthesis, and Respiration in a Starchless Mutant of Arabidopsis thaliana (L.) Deficient in Chloroplast Phosphoglucomutase Activity. Plant Physiol. **79**: 11–7.

Chen, M. and Chory, J. (2011). Phytochrome signaling mechanisms and the control of plant development. Trends Cell Biol. **21**: 664–671.

Chen, M., Chory, J., and Fankhauser, C. (2004). Light signal transduction in higher plants. Annu. Rev. Genet. **38**: 87–117.

Chew, Y.H. et al. (2014). Multiscale digital Arabidopsis predicts individual organ and whole-organism growth. Proc. Natl. Acad. Sci. **112**: 201506983.

Cho, J.-N., Ryu, J.-Y., Jeong, Y.-M., Park, J., Song, J.-J., Amasino, R.M., Noh, B., and Noh, Y.-S. (2012). Control of seed germination by light-induced histone arginine demethylation activity. Dev. Cell **22**: 736–48.

Cho, Y.-H., Yoo, S.-D., and Sheen, J. (2006). Regulatory Functions of Nuclear Hexokinase1 Complex in Glucose Signaling. Cell **127**: 579–589.

Chory, J., Chatterjee, M., Cook, R.K., Elich, T., Fankhauser, C., Li, J., Nagpal, P., Neff, M., Pepper, A., Poole, D., Reed, J., and Vitart, V. (1996). From seed germination to flowering, light controls plant development via the pigment phytochrome. Proc. Natl. Acad. Sci. **93**: 12066–12071.

Clack, T., Mathews, S., and Sharrock, R.A. (1994). The phytochrome apoprotein family in Arabidopsis is encoded by five genes: the sequences and expression of PHYD and PHYE. Plant Mol. Biol. **25**: 413–27.

Colebrook, E.H., Thomas, S.G., Phillips, A.L., and Hedden, P. (2014). The role of gibberellin signalling in plant responses to abiotic stress. J. Exp. Biol. **217**: 67–75.

Cross, J.M., Korff, M. Von, Altmann, T., Bartzetko, L., Sulpice, R., Gibon, Y., Palacios, N., and Stitt, M. (2006). Variation of Enzyme Activities and Metabolite Levels in 24 Arabidopsis Accessions Growing in Carbon-Limited Conditions. Plant Physiol. **142**: 1574–1588.

Das, P.K., Shin, D.H., Choi, S.B., and Park, Y.I. (2012). Sugar-hormone cross-talk in anthocyanin biosynthesis. Mol. Cells **34**: 501–507.

Davison, B.H., Parks, J., Davis, M.F., and Donohoe, B.S. (2013). Plant Cell Walls: Basics of Structure, Chemistry, Accessibility and the Influence on Conversion. In Aqueous Pretreatment of Plant Biomass for Biological and Chemical Conversion to Fuels and Chemicals (John Wiley & Sons, Ltd: Chichester, UK), pp. 23–38.

Debrieux, D., Trevisan, M., and Fankhauser, C. (2013). Conditional Involvement of CONSTITUTIVE PHOTOMORPHOGENIC1 in the Degradation of Phytochrome A. Plant Physiol. **161**: 2136–2145.

Dekkers, B.J.W., Schuurmans, J.A.M.J., and Smeekens, S.C.M. (2004). Glucose delays seed germination in Arabidopsis thaliana. Planta **218**: 579–588.

Deng, X., Caspar, T., and Quail, P.H. (1991). Cop1 : a regulatory locus involved m hght-controlled development and gene expression in Arabidopsis. Genes Dev. **5**: 1172–1182.

Deprost, D., Yao, L., Sormani, R., Moreau, M., Leterreux, G., Nicolaï, M., Bedu, M., Robaglia, C., and Meyer, C. (2007). The Arabidopsis TOR kinase links plant growth, yield, stress resistance and mRNA translation. EMBO Rep. **8**: 864–70.

Devlin, P.F. (2016). Plants wait for the lights to change to red. Proc. Natl. Acad. Sci. **113**: 201608237.

Devlin, P.F., Robson, P.R., Patel, S.R., Goosey, L., Sharrock, R. a, and Whitelam, G.C. (1999). Phytochrome D acts in the shade-avoidance syndrome in Arabidopsis by controlling elongation growth and flowering time. Plant Physiol. **119**: 909–915.

Dijkwel, P.P., Huijser, C., Weisbeek, P.J., Chua, N.H., and Smeekens, S.C. (1997). Sucrose control of phytochrome A signaling in Arabidopsis. Plant Cell **9**: 583–95.

Dijkwel, P.P., Kock, P., Bezemer, R., Weisbeek, P.J., and Smeekens, S. (1996). Sucrose Represses the Developmentally Controlled Transient Activation of the Plastocyanin Gene in Arabidopsis thaliana Seedlings. Plant Physiol. **110**: 455–463.

Duek, P.D. and Fankhauser, C. (2005). bHLH class transcription factors take centre stage in phytochrome signalling. Trends Plant Sci. **10**: 51–54.

Ermert, A.L., Mailliet, K., and Hughes, J. (2016). Holophytochrome-Interacting Proteins in Physcomitrella: Putative Actors in Phytochrome Cytoplasmic Signaling. Front. Plant Sci. **7**: 613.

Fankhauser, C. and Staiger, D. (2002). Photoreceptors in Arabidopsis thaliana: light perception, signal transduction and entrainment of the endogenous clock. Planta **216**: 1–16.

Fankhauser, C., Yeh, K.C., Lagarias, J.C., Zhang, H., Elich, T.D., and Chory, J. (1999). PKS1, a substrate phosphorylated by phytochrome that modulates light signaling in Arabidopsis. Science **284**: 1539–1541.

Feng, S. et al. (2008). Coordinated regulation of Arabidopsis thaliana development by light and gibberellins. Nature **451**: 475–479.

Fitter, A.H. and Fitter, R.S.R. (2002). Rapid changes in flowering time in British plants. Science (80-.). **296**: 1689–1691.

Franklin, K.A. (2003). Phytochromes B, D, and E Act Redundantly to Control Multiple Physiological Responses in Arabidopsis. Plant Physiol. **131**: 1340–1346.

Franklin, K.A., Davis, S.J., Stoddart, W.M., Vierstra, R.D., and Whitelam, G.C. (2003). Mutant analyses define multiple roles for phytochrome C in Arabidopsis photomorphogenesis. Plant Cell **15**: 1981–9.

Franklin, K.A. and Whitelam, G.C. (2007). Light-quality regulation of freezing tolerance in Arabidopsis thaliana. Nat. Genet. **39**: 1410–3.

Franklin, K.A. and Whitelam, G.C. (2005). Phytochromes and shade-avoidance responses in plants. Ann. Bot. **96**: 169–175.

Franklin, K. a and Quail, P.H. (2010). Phytochrome functions in Arabidopsis development. J. Exp. Bot. **61**: 11–24.

Fukushima, A., Kusano, M., Nakamichi, N., Kobayashi, M., Hyashi, N., Sakakibara, H., Mizuno, T., and Saito, K. (2009). Correction for Fukushima et al., Impact of clock-associated Arabidopsis pseudo-response regulators in metabolic coordination. Proc. Natl. Acad. Sci. **106**: 8791–8791.

Galvão, V.C. and Fankhauser, C. (2015). Sensing the light environment in plants: photoreceptors and early signaling steps. Curr. Opin. Neurobiol. **34**: 46–53.

Gan, S. and Amasino, R.M. (1997). Making Sense of Senescence (Molecular Genetic Regulation and Manipulation of Leaf Senescence). Plant Physiol. **113**: 313–319.

Gao, Y., Jiang, W., Dai, Y., Xiao, N., Zhang, C., Li, H., Lu, Y., Wu, M., Tao, X., Deng, D., and Chen, J. (2015). A maize phytochrome-interacting factor 3 improves drought and salt stress tolerance in rice. Plant Mol. Biol. **87**: 413–428.

Ghassemian, M., Lutes, J., Tepperman, J.M., Chang, H.-S., Zhu, T., Wang, X., Quail, P.H., and Lange, B.M. (2006). Integrative analysis of transcript and metabolite profiling data sets to evaluate the regulation of biochemical pathways during photomorphogenesis. Arch. Biochem. Biophys. **448**: 45–59.

Gibon, Y., Bläsing, O.E., Palacios-Rojas, N., Pankovic, D., Hendriks, J.H.M., Fisahn, J., Höhne, M., Günther, M., and Stitt, M. (2004). Adjustment of diurnal starch turnover to short days: Depletion of sugar during the night leads to a temporary inhibition of carbohydrate utilization, accumulation of sugars and post-translational activation of ADP-glucose pyrophosphorylase in the followin. Plant J. **39**: 847–862.

Gibon, Y., Pyl, E.-T., Sulpice, R., Lunn, J.E., Höhne, M., Günther, M., and Stitt, M. (2009). Adjustment of growth, starch turnover, protein content and central metabolism to a decrease of the carbon supply when Arabidopsis is grown in very short photoperiods. Plant. Cell Environ. **32**: 859–74.

Graf, A., Schlereth, A., Stitt, M., and Smith, A.M. (2010). Circadian control of carbohydrate availability for growth in Arabidopsis plants at night. Proc. Natl. Acad. Sci. **107**: 9458–9463.

Grant, O. (2012). Abiotic Stress Responses in Plants P. Ahmad and M.N.V. Prasad, eds (Springer New York: New York, NY).

Grbic, V., Grbic, V., Bleecker, A.B., and Bleecker, A.B. (1995). Ethylene Regulates the Timing of Leaf Senescence in Arabidopsis. Plant J. **8**: 595–602.

De Greef, J., Butler, W.L., Roth, T.F., and Fredericq, H. (1971). Control of

Senescence in Marchantia by Phytochrome. Plant Physiol **48**: 407–412.

Guo, Y. and Gan, S. (2006). AtNAP, a NAC family transcription factor, has an important role in leaf senescence. Plant J. **46**: 601–612.

Häffner, E., Karlovsky, P., Splivallo, R., Traczewska, A., and Diederichsen, E. (2014). ERECTA, salicylic acid, abscisic acid, and jasmonic acid modulate quantitative disease resistance of Arabidopsis thaliana to Verticillium longisporum. BMC Plant Biol. **14**: 85.

Halliday, K. and Whitelam, G. (2003). Changes in photoperiod or temperature alter the functional relationships between phytochromes and reveal roles for phyD and phyE. Plant Physiol. **131**: 1913–1920.

Halliday, K.J., Koornneef, M., and Whitelam, G.C. (1994). Phytochrome B and at Least One Other Phytochrome Mediate the Accelerated Flowering Response of Arabidopsis thaliana L. to Low Red/Far-Red Ratio. Plant Physiol. **104**: 1311–1315.

Halliday, K.J., Salter, M.G., Thingnaes, E., and Whitelam, G.C. (2003). Phytochrome control of flowering is temperature sensitive and correlates with expression of the floral integrator FT. Plant J. **33**: 875–885.

HANNEMANN, J., POORTER, H., USADEL, B., BLÄSING, O.E., FINCK, A., TARDIEU, F., ATKIN, O.K., PONS, T., STITT, M., and GIBON, Y. (2009). Xeml Lab: a tool that supports the design of experiments at a graphical interface and generates computer-readable metadata files, which capture information about genotypes, growth conditions, environmental perturbations and sampling strategy. Plant. Cell Environ. **32**: 1185–1200.

Hanson, J. and Smeekens, S. (2009). Sugar perception and signaling—an update. Curr. Opin. Plant Biol. **12**: 562–567.

Hare, P.D.P., Cress, W. a., and van Staden, J. (1999). Proline synthesis and degradation: a model system for elucidating stress-related signal transduction. J. Exp. Bot. **50**: 413–434.

Hendriks, J.H.M. (2003). ADP-Glucose Pyrophosphorylase Is Activated by Posttranslational Redox-Modification in Response to Light and to Sugars in Leaves of Arabidopsis and Other Plant Species. Plant Physiol. **133**: 838–849.

Holm, M., Ma, L.G., Qu, L.J., and Deng, X.W. (2002). Two interacting bZIP proteins are direct targets of COP1-mediated control of light-dependent gene expression in Arabidopsis. Genes Dev. **16**: 1247–1259.

Hörtensteiner, S. (2006). CHLOROPHYLL DEGRADATION DURING SENESCENCE *. Annu. Rev. Plant Biol. **57**: 55–77.

Hu, W., Franklin, K.A., Sharrock, R.A., Jones, M.A., Harmer, S.L., and

Lagarias, J.C. (2013). Unanticipated regulatory roles for Arabidopsis phytochromes revealed by null mutant analysis. Proc. Natl. Acad. Sci. U. S. A. **110**: 1542–7.

Hudson, M. and Quail, P. (2003). Identification of promoter motifs involved in the network of phytochrome A-regulated gene expression by combined analysis of genomic sequence and microarray data. Plant Physiol. **133**: 1605–1616.

Hughes, J. (2012). Phytochrome Cytoplasmic Signaling. Annu. Rev. Plant Biol. **64**: 130318105636005.

Izumi, M., Hidema, J., Makino, A., and Ishida, H. (2013). Autophagy contributes to nighttime energy availability for growth in Arabidopsis. Plant Physiol. **161**: 1682–93.

Jang, I.-C., Henriques, R., Seo, H.S., Nagatani, A., and Chua, N.-H. (2010). Arabidopsis PHYTOCHROME INTERACTING FACTOR proteins promote phytochrome B polyubiquitination by COP1 E3 ligase in the nucleus. Plant Cell **22**: 2370–83.

Jiang, C., Belfield, E.J., Cao, Y., Smith, J.A.C., and Harberd, N.P. (2013). An Arabidopsis Soil-Salinity-Tolerance Mutation Confers Ethylene-Mediated Enhancement of Sodium/Potassium Homeostasis. Plant Cell **25**: 3535–3552.

Jiao, Y., Lau, O.S., and Deng, X.W. (2007). Light-regulated transcriptional networks in higher plants. Nat. Rev. Genet. **8**: 217–230.

Jiao, Y., Ma, L., Strickland, E., and Deng, X.W. (2005). Conservation and divergence of light-regulated genome expression patterns during seedling development in rice and Arabidopsis. Plant Cell **17**: 3239–56.

Johansson, H., Jones, H.J., Foreman, J., Hemsted, J.R., Stewart, K., Grima, R., and Halliday, K.J. (2014). Arabidopsis cell expansion is controlled by a photothermal switch. Nat. Commun. **5**: 4848.

Jumtee, K., Okazawa, A., Harada, K., Fukusaki, E., Takano, M., and Kobayashi, A. (2009). Comprehensive metabolite profiling of phyA phyB phyC triple mutants to reveal their associated metabolic phenotype in rice leaves. J. Biosci. Bioeng. **108**: 151–9.

Jyan-Chyun, J., Patricia, L., Li, Z., and Jen, S. (1997). Hexokinase as a Sugar Sensor in Higher Plants. Plant Cell **9**: 5–19.

Kangasjärvi, S., Neukermans, J., Li, S., Aro, E.-M., and Noctor, G. (2012). Photosynthesis, photorespiration, and light signalling in defence responses. J. Exp. Bot. **63**: 1619–36.

Kempa, S., Krasensky, J., Dal Santo, S., Kopka, J., and Jonak, C. (2008). A Central Role of Abscisic Acid in Stress-Regulated Carbohydrate

Metabolism. PLoS One **3**: e3935.

Kim, J.H., Woo, H.R., Kim, J., Lim, P.O., Lee, I.C., Choi, S.H., Hwang, D., and Nam, H.G. (2009). Trifurcate feed-forward regulation of age-dependent cell death involving miR164 in Arabidopsis. Science (80-.). **323**: 1053–1057.

Kirchenbauer, D., Viczián, A., Ádám, É., Hegedűs, Z., Klose, C., Leppert, M., Hiltbrunner, A., Kircher, S., Schäfer, E., and Nagy, F. (2016). Characterization of photomorphogenic responses and signaling cascades controlled by phytochrome-A expressed in different tissues. New Phytol. **211**: 584–598.

Kircher, S., Patricia, G., Kozma-Bognár, L., Fejes, E., Volker, S., Husselstein-Muller, T., Diana, B., Ádám, É., Schäfer, E., and Nagy, F. (2002). Nucleocytoplasmic Partitioning of the Plant Photoreceptors Phytochrome A, B, C, D, and E Is Regulated Differentially by Light and Exhibits a Diurnal Rhythm. Plant Cell **14**: 1541–1555.

Kircher, S. and Schopfer, P. (2012). Photosynthetic sucrose acts as cotyledon-derived long-distance signal to control root growth during early seedling development in Arabidopsis. Proc. Natl. Acad. Sci. **109**: 11217–11221.

Kölling, K., Müller, A., Flütsch, P., and Zeeman, S.C. (2013). A device for single leaf labelling with CO2 isotopes to study carbon allocation and partitioning in Arabidopsis thaliana. Plant Methods **9**: 45.

Koornneef, M., Alonso-Blanco, C., and Vreugdenhil, D. (2004). NATURALLY OCCURRING GENETIC VARIATION IN *ARABIDOPSIS THALIANA*. Annu. Rev. Plant Biol. **55**: 141–172.

Kozuka, T., Horiguchi, G., Kim, G.-T., Ohgishi, M., Sakai, T., and Tsukaya, H. (2005). The different growth responses of the Arabidopsis thaliana leaf blade and the petiole during shade avoidance are regulated by photoreceptors and sugar. Plant Cell Physiol. **46**: 213–23.

Kozuka, T., Kobayashi, J., Horiguchi, G., Demura, T., Sakakibara, H., Tsukaya, H., and Nagatani, A. (2010). Involvement of auxin and brassinosteroid in the regulation of petiole elongation under the shade. Plant Physiol. **153**: 1608–18.

Krasensky, J. and Jonak, C. (2012). Drought, salt, and temperature stress-induced metabolic rearrangements and regulatory networks. J. Exp. Bot. **63**: 1593–1608.

Kumar, S.V. and Wigge, P.A. (2010). H2A.Z-Containing Nucleosomes Mediate the Thermosensory Response in Arabidopsis. Cell **140**: 136–147.

Lastdrager, J., Hanson, J., and Smeekens, S. (2014). Sugar signals and

the control of plant growth and development. J. Exp. Bot. **65**: 799–807.

Lee, C.P., Eubel, H., and Millar, a H. (2010). Diurnal changes in mitochondrial function reveal daily optimization of light and dark respiratory metabolism in Arabidopsis. Mol. Cell. Proteomics **9**: 2125–39.

Lee, I.C., Hong, S.W., Whang, S.S., Lim, P.O., Nam, H.G., and Koo, J.C. (2011). Age-dependent action of an ABA-inducible receptor kinase, RPK1, as a positive regulator of senescence in arabidopsis leaves. Plant Cell Physiol. **52**: 651–662.

Lee, K.P., Piskurewicz, U., Turečková, V., Carat, S., Chappuis, R., Strnad, M., Fankhauser, C., and Lopez-Molina, L. (2012). Spatially and genetically distinct control of seed germination by phytochromes A and B. Genes Dev. **26**: 1984–96.

Leivar, P. and Monte, E. (2014). PIFs: systems integrators in plant development. Plant Cell **26**: 56–78.

Leivar, P. and Quail, P.H. (2011). PIFs: pivotal components in a cellular signaling hub. Trends Plant Sci. **16**: 19–28.

León, P. (2003). Sugar and hormone connections. Trends Plant Sci. **8**: 110–116.

Li, J., Li, G., Wang, H., and Wang Deng, X. (2011). Phytochrome signaling mechanisms. Arabidopsis Book **9**: e0148.

Li, K., Yu, R., Fan, L.-M., Wei, N., Chen, H., and Deng, X.W. (2016). DELLA-mediated PIF degradation contributes to coordination of light and gibberellin signalling in Arabidopsis. Nat. Commun. **7**: 11868.

Li, Y., Xu, J., Haq, N.U., Zhang, H., and Zhu, X.-G. (2014). Was low CO2 a driving force of C4 evolution: Arabidopsis responses to long-term low CO2 stress. J. Exp. Bot. **65**: 3657–67.

Li, Z., Peng, J., Wen, X., and Guo, H. (2013). ETHYLENE-INSENSITIVE3 Is a Senescence-Associated Gene That Accelerates Age-Dependent Leaf Senescence by Directly Repressing miR164 Transcription in Arabidopsis. Plant Cell **25**: 3311–3328.

Lilley, J.L.S., Gee, C.W., Sairanen, I., Ljung, K., and Nemhauser, J.L. (2012). An Endogenous Carbon-Sensing Pathway Triggers Increased Auxin Flux and Hypocotyl Elongation. Plant Physiol. **160**: 2261–2270.

Lim, P.O., Kim, H.J., and Nam, H.G. (2007). Leaf senescence. Annu. Rev. Plant Biol. **58**: 115–36.

Lin, C. (2000). Photoreceptors and Regulation of Flowering Time. PLANT Physiol. **123**: 39–50.

Lisec, J., Schauer, N., Kopka, J., Willmitzer, L., and Fernie, A.R. (2006).

Gas chromatography mass spectrometry-based metabolite profiling in plants. Nat. Protoc. **1**: 387–96.

Liu, X., Chen, C.-Y.Y., Wang, K.-C.C., Luo, M., Tai, R., Yuan, L., Zhao, M., Yang, S., Tian, G., Cui, Y., Hsieh, H.-L.L., and Wu, K. (2013). PHYTOCHROME INTERACTING FACTOR3 Associates with the Histone Deacetylase HDA15 in Repression of Chlorophyll Biosynthesis and Photosynthesis in Etiolated Arabidopsis Seedlings. Plant Cell **25**: 1258–73.

Liu, Z., Zhang, Y., Liu, R., Hao, H., Wang, Z., and Bi, Y. (2011). Phytochrome interacting factors (PIFs) are essential regulators for sucrose-induced hypocotyl elongation in Arabidopsis. J. Plant Physiol. **168**: 1771–1779.

Lorrain, S., Allen, T., Duek, P.D., Whitelam, G.C., and Fankhauser, C. (2008). Phytochrome-mediated inhibition of shade avoidance involves degradation of growth-promoting bHLH transcription factors. Plant J. **53**: 312–323.

Lu, X.D., Zhou, C.M., Xu, P.B., Luo, Q., Lian, H.L., and Yang, H.Q. (2015). Red-light-dependent interaction of phyB with SPA1 promotes COP1-SPA1 dissociation and photomorphogenic development in arabidopsis. Mol. Plant **8**: 467–478.

Lucas, M. et al. (2008). A molecular framework for light and gibberellin control of cell elongation. Nature **451**: 480–484.

Lucas, M. and Prat, S. (2014). PIFs get BRright: PHYTOCHROME INTERACTING FACTORs as integrators of light and hormonal signals. New Phytol. **202**: 1126–41.

Mattioli, R., Costantino, P., and Trovato, M. (2009). Proline accumulation in plants: not only stress. Plant Signal. Behav. **4**: 1016–1018.

Mazzella, M. a, Cerdán, P.D., Staneloni, R.J., and Casal, J.J. (2001). Hierarchical coupling of phytochromes and cryptochromes reconciles stability and light modulation of Arabidopsis development. Development **128**: 2291–2299.

Mclaren, J.S. and Smith, H. (1978). Phytochrome control of the growth and development of Rumex obtusifolius under simulated canopy light environments. Plant, Cell Environ. **1**: 61–67.

Meyer, R.C., Steinfath, M., Lisec, J., Becher, M., Witucka-Wall, H., Törjék, O., Fiehn, O., Eckardt, A., Willmitzer, L., Selbig, J., and Altmann, T. (2007). The metabolic signature related to high plant growth rate in Arabidopsis thaliana. Proc. Natl. Acad. Sci. U. S. A. **104**: 4759–64.

Michael, T.P., Breton, G., Hazen, S.P., Priest, H., Mockler, T.C., Kay, S.A., and Chory, J. (2008). A Morning-Specific Phytohormone Gene

Expression Program underlying Rhythmic Plant Growth. PLoS Biol. **6**: e225.

Moghaddam, M.R.B. and Ende, W. Van den (2013). Sugars, the clock and transition to flowering. Front. Plant Sci. **4**.

Moore, B. (2003). Role of the Arabidopsis Glucose Sensor HXK1 in Nutrient, Light, and Hormonal Signaling. Science (80-.). **300**: 332–336.

Nakamichi, N., Kusano, M., Fukushima, A., Kita, M., Ito, S., Yamashino, T., Saito, K., Sakakibara, H., and Mizuno, T. (2009). Transcript Profiling of an Arabidopsis PSEUDO RESPONSE REGULATOR Arrhythmic Triple Mutant Reveals a Role for the Circadian Clock in Cold Stress Response. Plant Cell Physiol. **50**: 447–462.

Nakashima, K., Satoh, R., Kiyosue, T., Yamaguchi-Shinozaki, K., and Shinozaki, K. (1998). A gene encoding proline dehydrogenase is not only induced by proline and hypoosmolarity, but is also developmentally regulated in the reproductive organs of Arabidopsis. Plant Physiol. **118**: 1233–1241.

Neff, M.M., Fankhauser, C., and Chory, J. (2000). Light: an indicator of time and place. Genes Dev. **14**: 257–271.

Ni, Z., Kim, E., and Chen, Z.J. (2009). Chlorophyll and starch assays. Protoc. Exch.: 23–25.

Nunes, C., O'Hara, L.E., Primavesi, L.F., Delatte, T.L., Schluepmann, H., Somsen, G.W., Silva, A.B., Fevereiro, P.S., Wingler, A., and Paul, M.J. (2013). The Trehalose 6-Phosphate/SnRK1 Signaling Pathway Primes Growth Recovery following Relief of Sink Limitation. PLANT Physiol. **162**: 1720–1732.

Oh, S. a, Park, J.H., Lee, G.I., Paek, K.H., Park, S.K., and Nam, H.G. (1997). Identification of three genetic loci controlling leaf senescence in Arabidopsis thaliana. Plant J. **12**: 527–535.

Pacin, M., Legris, M., and Casal, J.J. (2014). Rapid Decline in Nuclear COSTITUTIVE PHOTOMORPHOGENESIS1 Abundance Anticipates the Stabilization of Its Target ELONGATED HYPOCOTYL5 in the Light. Plant Physiol. **164**: 1134–1138.

Paik, I., Yang, S., and Choi, G. (2012). Phytochrome regulates translation of mRNA in the cytosol. Proc. Natl. Acad. Sci. U. S. A. **109**: 1335–40.

Pal, S.K. et al. (2013). Diurnal changes of polysome loading track sucrose content in the rosette of wildtype Arabidopsis and the starchless pgm mutant. Plant Physiol. **162**: 1246–1265.

Pandey, G.K., Grant, J.J., Cheong, Y.H., Kim, B.G., Li, L., and Luan, S. (2005). ABR1, an APETALA2-domain transcription factor that functions

as a repressor of ABA response in Arabidopsis. Plant Physiol. **139**: 1185–93.

Park, D.H. (1999). Control of Circadian Rhythms and Photoperiodic Flowering by the Arabidopsis GIGANTEA Gene. Science (80-.). **285**: 1579–1582.

Park, E., Park, J., Kim, J., Nagatani, A., Lagarias, J.C., and Choi, G. (2012). Phytochrome B inhibits binding of phytochrome-interacting factors to their target promoters. Plant J. **72**: 537–46.

Patel, D., Basu, M., Hayes, S., Majláth, I., Hetherington, F.M., Tschaplinski, T.J., and Franklin, K.A. (2013). Temperature-dependent shade avoidance involves the receptor-like kinase ERECTA. Plant J. **73**: 980–992.

Piao, W., Kim, E.-Y., Han, S.-H., Sakuraba, Y., and Paek, N.-C. (2015). Rice Phytochrome B (OsPhyB) Negatively Regulates Dark- and Starvation-Induced Leaf Senescence. Plants **4**: 644–663.

Plackett, A.R.G., Ferguson, A.C., Powers, S.J., Wanchoo-Kohli, A., Phillips, A.L., Wilson, Z.A., Hedden, P., and Thomas, S.G. (2014). DELLA activity is required for successful pollen development in the Columbia ecotype of Arabidopsis. New Phytol. **201**: 825–36.

PROVENIERS, M. (2013). Sugars speed up the circle of life. Elife.

Quail, P.H. (2002). Phytochrome photosensory signalling networks. Nat. Rev. Mol. Cell Biol. **3**: 85–93.

Rahmani, F., Hummel, M., Schuurmans, J., Wiese-Klinkenberg, A., Smeekens, S., and Hanson, J. (2009). Sucrose control of translation mediated by an upstream open reading frame-encoded peptide. Plant Physiol. **150**: 1356–67.

Rausenberger, J., Hussong, A., Kircher, S., Kirchenbauer, D., Timmer, J., Nagy, F., Schäfer, E., and Fleck, C. (2010). An Integrative Model for Phytochrome B Mediated Photomorphogenesis: From Protein Dynamics to Physiology. PLoS One **5**: e10721.

Rausenberger, J., Tscheuschler, A., Nordmeier, W., Wüst, F., Timmer, J., Schäfer, E., Fleck, C., and Hiltbrunner, A. (2011). Photoconversion and Nuclear Trafficking Cycles Determine Phytochrome A's Response Profile to Far-Red Light. Cell **146**: 813–825.

Reed, J.W., Elumalai, R.P., and Chory, J. (1998). Suppressors of an Arabidopsis thaliana phyB mutation identify genes that control light signaling and hypocotyl elongation. Genetics **148**: 1295–1310.

Reed, J.W., Nagpal, P., Poole, D.S., Furuya, M., and Chory, J. (1993). Mutations in the gene for the red/far-red light receptor phytochrome B

alter cell elongation and physiological responses throughout Arabidopsis development. Plant Cell **5**: 147–157.

Rockwell, N.C., Su, Y.-S., and Lagarias, J.C. (2006). Phytochrome structure and signaling mechanisms. Annu. Rev. Plant Biol. **57**: 837–58.

Rose, J.K.C., Braam, J., Fry, S.C., and Nishitani, K. (2002). The XTH family of enzymes involved in xyloglucan endotransglucosylation and endohydrolysis: Current perspectives and a new unifying nomenclature. Plant Cell Physiol. **43**: 1421–1435.

Rose, T.L., Bonneau, L., Der, C., Marty-Mazars, D., and Marty, F. (2006). Starvation-induced expression of autophagy-related genes in Arabidopsis. Biol. Cell **98**: 53–67.

Ruan, Y.-L. (2014). Sucrose metabolism: gateway to diverse carbon use and sugar signaling. Annu. Rev. Plant Biol. **65**: 33–67.

Ruberti, I., Sessa, G., Ciolfi, A., Possenti, M., Carabelli, M., and Morelli, G. (2012). Plant adaptation to dynamically changing environment: The shade avoidance response. Biotechnol. Adv. **30**: 1047–1058.

Sairanen, I., Novak, O., Pencik, A., Ikeda, Y., Jones, B., Sandberg, G., and Ljung, K. (2012). Soluble Carbohydrates Regulate Auxin Biosynthesis via PIF Proteins in Arabidopsis. Plant Cell **24**: 4907–4916.

Sakuraba, Y., Jeong, J., Kang, M.-Y., Kim, J., Paek, N.-C., and Choi, G. (2014). Phytochrome-interacting transcription factors PIF4 and PIF5 induce leaf senescence in Arabidopsis. Nat. Commun. **5**: 4636.

Sanchez-Villarreal, A. et al. (2013). TIME FOR COFFEE is an Essential Component in the Maintenance of Arabidopsis thaliana Metabolic Homeostasis. Plant J. **1**: 1–13.

Santelia, D. and Zeeman, S.C. (2011). Progress in Arabidopsis starch research and potential biotechnological applications. Curr. Opin. Biotechnol. **22**: 271–280.

Sasidharan, R., Chinnappa, C.C., Staal, M., Elzenga, J.T.M., Yokoyama, R., Nishitani, K., Voesenek, L.A.C.J., and Pierik, R. (2010). Light Quality-Mediated Petiole Elongation in Arabidopsis during Shade Avoidance Involves Cell Wall Modification by Xyloglucan Endotransglucosylase/Hydrolases. Plant Physiol. **154**: 978–990.

Sasidharan, R. and Pierik, R. (2010). Cell wall modification involving XTHs controls phytochrome-mediated petiole elongation in Arabidopsis thaliana. Plant Signal. Behav. **5**: 1491–1492.

Schluepmann, H., Berke, L., and Sanchez-Perez, G.F. (2011). Metabolism control over growth: a case for trehalose-6-phosphate in plants. J. Exp. Bot. **63**: 3379–3390.

Scialdone, A., Mugford, S.T., Feike, D., Skeffngton, A., Borrill, P., Graf, A., Smith, A.M., and Howard, M. (2013). Arabidopsis plants perform arithmetic division to prevent starvation at night. Elife **2013**: 1–24.

Seung, D., Soyk, S., Coiro, M., Maier, B.A., Eicke, S., and Zeeman, S.C. (2015). PROTEIN TARGETING TO STARCH Is Required for Localising GRANULE-BOUND STARCH SYNTHASE to Starch Granules and for Normal Amylose Synthesis in Arabidopsis. PLoS Biol. **13**: e1002080.

Sharrock, R.A. and Quail, P.H. (1989). Novel phytochrome sequences in Arabidopsis thaliana: structure, evolution, and differential expression of a plant regulatory photoreceptor family. Genes Dev. **3**: 1745–57.

Sheen, J. (1990). Metabolic repression of transcription in higher plants. Plant Cell **2**: 1027–38.

Sheerin, D.J., Menon, C., zur Oven-Krockhaus, S., Enderle, B., Zhu, L., Johnen, P., Schleifenbaum, F., Stierhof, Y.-D., Huq, E., and Hiltbrunner, A. (2015). Light-activated phytochrome A and B interact with members of the SPA family to promote photomorphogenesis in Arabidopsis by reorganizing the COP1/SPA complex. Plant Cell **27**: 189–201.

Shin, A.-Y., Han, Y.-J., Baek, A., Ahn, T., Kim, S.Y., Nguyen, T.S., Son, M., Lee, K.W., Shen, Y., Song, P.-S., and Kim, J.-I. (2016). Evidence that phytochrome functions as a protein kinase in plant light signalling. Nat. Commun. **7**: 11545.

Shinomura, T., Uchida, K., and Furuya, M. (2000). Elementary processes of photoperception by phytochrome A for high-irradiance response of hypocotyl elongation in Arabidopsis. Plant Physiol. **122**: 147–56.

Short, T.W. (1999). Overexpression of Arabidopsis phytochrome B inhibits phytochrome A function in the presence of sucrose. Plant Physiol. **119**: 1497–506.

Skirycz, A. and Inzé, D. (2010). More from less: plant growth under limited water. Curr. Opin. Biotechnol. **21**: 197–203.

Smith, A.M. and Stitt, M. (2007). Coordination of carbon supply and plant growth. Plant. Cell Environ. **30**: 1126–49.

Smith, H. and Whitelam, G.C. (1997). The shade avoidance syndrome: multiple responses mediated by multiple phytochromes. Plant Cell Environ. **20**: 840–844.

Song, Y., Yang, C., Gao, S., Zhang, W., Li, L., and Kuai, B. (2014). Age-Triggered and Dark-Induced Leaf Senescence Require the bHLH Transcription Factors PIF3, 4, and 5. Mol. Plant **7**: 1776–87.

Song, Y.H., Smith, R.W., To, B.J., Millar, A.J., and Imaizumi, T. (2012).

FKF1 Conveys Timing Information for CONSTANS Stabilization in Photoperiodic Flowering. Science (80-.). **336**: 1045–1049.

Stewart, J.L., Maloof, J.N., and Nemhauser, J.L. (2011). PIF genes mediate the effect of sucrose on seedling growth dynamics. PLoS One **6**: e19894.

Stitt, M., Lunn, J., and Usadel, B. (2010). Arabidopsis and primary photosynthetic metabolism - more than the icing on the cake. Plant J. **61**: 1067–1091.

Stitt, M. and Zeeman, S.C. (2012). Starch turnover: pathways, regulation and role in growth. Curr. Opin. Plant Biol. **15**: 282–292.

Strasser, B., Sanchez-Lamas, M., Yanovsky, M.J., Casal, J.J., and Cerdan, P.D. (2010). Arabidopsis thaliana life without phytochromes. Proc. Natl. Acad. Sci. **107**: 4776–4781.

Streb, S. and Zeeman, S.C. (2012). Starch Metabolism in Arabidopsis. Arab. B. **10**: e0160.

Su, M., Huang, G., Zhang, Q., Wang, X., Li, C., Tao, Y., Zhang, S., Lai, J., Yang, C., and Wang, Y. (2016). The LEA protein, ABR, is regulated by ABI5 and involved in dark-induced leaf senescence in Arabidopsis thaliana. Plant Sci. **247**: 93–103.

Subramanian, C., Kim, B.-H., Lyssenko, N.N., Xu, X., Johnson, C.H., and von Arnim, A.G. (2004). The Arabidopsis repressor of light signaling, COP1, is regulated by nuclear exclusion: Mutational analysis by bioluminescence resonance energy transfer. Proc. Natl. Acad. Sci. **101**: 6798–6802.

Sulpice, R. et al. (2009). Starch as a major integrator in the regulation of plant growth. Proc. Natl. Acad. Sci. U. S. A. **106**: 10348–53.

Sun, J., Qi, L., Li, Y., Chu, J., and Li, C. (2012). Pif4-mediated activation of yucca8 expression integrates temperature into the auxin pathway in regulating arabidopsis hypocotyl growth. PLoS Genet. **8**: e1002594.

Takatani, N., Ito, T., Kiba, T., Mori, M., Miyamoto, T., Maeda, S. -i., and Omata, T. (2014). Effects of High CO2 on Growth and Metabolism of Arabidopsis Seedlings During Growth with a Constantly Limited Supply of Nitrogen. Plant Cell Physiol. **55**: 281–292.

Tepperman, J.M., Hudson, M.E., Khanna, R., Zhu, T., Chang, S.H., Wang, X., and Quail, P.H. (2004). Expression profiling of phyB mutant demonstrates substantial contribution of other phytochromes to red-light-regulated gene expression during seedling de-etiolation. Plant J. **38**: 725–39.

Thimm, O., Bläsing, O., Gibon, Y., Nagel, A., Meyer, S., Krüger, P.,

Selbig, J., Müller, L. a., Rhee, S.Y., and Stitt, M. (2004). Mapman: a User-Driven Tool To Display Genomics Data Sets Onto Diagrams of Metabolic Pathways and Other Biological Processes. Plant J. **37**: 914–939.

Tilbrook, K., Arongaus, A.B., Binkert, M., Heijde, M., Yin, R., and Ulm, R. (2013). The UVR8 UV-B Photoreceptor: Perception, Signaling and Response. Arabidopsis Book **11**: e0164.

Toledo-Ortiz, G., Huq, E., and Quail, P.H. (2003). The Arabidopsis basic/helix-loop-helix transcription factor family. Plant Cell Online **15**: 1749–1770.

Torii, K.U., Mitsukawa, N., Oosumi, T., Matsuura, Y., Yokoyama, R., Whittier, R.F., and Komeda, Y. (1996). The Arabidopsis ERECTA gene encodes a putative receptor protein kinase with extracellular leucine-rich repeats. Plant Cell **8**: 735–746.

Urano, K., Maruyama, K., Ogata, Y., Morishita, Y., Takeda, M., Sakurai, N., Suzuki, H., Saito, K., Shibata, D., Kobayashi, M., Yamaguchi-Shinozaki, K., and Shinozaki, K. (2009). Characterization of the ABA-regulated global responses to dehydration in Arabidopsis by metabolomics. Plant J. **57**: 1065–1078.

Vanhaeren, H., Gonzalez, N., and Inzé, D. (2015). A Journey Through a Leaf: Phenomics Analysis of Leaf Growth in Arabidopsis thaliana. Arab. B. **13**: e0181.

Wada, S., Ishida, H., Izumi, M., Yoshimoto, K., Ohsumi, Y., Mae, T., and Makino, A. (2008). Autophagy Plays a Role in Chloroplast Degradation during Senescence in Individually Darkened Leaves. Plant Physiol. **149**: 885–893.

Wahl, V., Ponnu, J., Schlereth, A., Arrivault, S., Langenecker, T., Franke, A., Feil, R., Lunn, J.E., Stitt, M., and Schmid, M. (2013). Regulation of Flowering by Trehalose-6-Phosphate Signaling in Arabidopsis thaliana. Science (80-.). **339**: 704–707.

Wang, Y., Yu, B., Zhao, J., Guo, J., Li, Y., Han, S., Huang, L., Du, Y., Hong, Y., Tang, D., and Liu, Y. (2013). Autophagy contributes to leaf starch degradation. Plant Cell **25**: 1383–99.

Weaver, L.M. and Amasino, R.M. (2001). Senescence is induced in individually darkened Arabidopsis leaves, but inhibited in whole darkened plants. Plant Physiol. **127**: 876–886.

Weigel, D. (2012). Natural Variation in Arabidopsis: From Molecular Genetics to Ecological Genomics. PLANT Physiol. **158**: 2–22.

de Wit, M., Ljung, K., and Fankhauser, C. (2015). Contrasting growth responses in lamina and petiole during neighbor detection depend on

differential auxin responsiveness rather than different auxin levels. New Phytol. **208**: 198–209.

Woo, H.R., Chung, K.M., Park, J.H., Oh, S.A., Ahn, T., Hong, S.H., Jang, S.K., and Nam, H.G. (2001). ORE9, an F-box protein that regulates leaf senescence in Arabidopsis. Plant Cell **13**: 1779–1790.

Xu, X., Paik, I., Zhu, L., and Huq, E. (2015). Illuminating Progress in Phytochrome-Mediated Light Signaling Pathways. Trends Plant Sci. **20**: 641–650.

Yang, D., Seaton, D.D., Krahmer, J., and Halliday, K.J. (2016). Photoreceptor effects on plant biomass, resource allocation, and metabolic state. Proc. Natl. Acad. Sci. **113**: 7667–7672.

Yang, L., Xu, M., Koo, Y., He, J., and Poethig, R.S. (2013). Sugar promotes vegetative phase change in Arabidopsis thaliana by repressing the expression of MIR156A and MIR156C. Elife.

Yu, S., Cao, L., Zhou, C.-M., Zhang, T.-Q., Lian, H., Sun, Y., Wu, J., Huang, J., Wang, G., and Wang, J.-W. (2013). Sugar is an endogenous cue for juvenile-to-adult phase transition in plants. Elife.

Zhang, K., Xia, X., Zhang, Y., and Gan, S.S. (2012). An ABA-regulated and Golgi-localized protein phosphatase controls water loss during leaf senescence in Arabidopsis. Plant J. **69**: 667–678.

Zhang, Y., Liu, Z., Chen, Y., He, J.X., and Bi, Y. (2015). PHYTOCHROME-INTERACTING FACTOR 5 (PIF5) positively regulates dark-induced senescence and chlorophyll degradation in Arabidopsis. Plant Sci. **237**: 57–68.

Zhu, X.-G., Long, S.P., and Ort, D.R. (2008). What is the maximum efficiency with which photosynthesis can convert solar energy into biomass? Curr. Opin. Biotechnol. **19**: 153–159.

Appendix

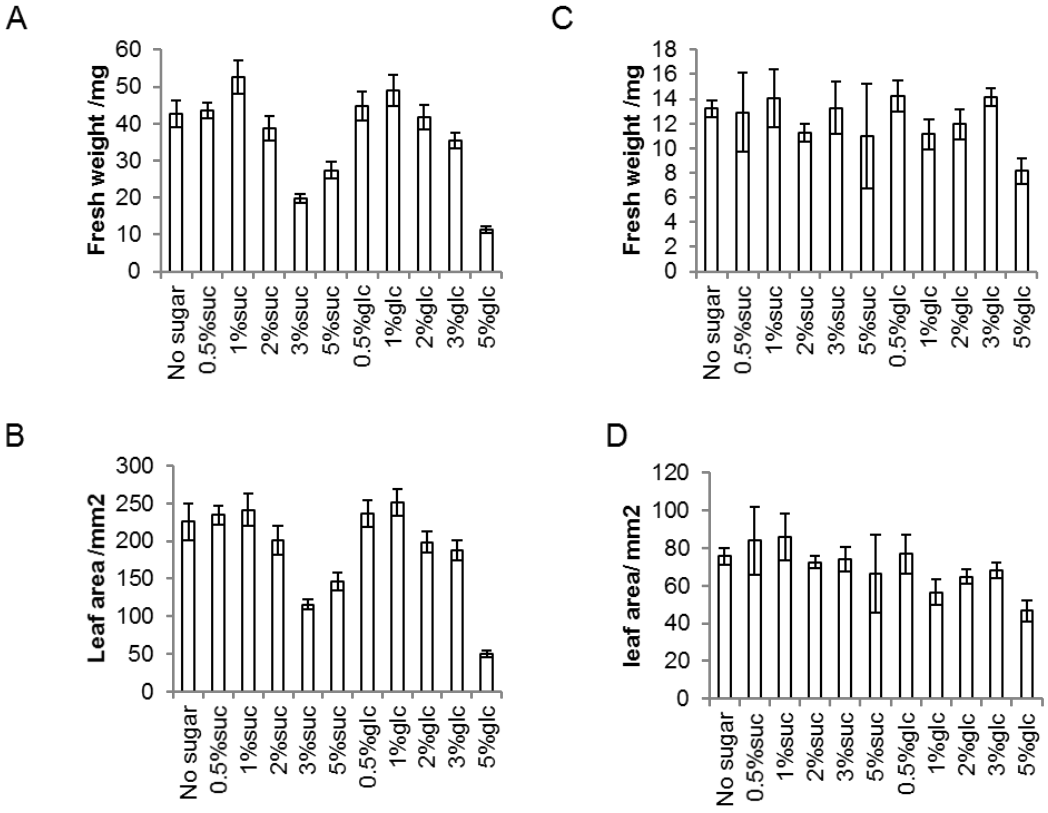

Appendix Figure 1. Plant fresh weight and leaf area are reduced when supplied with sugars in high light conditions.

(A-B) Plants were grown at 17℃ in 12h 80 μmol·m^{-2}sec^{-1} red light/ 12h dark conditions for 3 weeks before transferring to new media with or without sugars. (C-D) Plants were grown at 17℃ in 12h 20 μmol·m^{-2}sec^{-1} red light/ 12h dark conditions for 4 weeks before transferring to new media with or without sugars. Fresh weight, leaf area and leaf number were determined another 2 week after the sugar treatment. All the values are means ± SE from at least 7 plants for high light group and 4 for low light group.

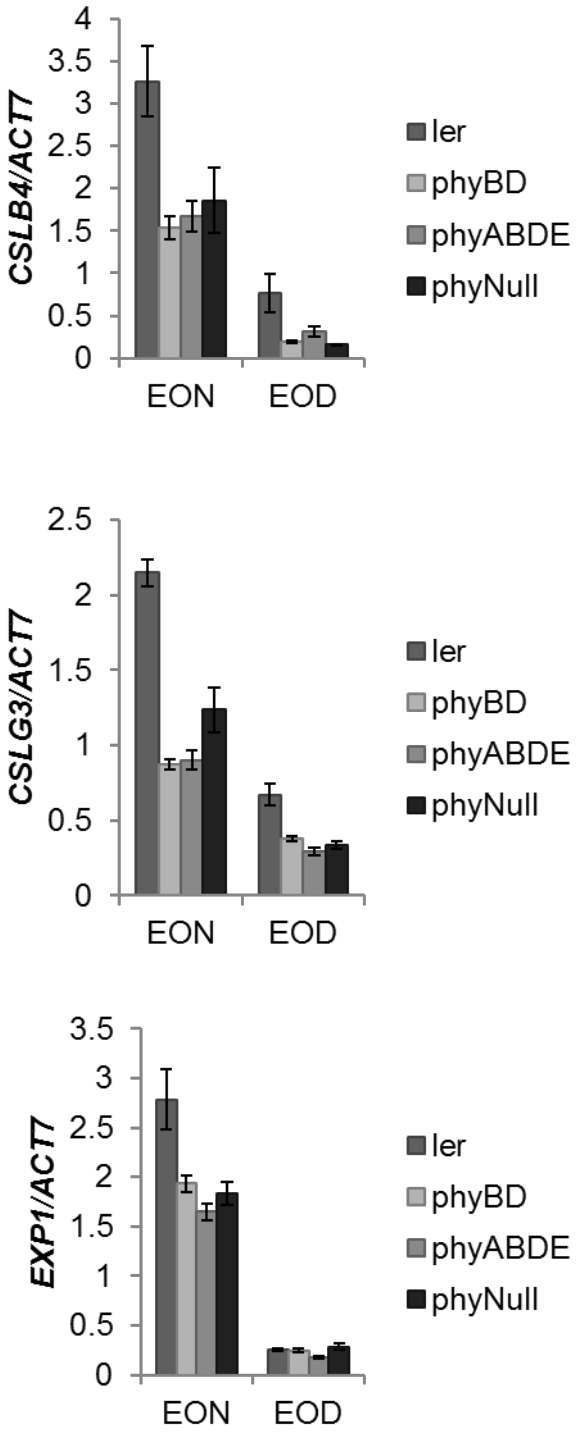

Appendix Figure 2. Q-PCR analysis of cell wall synthesis related genes in 5-week-old *phyBD*, *phyABDE* and phyNull (*phyABCDE*) at EON and EOD.

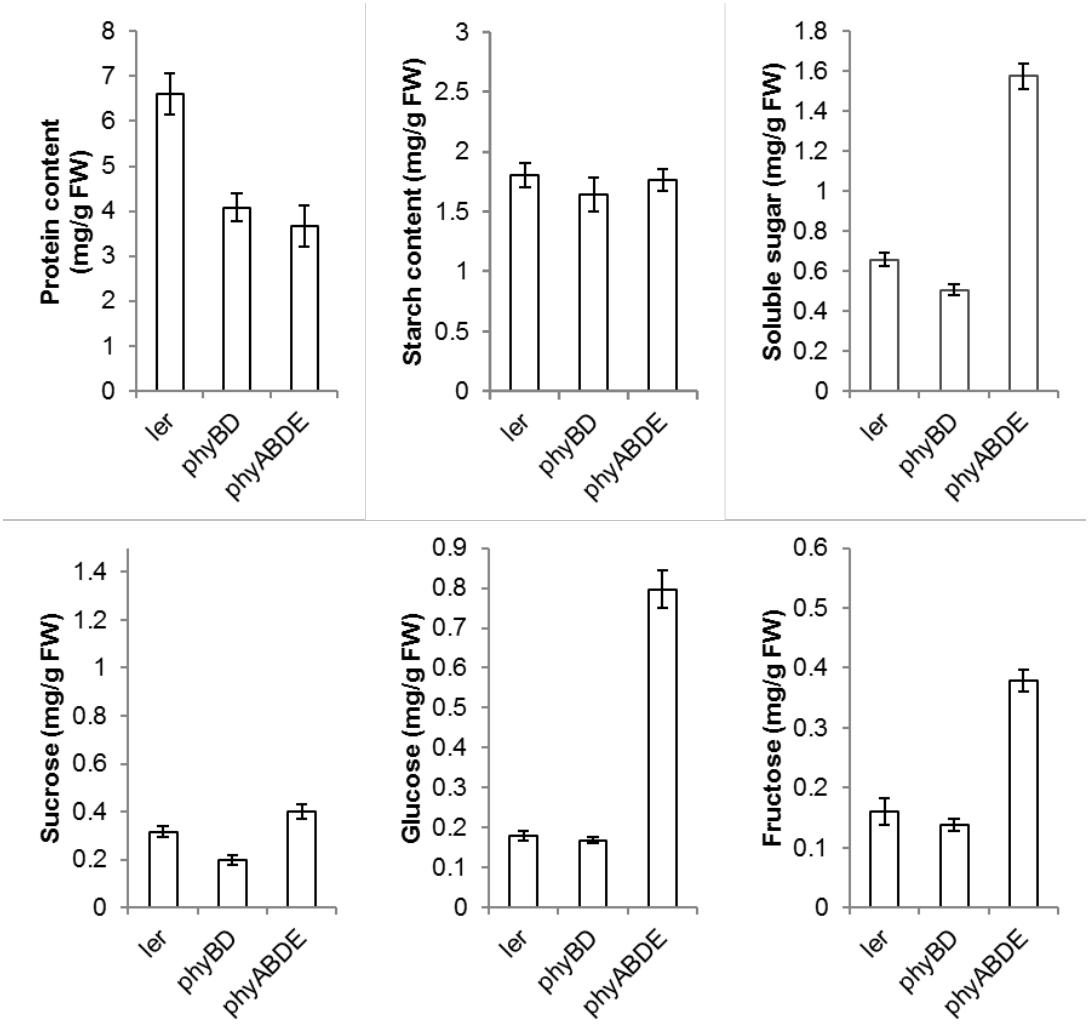

Appendix Figure 3. Protein, Starch and Soluble Sugar Quantification in 2-week-old Seedlings.

L*er*, *phyBD* and *phyABDE* were grown in short photoperiod (8L:16D) for 2 weeks at 18C. Samples were collected at EOD.

Appendix Table 1. Starch and sucrose quantification with statistical analysis results.

Values presented are mean ± SEM. Asterisks indicate a significant difference between values of the phytochrome mutants and WT at each time point, by means of t-test at ns: p ≥ 0.05, * p ≤ 0.05, ** p ≤ 0.01, *** p ≤ 0.001.

Sample information		SUCROSE				STARCH			
time	genotype	mean	se	p-value	significance	mean	se	p-value	significance
9am (ZT0)	*ler*	0.1698	0.0106			0.1747	0.0072		
	phyBD	0.3339	0.0136	6E-06	***	0.5566	0.009	4E-11	***
	phyABDE	0.3383	0.0265	0.0008	***	0.2978	0.014	7E-05	***
3pm (ZT6)	*ler*	0.5571	0.0389			2.242	0.0817		
	phyBD	0.547	0.0266	0.8341	ns	3.3551	0.1524	0.0002	***
	phyABDE	0.7272	0.0596	0.0577	ns	2.6523	0.0956	0.0526	ns
9pm (ZT12)	*ler*	0.6973	0.1092			3.6774	0.2519		
	phyBD	1.0048	0.0442	0.0368	*	5.9063	0.1496	6E-05	***
	phyABDE	1.2164	0.0395	0.0038	**	5.3446	0.1073	0.0136	*
3am (ZT18)	*ler*	0.6869	0.0519			1.5669	0.0399		
	phyBD	0.5612	0.0447	0.0969	ns	3.2274	0.0664	2E-07	***
	phyABDE	0.5129	0.0319	0.0205	*	2.5617	0.0736	2E-05	***
9am (ZT24)	*ler*	0.1062	0.0277			0.1799	0.0067		
	phyBD	0.2228	0.0321	0.0208	*	0.5094	0.0103	1E-09	***
	phyABDE	0.3158	0.0324	0.0006	***	0.3134	0.0112	6E-06	***

Appendix Table 2. Ion library used for quantifying each metabolite

Name	Retention Time	ref_ion1	ref_ion2	ref_ion1	ref_ion2	ion2to1	ion3to1	ion4to1
Name	RT	ref_ion1	ref_ion2	ref_ion3	ref_ion4	ion2to1	ion3to1	ion4to1
Lactic acid (2TMS)	3.398	117	88	118	190	0.104	0.1	0.1
Hydroxylamine(3TMS)	3.47	133	146	119	86	0.678	0.599	0.38
L-Alanine (2TMS)	3.738	116	117	72	130	0.106	0.05	0.048
Oxalic acid (2TMS)	4.611	72	133	100	86	0.925	0.788	0.613
L-Valine (2TMS)	4.89	144	145	218	100	0.161	0.122	0.06
Glycerol(3TMS)	5.246	205	103	117	133	0.983	0.919	0.391
Hydroxycarbamic acid (3TMS)	5.36	70	278	133	160	0.293	0.255	0.107
Leucine(2TMS)	5.468	158	159	102	NA	0.145	0.112	NA
Isoleucine(2TMS)	5.71	158	159	218	NA	0.17	0.153	NA
Glycine(3TMS)	5.807	174	86	175	100	0.434	0.199	0.194
L-Proline (2TMS)	6.05	142	143	144	72	0.117	0.041	0.034
Glyceric acid (3TMS)	6.141	189	103	102	133	0.832	0.509	0.497
Benzoic acid (1TMS)	6.203	105	77	179	135	0.847	0.645	0.581
Serine(3TMS)	6.374	204	218	100	116	0.882	0.455	0.247
Succinic acid (2TMS)	6.508	247	72	129	172	0.943	0.906	0.679
L-Threonine (3TMS)	6.547	117	218	219	101	0.638	0.607	0.538
Fumaric acid (2TMS)	6.606	245	143	246	115	0.253	0.177	0.128
Malic acid (3TMS)	7.82	233	133	101	72	0.842	0.807	0.719
proline, 4-Hydroxy (3TMS)	7.946	71	230	85	140	0.92	0.614	0.472
Aspartic acid (3TMS)	8.109	232	100	233	218	0.517	0.194	0.191
Ribitol (5TMS)-IS	8.876	103	217	129	205	0.712	0.444	0.392
Glutamic acid (3TMS)	8.985	246	128	84	247	0.525	0.256	0.191
Phenylalanine (2TMS)	9.413	218	192	100	82	0.832	0.474	0.407

Appendix Table 2. Ion library used for quantifying each metabolite (continued).

Asparagine (3TMS)	9.712	116	132	231	141	0.404	0.312	0.205
1,6-Anhydroglucose (3TMS)	9.847	204	217	103	117	0.813	0.225	0.211
2- Desoxyinosose methoxyamine (4TMS)	10.104	133	89	116	103	0.408	0.355	0.287
Fructose methoxyamine (5TMS)	10.224	103	217	307	133	0.37	0.15	0.092
Glucose methoxyamine (5TMS)	10.42	205	160	319	103	0.87	0.786	0.724
Citric acid (4TMS)	10.459	273	133	72	347	0.187	0.165	0.165
Glutamine(3TMS)	10.549	156	155	245	157	0.337	0.178	0.146
Diethyleneglycol (2TMS)	10.6	117	116	103	101	0.548	0.259	0.181
Tetradecanoic acid(1TMS)	10.883	117	129	132	285	0.301	0.271	0.262
Dehydroascorbic acid dimer; L(+)-Ascorbic acid {BP}	11.041	173	157	129	89	0.89	0.572	0.318
myo-Inositol (6TMS)	11.544	217	305	191	318	0.819	0.545	0.397
Galactose methoxyamine (5TMS)	11.704	319	205	103	320	0.821	0.599	0.322
Hexadecanoic acid (1TMS)	12.287	117	129	132	313	0.331	0.314	0.26
2-O-Glycerol-beta-D-galactopyranoside (6TMS)	12.546	204	205	217	131	0.208	0.115	0.094
Spermidine (5TMS)	12.753	144	116	174	156	0.829	0.378	0.341
Indole-3-acetonitrile	12.788	228	129	213	101	0.943	0.313	0.1
Octadecanoic acid (1TMS)	13.581	117	132	129	341	0.361	0.346	0.258
Sucrose (8TMS)	14.769	361	217	103	129	0.532	0.44	0.346
Docosanol (1TMS)	15.159	383	103	159	89	0.766	0.644	0.383
Maltose methoxyamine {BP} (8TMS)	15.457	204	361	217	103	0.499	0.442	0.355
Galactinol(9TMS)	16.377	204	129	191	217	0.963	0.831	0.699
Trehalose (8TMS)	17.216	361	103	217	129	0.474	0.355	0.33
Raffinose (11TMS)	18.079	361	217	204	103	0.556	0.45	0.366

Appendix Table 3. Relative metabolite contents of EON and EOD samples of WT and phytochrome mutants.

Data was normalized to WT EOD sample. NA indicates no detection of such metabolite in the given sample.

	EOD								EON							
Compound	**WT**	**SE**	**phyBD**	**SE**	**phyABDE**	**SE**	**phyABCDE**	**SE**	**WT**	**SE**	**phyBD**	**SE**	**phyABDE**	**SE**	**phyABCDE**	**SE**
1,6-Anhydroglucose (3TMS)	1.000	0.147	0.821	0.107	0.750	0.177	0.884	0.159	1.215	0.089	0.934	0.101	0.735	0.071	0.735	0.096
2- Desoxyinososе methoxyamine (4TMS)	1.000	0.075	1.402	0.095	1.396	0.082	1.461	0.194	0.358	0.025	1.109	0.061	0.353	0.048	0.504	0.039
2-O-Glycerol-beta-D-galactopyranoside (6TMS)	1.000	0.023	1.065	0.040	1.062	0.014	0.893	0.169	0.818	0.156	1.213	0.051	1.090	0.028	1.118	0.040
Asparagine (3TMS)	1.000	0.124	0.748	0.128	0.971	0.176	1.339	0.302	0.748	0.120	1.113	0.237	0.919	0.194	1.398	0.129
Aspartic acid (3TMS)	1.000	0.060	1.211	0.041	1.206	0.087	1.148	0.078	0.979	0.092	1.426	0.196	1.345	0.062	1.502	0.071
Benzoic acid (1TMS)	1.000	0.062	1.215	0.178	1.068	0.040	1.121	0.067	0.666	0.122	0.903	0.113	0.808	0.070	0.854	0.155
Citric acid (4TMS)	1.000	0.208	0.917	0.073	1.459	0.119	1.489	0.122	0.732	0.066	1.522	0.225	1.243	0.112	1.470	0.117
Dehydroascorbic acid dimer; L(+)-Ascorbic acid {BP}	1.000	0.031	0.836	0.064	0.942	0.054	0.964	0.068	1.076	0.035	1.056	0.065	1.446	0.057	1.502	0.058
Diethyleneglycol (2TMS)	1.000	0.054	1.107	0.116	1.028	0.035	0.999	0.066	0.996	0.020	1.158	0.060	1.010	0.037	0.938	0.044
Docosanol (1TMS)	1.000	0.188	0.894	0.171	0.808	0.178	0.822	0.145	0.885	0.196	1.035	0.078	0.993	0.060	0.952	0.086
Fructose methoxyamine (5TMS)	1.000	0.098	1.076	0.195	1.218	0.068	0.593	0.087	0.260	0.013	0.334	0.040	0.278	0.026	0.290	0.057
Fumaric acid (2TMS)	1.000	0.061	1.106	0.064	1.327	0.175	1.578	0.074	0.405	0.026	0.656	0.061	1.048	0.079	1.010	0.053
Galactinol(9TMS)	1.000	0.146	1.030	0.106	1.250	0.326	1.122	0.206	0.783	0.214	1.119	0.204	1.106	0.298	0.964	0.261
Galactose methoxyamine (5TMS)	1.000	0.063	1.086	0.053	0.955	0.028	1.013	0.041	1.074	0.103	1.054	0.119	0.723	0.071	0.957	0.074

Appendix Table 3. Relative metabolite contents of EON and EOD samples of WT and phytochrome mutants (continued).

	EOD								EON							
Compound	**WT**	**SE**	**phyBD**	**SE**	**phyABDE**	**SE**	**phyABCDE**	**SE**	**WT**	**SE**	**phyBD**	**SE**	**phyABDE**	**SE**	**phyABCDE**	**SE**
Glucose methoxyamine (5TMS)	1.000	0.023	1.948	0.321	2.085	0.201	1.101	0.102	0.334	0.034	0.665	0.087	0.314	0.022	0.420	0.055
Glutamic acid (3TMS)	1.000	0.059	1.185	0.058	1.361	0.042	1.846	0.121	1.002	0.065	1.263	0.170	1.356	0.108	1.411	0.051
Glutamine(3TMS)	1.000	0.106	1.352	0.061	1.493	0.195	2.139	0.397	0.291	0.041	0.634	0.131	0.465	0.038	0.863	0.097
Glyceric acid (3TMS)	1.000	0.058	1.080	0.102	0.870	0.044	1.025	0.065	NA	0.000	NA	0.000	NA	0.000	0.247	0.048
Glycerol(3TMS)	1.000	0.253	1.054	0.167	1.273	0.322	1.549	0.400	0.828	0.044	0.850	0.060	0.846	0.082	0.655	0.045
Glycine(3TMS)	1.000	0.022	0.980	0.064	1.053	0.097	1.381	0.139	NA	0.000	0.037	0.006	0.082	0.025	0.106	0.010
Hexadecanoic acid (1TMS)	1.000	0.096	1.250	0.134	1.049	0.115	1.047	0.041	0.988	0.082	1.155	0.082	0.956	0.052	1.009	0.069
Hydroxycarbamic acid (3TMS)	1.000	0.078	4.047	0.430	3.672	0.502	3.614	0.504	0.644	0.046	3.055	0.115	2.532	0.187	2.103	0.178
Hydroxylamine(3TMS)	1.000	0.039	0.949	0.063	0.872	0.043	0.851	0.072	0.806	0.053	0.918	0.086	0.655	0.039	0.604	0.025
Indole-3-acetonitrile	1.000	0.254	0.838	0.211	0.886	0.196	0.548	0.123	0.703	0.130	NA	0.000	0.661	0.161	NA	0.000
Isoleucine(2TMS)	NA	NA	NA	NA	NA	NA	NA	NA	NA	NA	NA	NA	NA	NA	NA	NA
Lactic acid (2TMS)	1.000	0.142	1.022	0.177	1.068	0.294	1.104	0.326	0.739	0.088	1.542	0.602	1.321	0.263	1.710	0.495
L-Alanine (2TMS)	1.000	0.030	1.143	0.057	0.985	0.085	1.380	0.084	0.882	0.048	0.854	0.063	0.786	0.048	0.968	0.049
Leucine(2TMS)	1.000	0.081	1.357	0.099	1.360	0.084	1.450	0.207	0.743	0.134	1.693	0.134	1.943	0.141	2.005	0.093
L-Proline (2TMS)	1.000	0.035	3.708	0.183	3.743	0.284	3.622	0.354	0.527	0.021	2.866	0.117	2.502	0.214	2.037	0.249
L-Threonine (3TMS)	1.000	0.048	1.038	0.022	0.821	0.024	0.856	0.026	0.481	0.015	0.644	0.038	0.455	0.036	0.550	0.030
L-Valine (2TMS)	1.000	0.050	1.241	0.051	1.135	0.036	1.218	0.106	0.632	0.028	0.925	0.058	0.923	0.040	1.008	0.041

Appendix Table 3. Relative metabolite contents of EON and EOD samples of WT and phytochrome mutants (continued).

	EOD								EON							
Compound	**WT**	**SE**	**phyBD**	**SE**	**phyABDE**	**SE**	**phyABCDE**	**SE**	**WT**	**SE**	**phyBD**	**SE**	**phyABDE**	**SE**	**phyABCDE**	**SE**
Malic acid (3TMS)	1.000	0.126	1.854	0.102	1.964	0.072	3.019	0.195	0.286	0.026	0.902	0.132	0.857	0.046	1.422	0.074
Maltose methoxyamine {BP} (8TMS)	1.000	0.170	1.536	0.067	1.263	0.399	1.332	0.271	1.649	0.108	1.851	0.197	0.764	0.049	1.864	0.125
myo-Inositol (6TMS)	1.000	0.064	1.115	0.065	0.837	0.029	1.251	0.076	0.979	0.036	1.201	0.113	0.860	0.027	1.110	0.143
Octadecanoic acid (1TMS)	1.000	0.075	1.257	0.177	1.109	0.071	1.100	0.056	0.981	0.068	1.185	0.094	0.924	0.029	1.055	0.081
Oxalic acid (2TMS)	1.000	0.068	1.103	0.087	1.082	0.125	1.104	0.075	1.093	0.069	1.284	0.079	0.956	0.065	0.947	0.030
Phenylalanine (2TMS)	1.000	0.111	0.891	0.055	1.268	0.055	1.108	0.075	0.251	0.061	0.382	0.094	0.499	0.063	0.571	0.053
proline, 4-Hydroxy (3TMS)	1.000	0.234	0.789	0.079	0.867	0.161	0.893	0.059	0.909	0.171	0.957	0.077	0.955	0.092	0.978	0.101
Raffinose (11TMS)	1.000	0.175	4.763	1.058	2.999	0.313	1.961	0.250	0.558	0.126	4.558	0.876	0.941	0.074	1.060	0.180
Ribitol (5TMS) IS	1.000	0.020	0.992	0.010	0.983	0.003	0.989	0.006	0.971	0.014	0.992	0.006	0.990	0.010	0.987	0.007
Serine(3TMS)	1.000	0.071	1.262	0.064	1.130	0.063	1.401	0.052	0.293	0.024	0.389	0.049	0.328	0.026	0.451	0.033
Spermidine (5TMS)	1.000	0.065	1.128	0.105	0.856	0.031	0.795	0.043	0.677	0.026	0.967	0.088	0.563	0.038	0.617	0.049
Succinic acid (2TMS)	1.000	0.175	2.154	0.399	1.853	0.167	3.285	0.244	1.535	0.100	4.018	0.375	3.030	0.193	4.179	0.149
Sucrose (8TMS)	1.000	0.042	1.120	0.061	1.116	0.026	1.061	0.027	0.837	0.051	0.939	0.063	0.789	0.031	0.872	0.027
Tetradecanoic acid(1TMS)	1.000	0.056	1.120	0.083	0.993	0.037	1.031	0.055	0.753	0.044	0.870	0.067	0.745	0.022	0.752	0.030
Trehalose (8TMS)	1.000	0.173	0.738	0.131	0.943	0.214	0.997	0.145	0.864	0.110	1.044	0.195	0.990	0.148	1.120	0.100

Appendix Table 4. XTHs are regulated differently in *phyABDE* compared to WT.

This table lists all the XTHs that have altered expression in *phyABDE* seedlings grown in 50Um continuous red light compared to WT. Results re-analyzed from published microarray data (Hu et al., 2013).

ID	adj.P.Val	P.Value	t	B	logFC	Gene. symbol	Gene.title
247162_at	1.94E-07	5.78E-11	-3.38E+01	15.54792	-6.7	XTH6	probable xyloglucan endotransglucosylase/hydrolase protein 6
253040_at	3.17E-07	2.98E-10	-2.82E+01	14.15331	-4.34	XTH7	xyloglucan endotransglucosylase/hydrolase protein 7
254044_at	1.45E-04	6.08E-06	-9.21	4.199799	-3.39	XTH14	xyloglucan endotransglucosylase/hydrolase protein 14
247871_at	4.46E-06	2.83E-08	-1.70E+01	9.807188	-2.87	XTH12	probable xyloglucan endotransglucosylase/hydrolase protein 12
247914_at	9.88E-05	3.52E-06	-9.82	4.781051	-2.37	XTH13	xyloglucan endotransglucosylase/hydrolase 13
253763_at	2.69E-04	1.47E-05	-8.28	3.258702	-1.68	XTH26	xyloglucan endotransglucosylase/hydrolase 26
263598_at	9.13E-05	3.11E-06	-9.97	4.913465	-1.28	EXGT-A3	endoxyloglucan transferase A3
253666_at	7.26E-04	5.73E-05	-6.99	1.798882	-1	XTH24	xyloglucan endotransglucosylase/hydrolase protein 24
247925_at	1.96E-02	4.72E-03	-3.7	-2.88726	**-7.38E-01**	**XTH22**	xyloglucan endotransglucosylase/hydrolase protein 22
261550_at	5.20E-03	8.31E-04	-4.87	-1.05673	-7.05E-01	RHS8	xyloglucan-specific galacturonosyltransferase
259041_at	5.28E-03	8.51E-04	-4.85	-1.08237	-6.51E-01	CSLC6	putative xyloglucan glycosyltransferase 6
262842_at	6.26E-03	1.06E-03	-4.69	-1.31998	-6.35E-01	XTH28	probable xyloglucan endotransglucosylase/hydrolase protein 28
265845_at	1.40E-01	6.09E-02	-2.13	-5.4737	-3.14E-01	XEG113	xyloglucanase 113
266376_at	2.38E-01	1.25E-01	-1.69	-6.14507	-2.25E-01	XTH10	xyloglucan endotransglucosylase/hydrolase protein 10
266215_at	7.13E-01	5.83E-01	-5.70E-01	-7.34159	-9.90E-02	XTH4	endoxyloglucan transferase A1
265283_at	8.41E-01	7.54E-01	-3.23E-01	-7.46053	-6.65E-02	MUR3	xyloglucan galactosyltransferase KATAMARI1
254801_at	9.78E-01	9.61E-01	-5.03E-02	-7.51644	-6.58E-03	XTH1	xyloglucan endotransglucosylase/hydrolase 1
257102_at	9.78E-01	9.62E-01	-4.84E-02	-7.51654	-6.22E-03	XTH3	xyloglucan endotransglucosylase/hydrolase 3
255433_at	6.78E-01	5.42E-01	6.33E-01	-7.30094	**1.06E-01**	**XTH9**	xyloglucan endotransglucosylase/hydrolase 9
254598_at	4.53E-01	3.02E-01	1.09	-6.89598	1.63E-01	XTH29	probable xyloglucan endotransglucosylase/hydrolase protein 29
251192_at	3.24E-01	1.90E-01	1.41	-6.51687	1.95E-01	XT1	xyloglucan 6-xylosyltransferase

Appendix Table 4. XTHs are regulated differently in *phyABDE* compared to WT (continued).

ID	adj.P.Val	P.Value	t	B	logFC	Gene. symbol	Gene.title
248732_at	4.48E-01	2.97E-01	1.1	-6.88462	2.00E-01	XTH20	xyloglucan endotransglucosylase/hydrolase protein 20
266066_at	1.74E-01	8.17E-02	1.95	-5.75361	3.44E-01	XTH21	probable xyloglucan endotransglucosylase/hydrolase protein 21
257203_at	6.32E-02	2.15E-02	2.77	-4.44412	**4.06E-01**	**XTH16**	xyloglucan endotransglucosylase/hydrolase protein 16
254802_at	1.91E-02	4.56E-03	3.72	-2.85169	4.92E-01	XTH2	xyloglucan endotransglucosylase/hydrolase 2
254042_at	2.77E-02	7.37E-03	3.42	-3.35106	5.42E-01	XTR6	probable xyloglucan endotransglucosylase/hydrolase protein 23
250591_at	1.53E-02	3.43E-03	3.91	-2.55462	5.48E-01	AT5G07720	xyloglucan 6-xylosyltransferase
260222_at	3.94E-03	5.69E-04	5.14	-0.65383	6.91E-01	XXT5	xyloglucan xylosyltransferase 5
253628_at	4.29E-02	1.30E-02	3.07	-3.93386	8.55E-01	XTH18	probable xyloglucan endotransglucosylase/hydrolase protein 18
263841_at	4.81E-04	3.26E-05	7.5	2.405465	9.46E-01	XTH32	probable xyloglucan endotransglucosylase/hydrolase protein 32
257071_at	2.33E-04	1.19E-05	8.49	3.479128	1.06	CSLC04	xyloglucan glycosyltransferase 4
245794_at	8.31E-04	6.88E-05	6.83	1.604475	1.07	XTH30	probable xyloglucan endotransglucosylase/hydrolase 30
261825_at	1.31E-04	5.33E-06	9.35	4.340377	1.26	XTH8	probable xyloglucan endotransglucosylase/hydrolase protein 8
252320_at	7.95E-04	6.47E-05	6.88	1.669598	1.34	XTH11	probable xyloglucan endotransglucosylase/hydrolase 11
250214_at	1.87E-04	8.76E-06	8.81	3.809171	1.5	XTH5	endoxyloglucan transferase A4
264157_at	8.13E-03	1.50E-03	4.46	-1.68318	**1.5**	**XTH17**	probable xyloglucan endotransglucosylase/hydrolase protein 17
247866_at	1.14E-01	4.68E-02	2.29	-5.21822	1.75	XTH25	probable xyloglucan endotransglucosylase/hydrolase protein 25
263207_at	1.08E-05	1.22E-07	1.45E+01	8.314768	1.85	XTH33	probable xyloglucan endotransglucosylase/hydrolase protein 33
252607_at	1.11E-04	4.17E-06	9.63	4.600906	1.96	XTH31	xyloglucan endotransglucosylase/hydrolase
253608_at	7.56E-05	2.38E-06	1.03E+01	5.197637	**2.02**	**XTH19**	xyloglucan endotransglucosylase/hydrolase 19
245325_at	3.21E-06	1.66E-08	1.81E+01	10.34516	**3.12**	**XTH15**	probable xyloglucan endotransglucosylase/hydrolase protein 15